

Application of Platelet-Rich Plasma in Combination with Cell-Based Therapy for Cartilage Repair

by

Jr-Jiun Liou

BS Biochemistry, National Taiwan University, 2012

MEng Biomedical Engineering, Cornell University, 2013

Submitted to the Graduate Faculty of
Swanson School of Engineering in partial fulfillment
of the requirements for the degree of
Doctor of Philosophy

University of Pittsburgh

2019

UNIVERSITY OF PITTSBURGH
SWANSON SCHOOL OF ENGINEERING

This dissertation was presented

by

Jr-Jiun Liou

It was defended on

April 6, 2018

and approved by

Yadong Wang, PhD, Professor, Department of Biomedical Engineering, Cornell University

Partha Roy, PhD, Associate Professor, Department of Bioengineering

Nam Vo, PhD, Associate Professor, Department of Orthopaedic Surgery

Volker Musahl, MD, Professor, Department of Orthopaedic Surgery

Dissertation Director: Rocky Tuan, PhD, Professor, Department of Orthopaedic Surgery

Copyright © by Jr-Jiun Liou

2019

-

Application of Platelet-Rich Plasma in Combination with Cell-Based Therapy for Cartilage Repair

Jr-Jiun Liou, PhD

University of Pittsburgh, 2019

Post-traumatic and focal cartilage defects of the knee affect over three million Americans annually. Autologous cell-based therapy, e.g., autologous chondrocyte implantation, is limited by the need for ex vivo chondrocyte expansion and donor site morbidity. Mesenchymal stem cells (MSCs), owing to their relative ease of isolation, higher replication activity, and chondrogenic potential, represent an alternative reparative cell type. Platelet-rich plasma (PRP) is an autologous, growth factor-rich biologic that has recently received increasing attention and use as a therapeutic adjunct for the treatment of degenerative joint diseases, and there is evidence suggesting that PRP acts by promoting stem cell proliferation and tissue healing. In this research, we have examined the effects of PRP treatment on chondrogenic differentiation of adult human MSCs derived from the infrapatellar fat pad (IFP-ASCs), maintained in high-density pellet cultures and hydrogel-encapsulated cultures. Cells derived from the infrapatellar fat pad were shown to possess a greater chondrogenic potential than those derived from subcutaneous tissue, and ideally provide a convenient cell source for tissue regenerative procedures. Our results showed that IFP-ASC chondrogenesis is inhibited with increasing PRP concentrations and duration of exposure, based on histological, biochemical, and gene expression analyses. We identified vascular endothelial growth factor (VEGF) as a component of PRP that acts to impair the pro-chondrogenic activity of PRP on IFP-ASCs. We further tested the combination of ASCs with VEGF-depleted PRP

encapsulated with hydrogels for in vivo osteochondral defect repair in a rabbit model. Findings from this research provide information on the potential application of PRP in combination with cell-based therapy for cartilage repair. Our goal is to develop an optimal cell and biologic formulation for a potential point-of-care treatment of post-traumatic and focal cartilage defects, for the restoration of joint function and improvement of the quality of life.

Table of Contents

Preface.....	xiii
1.0 Introduction.....	1
1.1 Cartilage	2
1.1.1 Structure and Function	2
1.1.2 Injury and Intrinsic Healing	4
1.1.3 Current Treatment Approaches	5
1.2 Cartilage Tissue Engineering	6
1.2.1 Cells	7
1.2.2 Biomimetic Scaffolds.....	11
1.2.3 Bioactive Factors	12
1.3 Platelet-Rich Plasma	14
1.3.1 Platelet Biology	15
1.3.2 Platelet-Rich Plasma for Pain Relief	18
1.3.3 Platelet-Rich Plasma for Cartilage Repair	19
1.4 Research Overview	20
2.0 Effect of Platelet-Rich Plasma on Chondrogenic Differentiation of Adipose- and	
Bone Marrow-Derived Mesenchymal Stem Cells	22
2.1 Introduction	22
2.2 Methods	24
2.2.1 Materials and Reagents	24
2.2.2 PRP Releasate Preparation	24

2.2.3 Cell Isolation	26
2.2.4 Cell Characterization.....	27
2.2.5 Colony Formation Assay	27
2.2.6 Differentiation Assay	27
2.2.7 Three-Dimensional Hydrogel Culture.....	28
2.2.8 Gene Expression Analysis	29
2.2.9 Histological Analysis	30
2.2.10 Biochemical Analysis	30
2.2.11 Statistical Analysis	31
2.3 Results.....	31
2.3.1 Comparison of IFP-ASCs and SQ-ASCs	31
2.3.2 Effect of PRP on chondrogenic differentiation in pellet culture.....	34
2.3.3 Effect of PRP on chondrogenic differentiation in hydrogel culture.....	42
2.4 Discussion	44
2.5 Conclusion.....	50
3.0 Vascular Endothelial Growth Factor Impairs Pro-Chondrogenic Activity of	
Platelet-Rich Plasma on Adipose Stem Cells.....	52
3.1 Introduction	52
3.2 Methods	55
3.2.1 Materials and Reagents	55
3.2.2 PRP Releasate Preparation	56
3.2.3 Cell Isolation and Preparation.....	56
3.2.4 PRP Characterization.....	57

3.2.5 Cell Characterization.....	58
3.2.6 Monolayer Culture and Proliferation Assay	58
3.2.7 Pellet Culture and Differentiation Assay	58
3.2.8 VEGF Knockdown	59
3.2.9 Mechanical Impacts	59
3.2.10 Western Blotting	60
3.2.11 Gene Expression Analysis	61
3.2.12 Histological Analysis	61
3.2.13 Biochemical Analysis	62
3.2.14 Statistical Analysis	62
3.3 Results.....	63
3.3.1 Growth factor and cytokine profile of PRP	63
3.3.2 Effect of PRP on IFP-ASC proliferation.....	65
3.3.3 Effect of exogenous VEGF supplementation	66
3.3.4 VEGF receptor surface expression.....	67
3.3.5 Effect of anti-VEGF treatment	68
3.3.6 Anti-inflammatory effect of PRP	69
3.4 Discussion	72
3.5 Conclusion	78
4.0 Discussion.....	79
4.1 Summary	82
4.2 Future Perspectives	83
4.2.1 Rabbit Model	83

4.2.2 Goat Model	94
4.2.3 Future Directions	95
Appendix A	97
Bibliography	104

List of Tables

Table 1. Effect of VEGF on chondrogenic differentiation for cartilage repair.	76
Table 2. Variables of PRP treatments for cartilage repair	83
Table 3. Relevant PRP rabbit studies.....	93
Table 4. Demography of human whole blood donors.....	97
Table 5. Sequences of human RT-PCR primers	98
Table 6. Antibodies for flow cytometry and antibody neutralization.....	99
Table 7. Demographic profile of donor rabbits for rabbit cell isolation.....	100
Table 8. Information of rabbit implantation	101
Table 9. Complete blood count of whole blood and PRP for rabbit surgery.....	102
Table 10. Information of goat implantation	103

List of Figures

Figure 1. Current surgical techniques for treating focal cartilage defects.	6
Figure 2. Cartilage tissue engineering.	13
Figure 3. Chondrogenic differentiation.....	14
Figure 4. PRP composition and function.	18
Figure 5. PRP releasate preparation.....	25
Figure 6. Characteristics of monolayer cultured IFP-ASCs.	33
Figure 7. Comparison of IFP-ASCs and SQ-ASCs.	34
Figure 8. Effect of treatment with 10% PRP for varying durations on IFP-ASC pellet cultures.	36
Figure 9. Effect of treatment with 10% PRP for varying durations on BM-MSC pellet cultures.	37
Figure 10. Effect of 1-day pulse PRP at varying concentrations on IFP-ASC pellet cultures.	39
Figure 11. Effect of 1-day pulse PRP at varying concentrations on BM-MSC pellet cultures.	40
Figure 12. Safranin O staining of IFP-ASC pellet cultures.	41
Figure 13. Alcian blue staining of IFP-ASC pellet cultures.	42
Figure 14. Effect of 21-day PRP at varying concentrations on IFP-ASC hydrogel cultures.....	43
Figure 15. Effect of 21-day PRP at varying concentrations on BM-MSC hydrogel cultures.	44
Figure 16. Growth factor and cytokine profile of PRP samples.	64
Figure 17. EGF and VEGF protein concentration in PRP samples.	65
Figure 18. Effect of PRP treatment on IFP-ASC metabolic activity and proliferation.	66
Figure 19. Effect of exogenous VEGF supplementation on IFP-ASC pellet cultures.	67
Figure 20. Surface expression of monolayer cultured IFP-ASCs, BM-MSCs, and UVECs.	68
Figure 21. Effect of anti-VEGF treatment on IFP-ASC pellet culture.	69

Figure 22. Effect of IL6 and IL1 β on IFP-ASC pellet cultures.	70
Figure 23. Effect of IL1 β on three-dimensional hydrogel cultures.	71
Figure 24. Tissue engineering approach for osteochondral defect repair.	80
Figure 25. Isolation of rabbit adipose tissue.	84
Figure 26. Tri-lineage differentiation of rabbit ASCs.	88
Figure 27. Cell implantation in rabbit osteochondral defects.	89

Preface

I would like to thank my Ph.D. advisor – Dr. Rocky Tuan for being so supportive all these years. He gave me the opportunity to be part of this big family – Center for Cellular and Molecular Engineering – and to improve my research skills and critical thinking. I want to thank my committee members Dr. Yadong Wang, Dr. Partha Roy, Dr. Nam Vo, and Dr. Volker Musahl.

I thank Dr. Benjamin Rothrauff and Dr. Peter Alexander for the mentorship, Dr. Mark Langhans and Dr. Riccardo Gottardi for the assistance in writing manuscripts, Dr. Hang Lin for the preparation of gelatin hydrogel solution, Dr. Jian Tan for the assistance in cell isolation, Dr. Tomoya Iseki and Dr. Shinsuke Kihara and Alyssa Falcione for the assistance in rabbit surgery, and Lynda Guzik for the help in flow cytometry. I would also like to thank the funding support of the U.S. Department of Defense (W81XWH-14-2-0003) and the International Foundation for Ethical Research.

Finally, I want to thank my parents and my boyfriend for supporting me throughout graduate school. Without them, I would never make this far.

1.0 Introduction

Cartilage injuries affect more than 10 million people in the United States every year (National Research Council and the Institute of Medicine, 2001). These injuries remain a significant clinical problem not only due to the intense pain and potential for mobility loss but also because they represent the primary reason for visits to the doctor's office and contribute to the majority of physical disabilities (National Research Council and the Institute of Medicine, 2001). The burden of musculoskeletal diseases is well recognized, afflicting more than 20% of the population, higher than cancer and cardiovascular disease combined (National Research Council and the Institute of Medicine, 2001). Understanding the nature and cause of musculoskeletal soft tissue injuries is thus highly relevant. This chapter reviews the nature and current treatments for cartilage injuries, and the knowledge gaps in effective therapies. The potential of tissue engineering and regenerative medicine approaches is highlighted with examples, featuring both promises and challenges for future investigations.¹

¹The Introduction contains materials from the publication - Liou, J. J., Langhans, M. T., Gottardi, R., & Tuan, R. S. (2016) Injury and Repair of Tendon, Ligament and Meniscus, *Advances in Translational Medicine Regenerative Medicine*, Chapter 6.

1.1 Cartilage

1.1.1 Structure and Function

Articular cartilage (AC) of the knee covers the femoral and tibial surface and can also be found on the back of patella. AC primary functions include transmission of applied loads across the mobile surface, alignment of the ends of bones as well as permitting rolling or sliding during movement (Masouros, Bull, & Amis, 2010). Cartilage is composed of 1% chondrocytes, 29% extracellular matrix, and 70% water. Among all extracellular matrix proteins, collagen type II is the most abundant component that provides tensile strength to the cartilage tissue. Proteoglycan, another key molecule of AC, is composed of proteins and sugars that contain negative charges. The repulsive force between negative charges provides increased compressive strength for the cartilage tissue (Han, Chen, Klisch, & Sah, 2011). Link protein, hyaluronan, core aggrecan protein, and glycosaminoglycan are four components of proteoglycans. The complexity of the organization between the cells and extracellular matrix constituents is critical for the unique biomechanics of cartilage.

Because of the limited availability of differentiated cartilage cells, i.e., chondrocytes, cartilage tissue engineering using adult tissue-derived, multipotent mesenchymal stem cells (MSCs) has been actively pursued for the past two decades. Adult MSCs can undergo condensation and chondrogenic differentiation and become mature chondrocytes with appropriate induction. Challenges on how to induce chondrogenic differentiation at the chosen time and the desired location remain. A variety of natural materials, including silk, fibrin, hyaluronic acid, collagen, gelatin, chitin, chitosan, tricalcium phosphate, and hydroxyapatite, have been utilized as

biomaterial scaffolds for neo-cartilage tissue formation; however, there is no agreed perfect material as of yet (J. Yang, Zhang, Yue, & Khademhosseini, 2017; P. J. Yang & Temenoff, 2009).

Collagen scaffolds, in particular, have been utilized in a currently practiced surgical technique - matrix-assisted autologous chondrocyte implantation (MACI) – for repair of focal cartilage defects (Brittberg et al., 1994; Brittberg, Nilsson, Lindahl, Ohlsson, & Peterson, 1996; Freymann, Petersen, & Kaps, 2013; E Kon, Filardo, Di Matteo, Perdisa, & Marcacci, 2013; Makris, Gomoll, Malizos, Hu, & Athanasiou, 2015). In the first generation of MACI, a collagen membrane was used to cover chondrocyte implantation site. The second generation of MACI utilizes collagen hydrogel scaffold to encapsulate chondrocytes to support cell growth. Challenges of MACI include donor site morbidity, low availability of chondrocytes, and loss of chondrocyte phenotype during cell expansion.

To engineer a fully functional cartilage tissue, a principal concern is an adequate mechanical strength since the major function of articular cartilage is to support the applied loads for the entire body. Weight-bearing regions must withstand repetitive mechanical loading to ensure joint function after an operation. The neo-cartilage must possess both biological characteristics and mechanical properties of native cartilage; The compressive modulus of native cartilage is 1 MPa (Moutos et al., 2016). Currently, numerous investigators are exploring different combinations of natural or synthetic materials to optimize the mechanical properties of neo-cartilage tissues. Using condensed mesenchymal cell bodies, Young's modulus can reach up to 700 kPa (Bhumiratana et al., 2014), alginate reinforced with polycaprolactone scaffolds can reach as high as 6000 kPa (Schuurman et al., 2011), polyethylene glycol at 4000 KPa (Woodfield et al., 2004, 2005) with polycaprolactone-hydroxyapatite scaffolds an excess of 5000 kPa (C. H. Lee et al.,

2010). A review of current cartilage tissue engineering systems with relevant information of materials and mechanical properties is presented by (Mouser et al., 2017).

In the cartilage growth plate of the developing endochondral skeleton, mesenchymal cells condense and then differentiate into chondrocytes, form flat columnar chondrocytes, become pre-hypertrophic chondrocytes and hypertrophic chondrocytes, ultimately mature to terminal hypertrophic chondrocytes. Terminal hypertrophic chondrocytes are withdrawn from the cell cycle and commit to apoptosis (Ruijtenberg & van den Heuvel, 2016; Zuscik, Hilton, Zhang, Chen, & O'Keefe, 2008), exhibiting an inverse relationship between proliferation and differentiation (Ruijtenberg & van den Heuvel, 2016).

1.1.2 Injury and Intrinsic Healing

Cartilage injuries occur during traumatic injuries or repeated unbalanced stress. The major symptom is pain and loss of joint function. Cartilage lesions can be categorized into four different severity levels: Grade I to Grade IV. Grade I represents the cartilage with soft spots or superficial wears; Grade II represents minor tears with lesions less than half thickness of cartilage; Grade III usually represents lesions that are deeper than half thickness of cartilage; patients diagnosed as Grade IV usually have full-thickness cartilage defects with subchondral bone exposed.

Due to lack of vasculature in cartilage, intrinsic healing is poor, and to repair damaged cartilage, surgical procedures are usually required. Unlike muscle strain and bone fracture, physical therapy is of little help.

1.1.3 Current Treatment Approaches

Current surgical techniques for treating focal cartilage defects include osteochondral autograft/allograft transplantation, microfracture, and autologous chondrocyte implantation (**Figure 1A**). In osteochondral autograft/allograft transplantation, the surgery involves harvesting osteochondral plugs from the donor site and osteochondral plug transplantation to the defect site (**Figure 1B**). Another surgical procedure – microfracture – involves drilling into subchondral bone to induce bleeding and release bone marrow, which contains clotting factors and mesenchymal stem cells.

In autologous chondrocyte implantation (ACI), autologous chondrocytes are isolated from non-weight bearing cartilage, expanded *ex vivo*, and returned to the chondral defect as a cell suspension covered with a collagen membrane (Huang, Hu, & Athanasiou, 2016). More recently, matrix-assisted ACI (MACI) has been developed (**Figure 1C**). In MACI, autologous chondrocytes are seeded within a three-dimensional scaffold before implantation, for better integration with the surrounding native cartilage while also providing a biomimetic microenvironment capable of enhancing cartilage neotissue formation (Freyman et al., 2013; E Kon et al., 2013; Makris et al., 2015). Although both ACI and MACI have shown promise, challenges persist. Chondrocyte yield from non-weight bearing cartilage is low, requiring *ex vivo* cell expansion with an accompanying loss of the chondrogenic phenotype (Tuan, Chen, & Klatt, 2013). As a result, the patient must undergo two surgical procedures, and the quality of cartilage repair remains inconsistent. Identification of alternative cell sources and the application of chondroinductive scaffolds are needed to overcome these challenges, permitting a single-step procedure with robust cartilage formation.

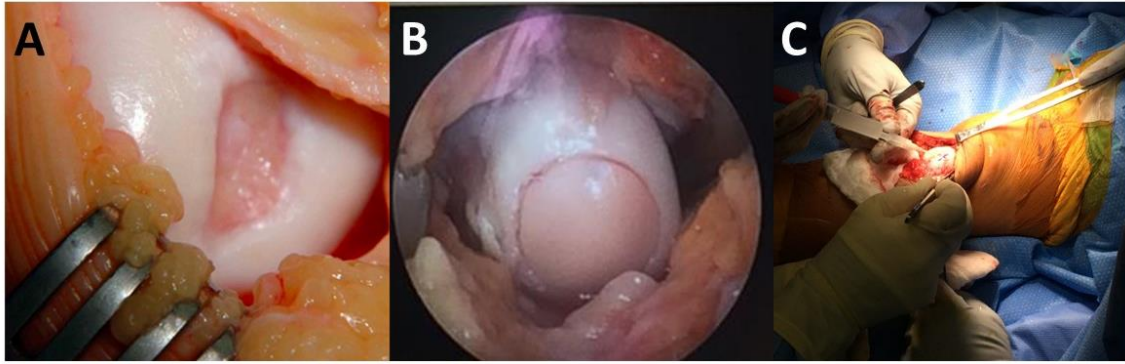


Figure 1. Current surgical techniques for treating focal cartilage defects.

Cartilage defects usually require a surgical procedure to repair. Photo adapted from the internet². (B) Osteochondral allograft transplantation is a technique that allograft is cored and trimmed to the appropriate dimensions and filled the defect. Photo credit: Jr-Jiun Liou. (C) Matrix-assisted autologous chondrocyte implantation is a two-step procedure: first procedure autologous articular cartilage is harvested, and the autologous chondrocytes are isolated and expanded *ex vivo*; during second procedure, autologous chondrocyte mixed in collagen solution is injected to the chondral defect with collagen membrane as a cover and fibrin gel as glue. Photo credit: Jr-Jiun Liou.

1.2 Cartilage Tissue Engineering

The field of tissue engineering was introduced more than two-and-a-half decades ago to describe the combination of biological principles and engineering technologies for developing functional replacement of degenerated, injured, or diseased tissues and organs. Regenerative medicine refers to clinical applications of these therapeutic procedures. Successful tissue engineering and regenerative medicine approaches require cells, scaffolds or matrices, and

² <http://www.porcpotlas.hu/en/mozaikplasztika.html>

bioactive factors, that when combined can facilitate the productive, conductive, and inductive activities, respectively, of tissue regeneration.

1.2.1 Cells

Chondrocytes are mature cells present in cartilage tissues. Many studies have intensively investigated the potential of chondrocyte-derived tissues. However, chondrocytes undergo dedifferentiation during cell expansion and typically lose their cartilage phenotype, resulting in fibroblastic cells. Unlike fibroblasts or MSCs, doubling time of chondrocytes may be as long as 3.5 days; which presents challenges to reach sufficient cell populations for one-step procedures (Akens & Hurtig, 2005). Strategies for maintaining chondrocyte phenotype have been reported. When mixed with bone marrow-derived MSCs (BM-MSCs) in alginate hydrogels before subcutaneous implantation, chondrocytes were able to maintain their phenotype for up to 6 weeks; however, the mechanical strength of alginate hydrogel used in this study may not be sufficient when implanted into articular joint (Fedorovich et al., 2012). Another research group reported chondrocytes cultured on beta-glycerophosphate containing calcium polyphosphate for development of cartilage-bone interface (Allan, Pilliar, Wang, Grynepas, & Kandel, 2007). This study indicated that calcium phosphate and beta-glycerophosphate are both necessary for calcified cartilage development (Allan et al., 2007).

To understand the regulation of differentiation and de-differentiation of articular chondrocytes, researchers have also focused on studying how chondrocytes are formed during embryonic development. In early embryonic development, the endochondral ossification process of skeletogenesis is initiated by mesenchymal condensation, followed by chondrogenic differentiation to form a cartilage template (Carlevaro, Cermelli, Cancedda, & Descalzi Cancedda,

2000; Kronenberg, 2003). Growth and maturation of the cartilage template in the growth plate result in chondrocyte hypertrophy, accompanied by the upregulation of vascular endothelial growth factor (VEGF) and subsequent vascularization (Carlevaro et al., 2000; Karimian, Chagin, & Säwendahl, 2011). During this event, the hypertrophic chondrocytes undergo apoptosis and are replaced by osteoblasts, ultimately resulting in bone formation (Carlevaro et al., 2000; Karimian et al., 2011). While the critical steps that lead to hypertrophy are still incompletely understood, VEGF is believed to play an important role.

Due to the limitations in culturing chondrocytes, stem cells have become an alternative cell source. Stem cells can be divided into two different categories: pluripotent stem cells (e.g., embryonic stem cells, ESCs, and induced pluripotent stem cells, iPSCs) and multipotent stem cells. iPSCs were first produced from mouse fibroblasts via viral transduction of four transcription factors – Oct4, Sox2, cMyc, and Klf4 in 2006 (Kazutoshi Takahashi & Yamanaka, 2006). Like ESCs, iPSCs were shown to possess unlimited self-renewal and proliferation potential (K. Takahashi et al., 2007; Wernig et al., 2007; Yamanaka, 2007; J. Yu et al., 2007). Compared to adult MSCs, iPSCs have longer telomere length and can potentially become a practically unlimited cell source without compromising the differentiation capacity (Marión & Blasco, 2010). During embryonic development, embryonic stem cells develop into three different germ layers: the endoderm, mesoderm, and ectoderm (Langhans, Yu, & Tuan, 2015). As the applicability of iPSCs for tissue engineering is still an area of active research and has not been established, it is not within the scope of this dissertation.

The other category is adult mesenchymal stem cells (MSCs). MSCs have the ability of self-renewal and multi-potency. For example, they can undergo condensation and chondrogenic differentiation and become mature chondrocytes with appropriate induction. MSCs have

traditionally been isolated from the bone marrow, an invasive and often painful procedure that yields a relatively low percentage of MSCs. Alternatively, adipose tissue contains a higher percentage of MSCs, is abundantly available, and can be harvested through a minimally invasive lipoaspiration procedure (Hildner et al., 2015). Recently, human MSCs derived from the infrapatellar fat pad (IFP-ASCs) were shown to possess a greater chondrogenic potential than subcutaneous ASCs (SQ-ASCs) (Lopa et al., 2014) and may ideally provide a stem cell source in one-step procedures.

Infrapatellar fat pad (IFP), or Hoffa's fat pad, is located underneath the patellar tendon. Hoffa's disease is caused by acute injuries or chronic unbalanced stresses, and the major symptom is pain due to impingement from femur or tibia to the fat tissue. The fat tissue is approximately 21-39 mL in size, dependent on the individual (Jason L. Dragoo, Johnson, & McConnell, 2012). IFP, like other fat tissues, is highly vascularized and innervated. Cells resident within the IFP include adipocytes, fibroblasts, and multipotent MSCs (IFP-ASCs), which have been harvested and utilized in tissue engineering approaches. The exact function of IFP is still unclear, but it has been hypothesized that IFP serves as cushioning and a reservoir of reparative cells (Jason L. Dragoo et al., 2012). Surgically, the IFP can be harvested by a small incision arthroscopically (Koh & Choi, 2012). This procedure is less invasive when compared to bone marrow harvest. The total cell numbers harvested from 21 mL of IFP average 5.5×10^6 cells, while the average from 30 mL of bone marrow aspirate is 1.0×10^5 cells (Bruder, Jaiswal, & Haynesworth, 1997; J L Dragoo et al., 2003). Due to their less invasive derivation and autologous nature, IFP-ASCs were chosen to be the main cell type used in this dissertation research.

However, the volume of IFP is still relatively small when compared to subcutaneous tissues, which usually range 200 mL, so the total cell number of IFP is limited (G. Yu et al., 2010).

Therefore, ex vivo culture expansion of IFP-ASCs would likely be required to obtain a sufficient cell number for implantation. Alternatively, it may be possible to promote IFP-ASC proliferation at the site of implantation, thereby allowing the intraoperative isolation of IFP-ASCs and implantation into a chondral defect.

Adult multipotent stem/progenitor cells, by virtue of their extensive proliferative activity and multi-lineage differentiation potential, are thus considered prime candidate cells for tissue engineering and regenerative medicine. For musculoskeletal applications, adult stem cells, such as MSCs, most commonly derived from bone marrow and adipose tissue, are of interest due to the relative ease of their isolation and enrichment, safety, and freedom from ethical issues. MSCs cultured in the presence of specific growth factors and inductive supplements may be induced to differentiate into specific musculoskeletal tissue lineages, including chondrocytes and osteoblasts. For the induction and enhancement of MSC chondrogenesis, several growth factors have been shown to be highly active, in particular transforming growth factor (TGF β). Of interest is the recent attention on platelet enriched products, including plasma platelet-rich plasma (PRP) and platelet-rich fibrin (PRF), as bioactive additives to enhance the repair of cartilage.

ASCs have been widely studied because of the abundance of fat disposed after surgery. MSCs may be derived from either autologous or allogeneic sources. Open surgery, ex vivo cell expansion and iatrogenic damage caused by autologous stem cell harvesting are not preferable. The other disadvantage of using autologous stem cells, particularly from elderly individuals, relates to the age-associated reduction in proliferative and differentiation activities of MSCs.

1.2.2 Biomimetic Scaffolds

In addition to cells, a biocompatible scaffold is beneficial in promoting cell growth and differentiation, as well as acting as a 3-dimensional volumetric adduct. As mentioned, the MACI technique utilizes collagen hydrogel as seeding scaffold. Materials including synthetic materials that degrade over time and native biomaterials derived from tissues have been investigated. Poly(lactic-co-glycolic acid) (PLGA), poly(L-lactic acid) (PLLA) and poly(ϵ -caprolactone) (PCL) are the most common synthetic biodegradable polymers in use. Kuo et al. summarized current synthetic polymeric scaffolds and native biomaterials in tendon and ligament tissue engineering (Kuo, Marturano, & Tuan, 2010). PLLA showed better performance compared to PLGA scaffold regarding degradation profiles (Kuo et al., 2010). A recent study adopted a rational design of nanofiber scaffolds for tendon regeneration using PLGA and PCL seeded with stem cells and implanted into different animal models, and reported favorable outcomes; however, the prevention of adhesion after the repair was not investigated (Ma, Xie, Jiang, Shuler, & Bartlett, 2013).

Native biomaterials derived from the extracellular matrix, such as collagen and fibrin, are also in common use. Silk fibroin, a native biomaterial, has the best elastic modulus and tensile strength among all natural scaffolds for cell support and tissue ingrowth (Kuo et al., 2010). Extracellular matrix derived from decellularized cartilage has also been studied to provide a more homogenous and porous scaffold for cartilage tissue engineering (Rothrauff et al., 2018).

1.2.3 Bioactive Factors

Bioactive factors are critical in regulating the differentiation of stem cells to target cell lineages. These factors, for cartilage tissue engineering, predominantly are within transforming growth factor beta (TGF β) superfamily.

For applications in skeletal soft tissues, the most commonly used biologics are platelet-rich plasma (PRP), platelet-rich fibrin (PRF), and the orthokines. PRP, isolated from human whole blood as a cocktail of growth factors released from activated platelets, has been used in clinics since the 1990s. Although the use of PRP treatment for tissue healing and regeneration has become clinically popular in the last decade, scientific evidence remains insufficient with many conflicting results reported on its efficacy. Several reasons contribute to the observed variability, including variations in PRP composition, cellularity of the damaged or diseased target tissue, and the lack of controlled studies. Several trials have reportedly focused on assessment of PRP effects compared to placebo controls. In the next section, platelet biology and use of PRP will be discussed in detail.

PRF, also called fibrin clot, is used to improve tissue regeneration as well. The use of PRF is considered more desirable than the use of PRP since bovine thrombin and anticoagulants are not required. A commercial product, Orthokine, is based on autologous serum generated by incubating venous blood with etched glass beads, thus allowing peripheral blood leukocytes to produce elevated amounts of the interleukin-1 receptor antagonist and other anti-inflammatory mediators that are recovered in the serum (36). Orthokine has been used in various applications to treat knee osteoarthritis; however, the effectiveness of orthokine, which is not FDA-approved, is unclear, and no controlled clinical trials are ongoing.

Cartilage tissue engineering involves cells, biomimetic scaffolds, and bioactive factors (**Figure 2**). As mentioned above, the most common cell sources are bone marrow, subcutaneous

tissue, and infrapatellar fat pad (the focus of this dissertation). Popular biomimetic scaffolds are collagen, gelatin, and fibrin scaffolds. In addition, bioactive factors (e.g., transforming growth factors) are necessary for cartilage tissue engineering to induce and promote cartilage matrix deposition.

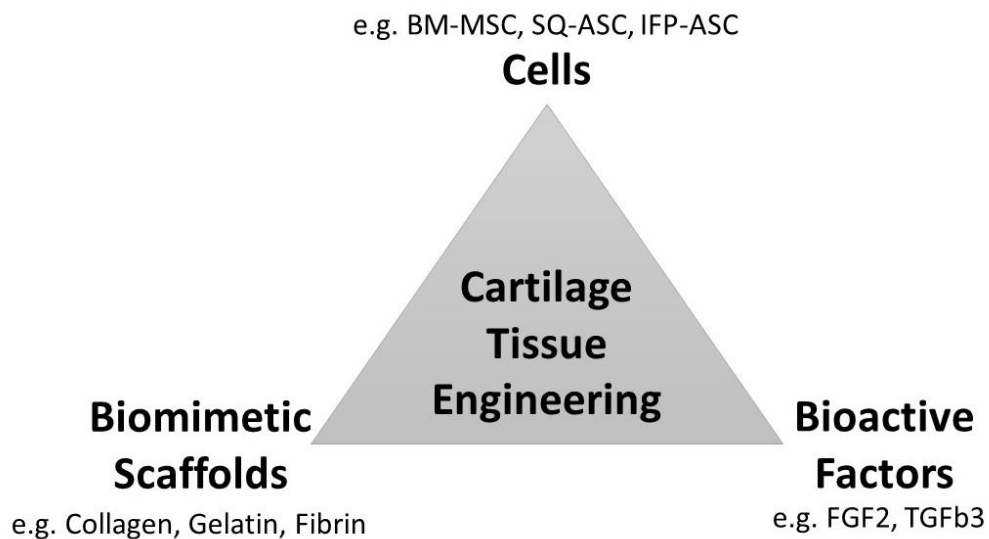


Figure 2. Cartilage tissue engineering.

Cartilage tissue engineering involves cells, biomimetic scaffolds, and bioactive factors. Cell sources can be bone marrow-derived mesenchymal stem cells (BM-MSCs), subcutaneous tissue-derived adipose stem cells (SQ-ASCs), and infrapatellar fat pad-derived adipose stem cells (IFP-ASCs). Examples of biomimetic scaffolds are collagen, gelatin, and fibrin scaffolds. Bioactive factors are the key to induce proliferation (e.g., basic fibroblast growth factor, FGF2) and chondrogenic differentiation (e.g., transforming growth factor 3, TGFβ3). Adapted from (Ohba, Yano, & Chung, 2009).

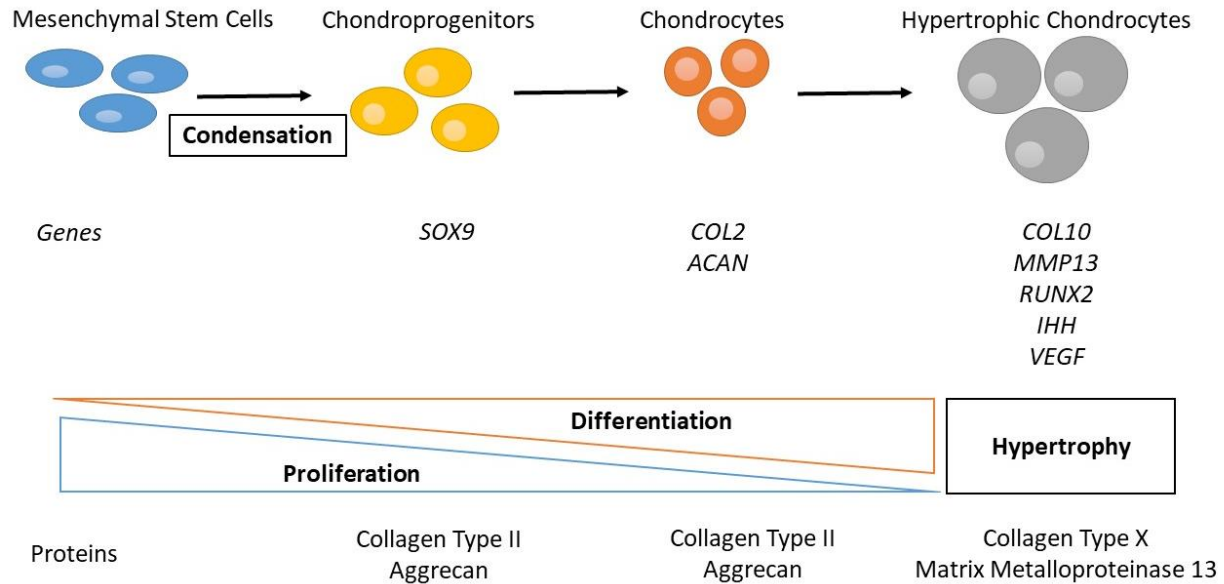


Figure 3. Chondrogenic differentiation

Chondrogenic differentiation begins with mesenchymal stem cells undergoing condensation, chondroprogenitors expressing *SOX9*, maturation of chondrocytes (expression of *COL2* and *ACAN*), and terminal differentiation – hypertrophic chondrocytes (expression of *COL10*, *MMP13*, *RUNX2*, *IHH*, and *VEGF*). Proteins that are highly expressed during chondrogenic differentiation are collagen type II and IX and aggrecan; once the cells become hypertrophic, cells start to produce collagen type X and matrix metalloproteinase 13. Adapted from (Zuscik et al., 2008).

1.3 Platelet-Rich Plasma

Platelet-rich plasma (PRP) has recently received considerable attention as a potential therapeutic agent for cartilage repair, due to its cost-effective and autologous nature. PRP contains many growth factors and inflammatory mediators that are released from activated platelets, and it has been shown to promote stem cell proliferation and tissue regeneration. We expect that the

combination of IFP-ASCs and autologous PRP can overcome the challenge of limited cell number and cell expansion given the proliferative capabilities of IFP-ASCs and the growth factors in PRP.

1.3.1 Platelet Biology

Platelets are essential to wound healing given their function of providing primary hemostasis and coagulation. Specifically, when an injury occurs, the clotting cascade generates active thrombin from pro-thrombin, thrombin activates platelets and releases fibrinogen. Fibrinogen reacts with thrombin or calcium and forms fibrin clots. The bleeding then stops, i.e., hemostasis.

Within platelets, there are alpha granules, dense granules, mitochondria, and other intracellular bodies (Kickler, 2006) (**Figure 4**). Upon platelet activation, growth factors and cytokines are released from alpha granules within seconds. These growth factors (e.g., platelet-derived growth factor, epidermal growth factor, vascular endothelial growth factor) and cytokines (e.g., matrix metalloproteinases, interleukins) act to maintain the balance between anabolic and catabolic responses locally. Under physiological condition, plasminogen is activated to become plasmin which proteolytically degrades fibrin to produce fibrin degradation products. Physiologically, the concentration of platelets is 150,000-350,000 platelets per microliter in the peripheral blood (Kickler, 2006).

A concentrate of platelets injected into the joint can potentially recruit reparatory cells and secrete growth factors and anti-inflammatory cytokines. Among all growth factors, transforming growth factor beta (TGF β) superfamily which includes TGF β s and bone morphogenetic proteins (BMP) is of interest. TGF β s and BMPs are ligands that bind to TGF β receptors, which are transmembrane proteins with cytosolic domains that exhibit serine/threonine kinase activity.

Signal transduction starts with direct activation of cytosolic Smad. TGF β 1 and TGF β 3 are known to promote chondrogenic differentiation for cartilage tissue engineering. However, studies have indicated that TGF β 1 may be associated with fibrosis and fibrocartilage formation in cartilage repair.

Platelets also release several pro-inflammatory cytokines that have been shown to involve in osteoarthritis pathogenesis. Interleukin 6 (IL6), for instance, is highly upregulated in osteoarthritic cartilage (L. Sun, Wang, & Kaplan, 2011). In vitro, IL6 inhibits collagen type II gene expression, decreases proteoglycan deposition, and glycosaminoglycan/DNA content in BM-MS-C cultures (Pricola, Kuhn, Haleem-Smith, Song, & Tuan, 2009). IL6 and soluble IL6 receptor alpha result in concentration-dependent increases in cartilage matrix deposition and collagen type II, aggrecan, and collagen type X gene expression in MSC pellet cultures (Kondo et al., 2015). IL6 trans-signaling requires soluble IL6 receptor and is potentially active in all cells of the body since all cells express the gp130 protein (Rose-John, 2012).

Another pro-inflammatory cytokine – interleukin 1 beta (IL1 β) is of interest as well. PRP decreases IL1 β -induced expression of TIMP1 and ADAMTS5 in cartilage and expression of TIMP1, ADAMTS, and VEGF in synovium, suggesting that PRP has anti-inflammatory effect on gene expression (Osterman et al., 2015). IL1 β decreases COL2 and ACAN expression and increases ADAMTS4 and PTGS2 expression; PRP reverses IL1 β -induced effects suggesting PRP has anti-inflammatory effect (van Buul et al., 2011). IL1 β significantly decreased cartilage matrix accumulation and decreased Young's modulus in bovine cartilage rings centrally embedded with chondrocyte-encapsulated agarose hydrogels (Djouad, Rackwitz, Song, Janjanin, & Tuan, 2009). IL1 β alone or in combination with TNF α increase collagenase and aggrecanase production and also suppress chondrocyte synthesis of aggrecan and collagen type II (L. Sun et al., 2011).

Combination of IL1 β and TNFa significantly upregulates MMP1, MMP3, MMP13. ADAMTS4, and ADAMTS5 gene expression while downregulating ACAN (L. Sun et al., 2011). Interestingly, one study has shown that pre-treatment of IL1 β for 14 days prior to pellet culture can increase the wet weight of synovium-derived MSC pellets (Matsumura et al., 2017).

Unfortunately, PRP is currently not regulated by the United States Food and Drug Administration (FDA). In principle, according to FDA regulations, PRP is considered, by definition, a blood-derived biologic and should be regulated by the Center for Biologics Evaluation and Research (CBER) (Beitzel et al., 2015). However, the commercially available PRP Preparation Devices, such as Arthrex ACP and Zimmer Biomet GPS, are released to the market via a different pathway - the 510(k) clearances. Such devices are determined to be “substantially equivalent” to a previously cleared device. For example, one of the PRP Preparation Devices – Arthrex ACP is meant to be mixed with the Arthrex BioCartilage in a clinical setting. This PRP product is not for direct injections but mixed with autologous or allogeneic bone grafts to enhance bone repair. For direct injections, PRP is considered “off-label” which refers to the devices that are not FDA-regulated; any manipulation, including platelet activation or addition of exogenous factors, is not yet allowed in the clinics. The main challenge of regulating PRP is that there is no consensus of which protocol is the best, and the number of platelets varies based on the individual difference among the patients, the timing of blood draw, and timing of PRP isolation given its autologous nature.

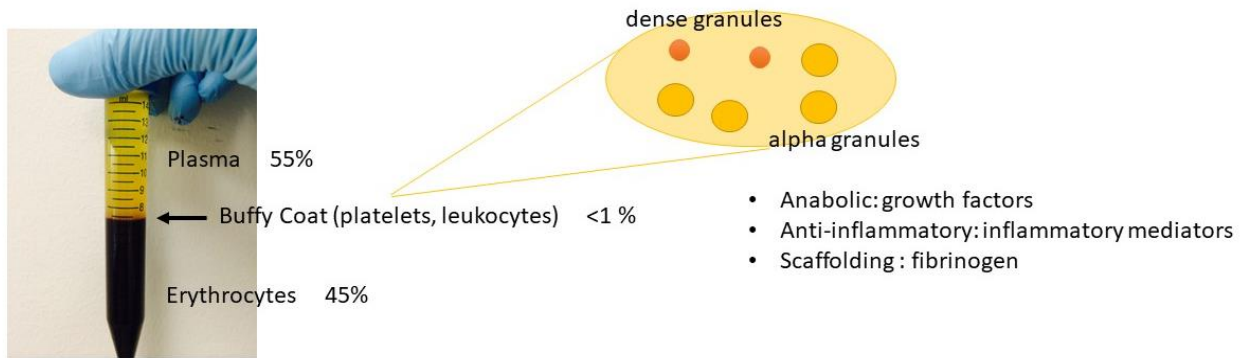


Figure 4. PRP composition and function.

Typically, after the first spin of whole blood, three layers are plasma (approximately 55% v/v) on top, buffy coat in the middle (1%) which is enriched in platelets and leukocytes, and erythrocytes (45%) on the bottom. Within platelets, there are dense granules and alpha granules. When the platelet is activated, anabolic growth factors, anti-inflammatory factors, and fibrinogen that can provide scaffolding effect are released from alpha granules.

1.3.2 Platelet-Rich Plasma for Pain Relief

Clinical studies have shown that PRP treatment improves pain management and inflammation in osteoarthritis (Andia & Maffulli, 2013). In a randomized controlled trial in Spain, three injections of PRP (n = 110 patients) significantly reduced pain and stiffness scores with increased physical function (Sánchez et al., 2012).

Similarly, intra-articular PRP injections (n = 60 patients) significantly improved mean Western Ontario and McMaster (WOMAC) score in gonarthrosis at 24 weeks, which is an indication of pain reduction and improved joint function, when compared to intra-articular hyaluronic acid injections (n = 60 patients) reported in a randomized controlled trial in Italy (Cerza et al., 2012).

PRP has been compared to placebo (saline) in a clinical trial in India (Patel, Dhillon, Aggarwal, Marwaha, & Jain, 2013). Single injection and double injections of PRP significantly improve pain, stiffness, and physical function when compared to single injection of saline at six months follow-up (Patel et al., 2013).

The anti-inflammatory effects of PRP may be partially attributed to the release of anti-inflammatory mediators from activated platelets and reduced canonical nuclear factor kappa B (NFkB) signaling (T. Lawrence, 2009). Anti-inflammatory mediators include interleukin 1 receptor antagonist, soluble tumor necrosis factor receptor, interleukin 4, interleukin 10, interleukin 13, and interferon gamma (Xie, Zhang, & Tuan, 2014). These factors can act to block the receptor and downstream signaling of IL1 β or tumor necrosis factor alpha (TNF α), consistent with other studies that show that PRP decreases catabolic gene expression and protein secretion. Previously, van Buul et al. showed PRP decreased expression of catabolic markers ADAMTS4 and COX2 on human chondrocytes within 48 hours (van Buul et al., 2011). PRP was able to rescue human nucleus pulposus cells from the IL1 β and TNF α -induced expression of catabolic markers MMP3 and COX2 at 48 hours (H.-J. Kim et al., 2014). Osterman et al. also demonstrated that PRP was able to decrease expression of catabolic markers TIMP1 and ADAMTS5 as well as angiogenic marker VEGF within 72 hours on human cartilage explants (Osterman et al., 2015).

1.3.3 Platelet-Rich Plasma for Cartilage Repair

However, while some studies have reported pain reduction and improvement of joint function with PRP treatment (Bayar et al., 2008), others have found no improvement in cartilage formation (Brehm et al., 2006; Elizaveta Kon et al., 2010). Variations in PRP effectiveness include individual difference and PRP preparation which results in varied

growth factor/cytokine profile. Among all growth factors within PRP, studies have indicated that vascular endothelial growth factor (VEGF) may impair chondrogenesis and cartilage repair. More specifically, VEGF-transduced muscle-derived stem cells performed poorly in chondrogenesis, and a catabolic role of VEGF on matrix degeneration has been reported in a rat model (Kubo et al., 2009b; Matsumoto et al., 2009). When combined with soluble receptor to block VEGF signaling, soluble receptor-treated group had more collagen type II deposition in pellet culture (Mifune et al., 2013). Intravenous administration of anti-VEGF antibody improved articular cartilage repair in a rabbit model (Nagai et al., 2010). Taken together, results from these studies suggest that VEGF may impair the pro-chondrogenic potential of PRP.

1.4 Research Overview

The central hypothesis of this dissertation research is that PRP can modulate IFP-ASC chondrogenesis, and that removal of VEGF can further enhance IFP-ASC chondrogenesis for cartilage tissue engineering. The hypothesis was tested through the following specific aims:

Specific Aim 1: Characterization of the effect of PRP on IFP-ASC chondrogenesis in both pellet and hydrogel cultures;

Specific Aim 2: Assessment of the effect of VEGF as a component of PRP and cellular mechanism of VEGF action on IFP-ASC chondrogenesis;

Specific Aim 3: *In vivo* application of PRP in combination with ASCs encapsulated in a 3-dimensional hydrogel in a rabbit model of cartilage repair.

The studies in Aim 1 examined the general role of PRP on IFP-ASC chondrogenesis; studies in Aim 2 examined the effect of VEGF as a component of PRP on IFP-ASC chondrogenesis; and studies in Aim 3 further tested the optimized PRP on osteochondral defect repair *in vivo*. These studies together can provide information on the potential application of PRP in combination with cell-based therapy for cartilage repair. Our goal is to develop a point-of-care application for the population with post-traumatic and focal cartilage defects, ultimately restoring their joint function and improving the quality of life.

2.0 Effect of Platelet-Rich Plasma on Chondrogenic Differentiation of Adipose- and Bone Marrow-Derived Mesenchymal Stem Cells

2.1 Introduction

Cartilage degeneration affects 27 million people in the United States, and post-traumatic and focal cartilage defects comprise 12% of all cases (approximately 3 million Americans annually) (Brown, Johnston, Saltzman, Marsh, & Buckwalter, 2006; R. C. Lawrence et al., 2008).³ Current surgical techniques for treating focal cartilage defects include osteochondral autograft/allograft transplantation, microfracture, and autologous chondrocyte implantation (ACI). In ACI, autologous chondrocytes are isolated from non-weight-bearing cartilage, expanded in *ex vivo* cultures, and returned to the chondral defect as a cell suspension covered with a periosteal membrane (Brittberg et al., 1994, 1996). More recently, matrix-assisted ACI (MACI) has been developed. In MACI, for which there are now several variations, autologous chondrocytes are seeded within a three-dimensional (3D) scaffold before implantation, potentially enabling better integration with the surrounding native cartilage while also providing a biomimetic microenvironment capable of enhancing cartilage neotissue formation (Freyman et al., 2013; E Kon et al., 2013; Makris et al., 2015). Although both ACI and MACI have shown promise, challenges still persist. Chondrocyte yield from non-weight-bearing cartilage is low, requiring *ex*

³ This chapter contains materials from - Liou, J. J., Rothrauff, B. R., Alexander, P. G., & Tuan, R. S. (2018) Effect of platelet-rich plasma on chondrogenic differentiation of adipose- and bone marrow-derived mesenchymal stem cells. *Tissue Engineering Part A*

vivo cell expansion, with an accompanying loss of the chondrogenic phenotype (Tuan et al., 2013). As a result, the patient must undergo two surgical procedures, and the quality of cartilage repair remains inconsistent. Identification of alternative cell sources and application of improved chondroinductive conditions are needed to overcome these challenges, permitting a single-step procedure with robust cartilage formation.

Adult tissue-derived mesenchymal stem cells (MSCs) are capable of undergoing chondrogenic differentiation and have traditionally been isolated from the iliac crest, an invasive procedure that yields a relatively low percentage of MSCs. Alternatively, adipose tissue contains a higher percentage of MSCs, is abundantly available, and can be harvested through a minimally invasive lipoaspiration procedure (Hildner et al., 2015). However, MSCs derived from adipose tissue, adipose stem cells (ASCs), have been reported as less chondrogenic than MSCs derived from bone marrow (BM-MSCs) (Alegre-Aguarón et al., 2012; Kohli et al., 2015). Recently, the infrapatellar fat pad, readily accessible intra-operatively during arthroscopic and open knee surgeries, was examined as an alternative source of ASCs (IFP-ASCs), which were shown to possess a greater chondrogenic potential than subcutaneous ASCs (SQ-ASCs) (Lopa et al., 2014). Specifically, it was reported that IFP-ASCs were superior to SQ-ASCs in terms of sulfated glycosaminoglycan (GAG) deposition and chondrogenic gene expression, with higher gene expression levels of aggrecan, SOX9, and collagen type II, and lower levels of collagen types X and I. However, the total cell number of IFP-ASCs is more limited compared to SQ-ASCs due to smaller tissue volume. Therefore, *ex vivo* culture expansion of IFP-ASCs would likely be required to obtain a sufficient cell number for implantation.

Alternatively, a strategy that promotes *in situ* proliferation and chondrogenic differentiation of IFP-ASCs could provide a single-step treatment for chondral defects. Platelet-

rich plasma (PRP), derived from whole blood, contains a large number of growth factors, and has been shown to promote stem cell proliferation and neotissue formation in cartilage defects (Xie et al., 2014). *In vivo*, a number of studies have reported pain reduction and improvement of joint function with PRP treatment (Patel et al., 2013), while others have found no improvement in cartilage formation (Brehm et al., 2006; Elizaveta Kon et al., 2010). The effect of PRP on chondrogenic differentiation of MSCs *in vitro* is also equivocal (J. K. Lee, Lee, Han, Seong, & Lee, 2014; Xie et al., 2012), with recent findings suggesting that the effects are dependent on PRP concentration (do Amaral et al., 2015). The purpose of this study was to evaluate the effect of different PRP concentrations and exposure durations on proliferation and *in vitro* chondrogenic differentiation of IFP-ASCs and BM-MSCs when cultured as pellets or within a 3-dimensional (3D) hydrogel biomaterial scaffold.

2.2 Methods

2.2.1 Materials and Reagents

All chemicals and reagents were purchased from Sigma-Aldrich (St. Louis, MO), unless indicated otherwise.

2.2.2 PRP Releasate Preparation

PRP releasate was prepared according to an adapted protocol (J. Zhang & Wang, 2010). Briefly, anticoagulated human whole blood (Central Blood Bank, Pittsburgh, PA) was distributed

into 15 mL conical tubes and centrifuged at 480 x g for 20 minutes. Pelleted red blood cells were discarded and the supernatant (including the buffy coat) was aspirated and concentrated to obtain a platelet concentration of 1×10^6 platelets/ μL . To activate platelets, concentrated CaCl_2 was added to a final concentration of 22.8 mM, followed by incubation at 37 °C overnight. After another centrifugation at 2,000 x g for 10 minutes, the fibrin clot was discarded and the supernatant, referred to as PRP releasate, was stored at -20 °C until future use (**Figure 5**). According to the Platelet Activation White blood cells (PAW) classification system, the PRP releasate prepared here was categorized as P3-X-A α (DeLong, Russell, & Mazzocca, 2012). Before use in experiments, equal volumes of PRP releasate from three donors were pooled.

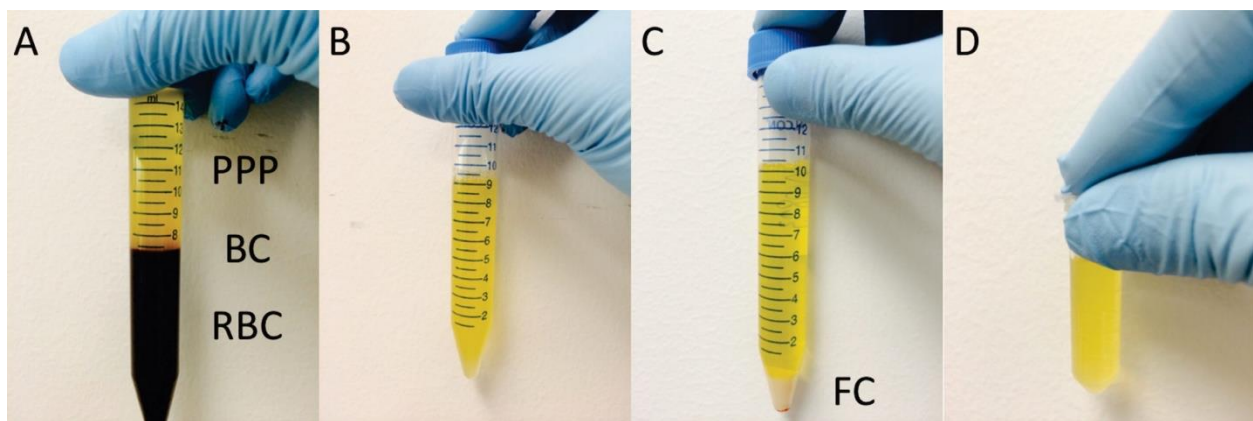


Figure 5. PRP releasate preparation.

(A) Anti-coagulated human whole blood was distributed into 15 mL conical tubes and centrifuged at 480 x g for 20 minutes. (B) The pelleted red blood cells (RBC) were discarded and the supernatant containing platelet-poor plasma (PPP) and buffy coat (BC) was partially aspirated to obtain a platelet concentration of 1×10^6 platelets/ μL . To activate platelets, 22.8 mM calcium chloride was added and incubated at 37 oC overnight. (C) After another centrifugation at 2,000 x g for 10 minutes, the fibrin clots (FC) were discarded. (D) The resulting supernatant was referred to as PRP releasate and frozen for future use.

2.2.3 Cell Isolation

All adult human cells were isolated according to Institutional Review Board (IRB) approved protocols (University of Washington and University of Pittsburgh).

Human IFP-ASCs were isolated from infrapatellar fat pads of three different donors undergoing total knee arthroplasty (48 years old female, 59 years old male, and 65 years old male). The tissue was digested with 1 mg/mL type I collagenase (Worthington Biochemical, Lakewood, NJ) and 1 mg/mL trypsin (Invitrogen, Carlsbad, CA) for 3 hours at 37 °C in an orbital shaker at 150 rpm. Cells were filtered through a 40 µm cell strainer (ThermoFisher, Pittsburgh, PA), pelleted by centrifugation at 1,200 rpm for 5 minutes, and expanded in growth medium (GM: Dulbecco's Modified Eagle's Medium [DMEM; Invitrogen], 10% v/v fetal bovine serum [FBS; Gemini Bio Product, West Sacramento, CA] and 1% v/v antibiotic-antimycotic [Invitrogen]).

Human subcutaneous ASCs (SQ-ASCs) were isolated from lipoaspirate-derived fat tissue of three donors (34 years old male, 38 years old female, and 49 years old female) using an automated cell isolation system (Icellator®, Tissue Genesis, Honolulu, HI). Cells were pelleted by centrifugation and culture-expanded in GM.

Human BM-MSCs were isolated from the bone marrow of three different patients undergoing arthroplasty (65 years old male, 67 years old male, and 68 years old male). Briefly, the trabecular bone marrow was rinsed with Minimum Essential Medium alpha (αMEM; Invitrogen) containing 1% v/v antibiotic-antimycotic and filtered through 40 µm strainers. Cells were pelleted by centrifugation and culture-expanded in GM.

2.2.4 Cell Characterization

The presence of surface markers, including CD31, CD34, CD44, CD45, CD73, CD90, and CD105, in SQ-ASCs and IFP-ASCs was assessed by flow cytometry using appropriate monoclonal antibodies (mouse anti-human antibodies; BD Biosciences, San Jose, CA).

2.2.5 Colony Formation Assay

Colony formation was analyzed by crystal violet staining. Briefly, cells were cultured as monolayers on 10-cm Petri dishes (ThermoFisher, Pittsburgh, PA) at a seeding density of 100 cells per dish in GM for 14 days. On day 14, monolayer cultures were stained with 0.5% crystal violet (Sigma-Aldrich) in 100% methanol (ThermoFisher) for 10 minutes prior to imaging.

2.2.6 Differentiation Assay

Monolayer Cultures Tri-lineage differentiation of SQ-ASCs and IFP-ASCs was analyzed via monolayer culture in, respectively: (1) *chondrogenic medium* (DMEM, 1% v/v antibiotic-antimycotic, 1x insulin-transferrin-selenium [ITS; ThermoFisher #41400045], 0.1 μ M dexamethasone, 40 μ g/mL proline, 50 μ g/mL ascorbic acid, and 10 ng/mL recombinant human transforming growth factor- β 3 [PeproTech #100-36E, Rocky Hill, NJ]; (2) *osteogenic medium* (DMEM, 10% v/v FBS, 1% v/v antibiotic-antimycotic, 0.1 μ M dexamethasone, 10 mM β -glycerophosphate, and 50 μ g/mL ascorbic acid); and (3) *adipogenic medium* (DMEM, 10% v/v FBS, 1% v/v antibiotic-antimycotic, 1x ITS, 1 μ M dexamethasone, and 0.5 mM 3-isobutyl-1-methylxanthine [IBMX]). On day 21, the cultures were stained with Alcian Blue, Alizarin Red,

and Oil Red O, using standard histological staining protocols, to assess chondrogenesis, osteogenesis, and adipogenesis, respectively.

High Density Pellet Culture Chondrogenesis was also examined under conditions that mimic mesenchymal condensation during developmental cartilage formation as high-density pellet cultures. 2.5×10^5 IFP-ASCs or BM-MSCs were pelleted by centrifugation, and then maintained in serum-free chondrogenic medium. The effect of PRP on chondrogenesis was measured by varying PRP concentration or exposure duration as follows: (1) pellets were cultured for 21 days in chondrogenic medium, which was supplemented with 10% v/v PRP releasate for the initial 0, 1, 3, 7, or 21 days (referred to as 1-, 3-, 7, or 21-day pulse, respectively); and (2) pellets were cultured for 21 days in chondrogenic medium, which was supplemented with PRP releasate at 0, 1, 5, 10, or 20% v/v for the first 24 hours. The 24-hour exposure to PRP was intended to mimic the transient bolus of growth factors provided by a single intraarticular injection of PRP, as commonly employed in clinical practice (Campbell et al., 2015). Culture medium was regularly changed three times a week, except for medium changes dictated by a particular PRP exposure duration indicated above.

2.2.7 Three-Dimensional Hydrogel Culture

We next examined the effect of PRP on MSC chondrogenesis in a 3D context more relevant to the translational application of MSCs in cartilage repair-based cartilage repair. MSCs were encapsulated in photocrosslinkable hydrogels previously shown to support robust chondrogenesis (H. Lin, Cheng, Alexander, Beck, & Tuan, 2014). Visible-light-activated methacrylated gelatin (mGL)/methacrylated hyaluronic acid (mHA) hydrogels were fabricated as described previously (H. Lin, Lozito, Alexander, Gottardi, & Tuan, 2014). Briefly, 15 g of gelatin (Sigma-Aldrich) was

dissolved in 500 mL H₂O at 37°C, and 15 mL of methacrylic anhydride (Sigma-Aldrich) was added dropwise. The mixture was incubated with shaking at 150 rpm for 24 hours, then dialyzed against water for 4 days, and mGL lyophilized for storage. The photoinitiator, lithium phenyl-2,4,6-trimethylbenzoylphosphinate (LAP), was prepared as described by Fairbanks et al. (Fairbanks, Schwartz, Bowman, & Anseth, 2009). For mHA, 5 gram of sodium hyaluronate (66 kDa, Lifecore Biomedical, Chaska, MN) was dissolved in 500 mL H₂O at 37°C, and 15 mL of methacrylic anhydride was added dropwise. At the end of every hour in the first 5 hours, pH was adjusted to 7. The mixture was then incubated with shaking at 150 rpm for 24 hours, dialyzed against water for 4 days, and lyophilized for storage. For hydrogel fabrication, mGL and mHA were dissolved in Hank's Balanced Salt Solution (HBSS) at final concentrations of 9% and 1% (w/v), respectively. After adjustment of pH to 7.4 with 10 N NaOH, 1% antibiotic-antimycotic and 0.15% w/v LAP were added. IFP-ASC or BM-MSC pellets were resuspended in mGL/mHA solution at a final concentration of 15×10^6 cells/mL, and 50 μ L of the suspension was transferred to a cylindrical mold measuring 5 mm diameter by 2 mm depth. The cell/monomer mixture was subjected to photoillumination (395 nm) for 90 seconds, forming a cell encapsulated mGL/mHA hydrogel. Constructs were cultured in Phenol Red-free chondrogenic medium supplemented with different PRP releasate concentrations (0, 1, 5, 10, and 20% v/v) for 21 days. Culture medium was changed twice a week.

2.2.8 Gene Expression Analysis

Both pellet and hydrogel cultures were collected on day 21, homogenized in Qiazol (Qiagen, Hilden, Germany), and total RNA isolated with RNeasy Plus Mini Kit (Qiagen). Gene expression levels of chondrogenesis markers (collagen type II, COL2; aggrecan, ACAN) and

hypertrophy markers (collagen type X, COL10; matrix metalloproteinase 13, MMP13) were assessed by real-time RT-PCR and normalized to that of 18S ribosomal RNA (gene primers sequences shown in Table S2). Relative fold changes in mRNA levels were calculated using the $\Delta\Delta\text{Ct}$ method.

2.2.9 Histological Analysis

Pellets and hydrogels collected on culture day 21 were fixed with 4% phosphate-buffered paraformaldehyde, dehydrated, and embedded in paraffin. Histological sections (8 μm) were stained with Safranin O/Fast Green and Alcian Blue/Nuclear Fast Red for sulfated GAG. For collagen type II immunohistochemistry, deparaffinized sections were washed with 0.02% bovine serum albumin and incubated with 0.1 U/mL chondroitinase ABC and 250 U/mL hyaluronidase for antigen retrieval, followed by blocking with 3% H_2O_2 in 1% horse serum. Sections were then incubated with rabbit anti-human collagen type II (Abcam #ab34712, Cambridge, UK) at 4 °C overnight, and then with biotinylated anti-rabbit secondary antibody. Immunolabeling was detected using the Vector ABC reagent (Vector, Burlingame, CA) and visualized with VIP Kit (Vector), with hematoxylin QS (Vector) as the counter-stain.

2.2.10 Biochemical Analysis

Pellet cultures were digested overnight at 65 °C in a digestion buffer (pH 6.0) containing 2% (v/v) of a commercially available papain solution (v/v, from Papaya latex, Sigma-Aldrich, containing 15-30 mg protein/ml with ≥ 16 units/mg), 0.1 M sodium acetate, 10 mM cysteine HCl, and 50 mM EDTA. Sulfated GAG content was measured with the Blyscan GAG Assay (BioColor,

Carrickfergus, UK) according to the manufacturer's instructions, with chondroitin sulfate as a standard. GAG content was normalized to DNA content determined with PicoGreen Assay (Invitrogen).

2.2.11 Statistical Analysis

Values of gene expression levels, GAG contents, and DNA contents are shown as mean \pm standard deviation. Three to six independent trials were performed for each experiment. Statistical difference from control (No PRP group) was analyzed by one-way ANOVA and Dunnett's multiple comparisons using GraphPad Prism 7 (GraphPad Software Inc, CA), with significance at $p \leq 0.05$.

2.3 Results

2.3.1 Comparison of IFP-ASCs and SQ-ASCs

In this study, ASCs obtained from both the infrapatellar fat pad (IFP-ASCs) and subcutaneous lipoaspirate (SQ-ASCs) were used. Both cell populations were confirmed by flow cytometry to exhibit MSC-associated surface markers. Positive expression of cell surface markers typical of adult MSCs, such as those derived from bone marrow (BM-MSCs), including CD44, CD73, CD90, and CD105, was detected, with negligible expression of epithelial and hematopoietic markers, including CD31, CD34, and CD45 (**Figure 6A**). In addition, IFP-ASCs and SQ-ASCs were both able to form colonies and differentiate into adipogenic, osteogenic, and chondrogenic

lineages (representative images shown for IFP-ASCs in **Figure 6B**). The chondrogenic capacity of ASCs isolated from the infrapatellar fat pad (IFP-ASCs) and subcutaneous lipoaspirate (SQ-ASCs) was next compared. Pellet cultures consisting of 2.5×10^5 IFP-ASCs or 2.5×10^5 SQ-ASCs each were maintained in chondrogenic medium. At culture day 21, the RT-PCR analysis showed that gene expression level of SOX9 and COL2 was significantly higher in the IFP-ASC pellets than in the SQ-ASCs pellets (**Figure 7**). Taken together, these results indicate the preferred chondrogenic ability of IFP-ASCs over SQ-ASCs, and their relevance as a candidate cell type for cell-based cartilage repair therapy.

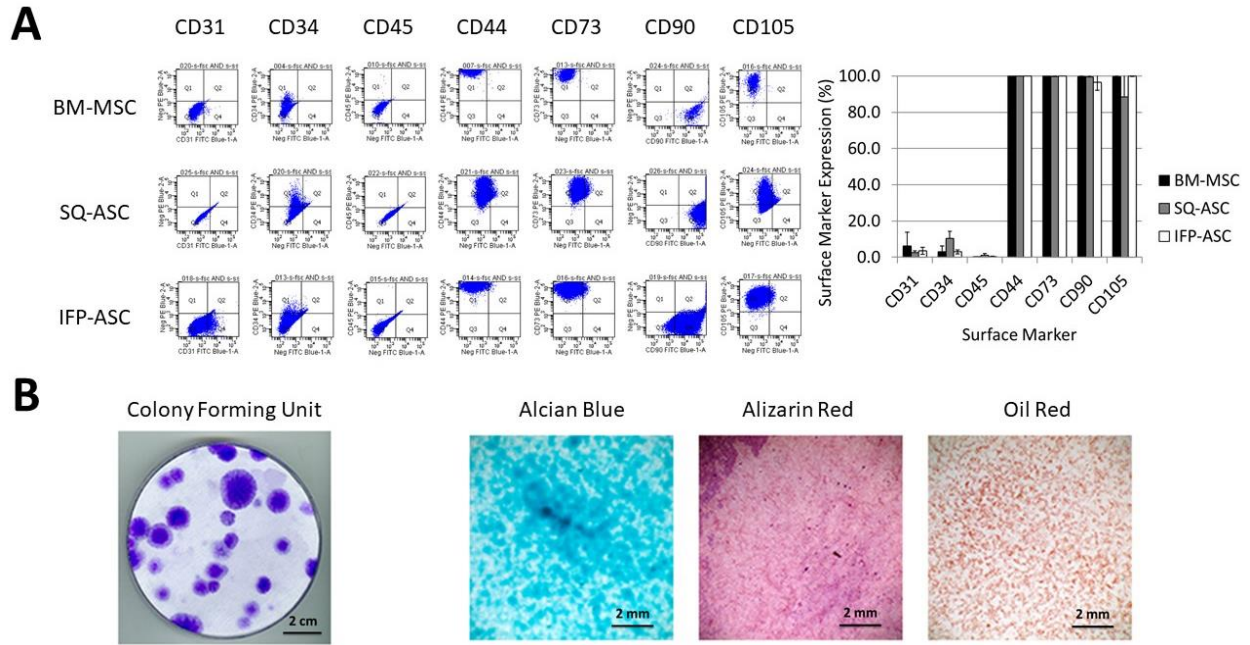


Figure 6. Characteristics of monolayer cultured IFP-ASCs.

(A) Surface marker profile. High mesenchymal stem cell characteristics of IFP-ASCs, similar to BM-MSCs and SQ-ASCs, is indicated by high expression of CD44, CD73, CD90, and CD105, and negligible expression of CD31, CD34, and CD45. (B) Colony formation ability and tri-lineage multipotent differentiation of IFP-ASCs.

Colony formation was detected by Crystal Violet staining (bar = 2 cm), and monolayer cultures of IFP-ASCs undergoing chondrogenesis, osteogenesis, and adipogenesis were assessed histologically by Alcian blue, Alizarin Red, and Oil Red O staining (bar = 2 mm).

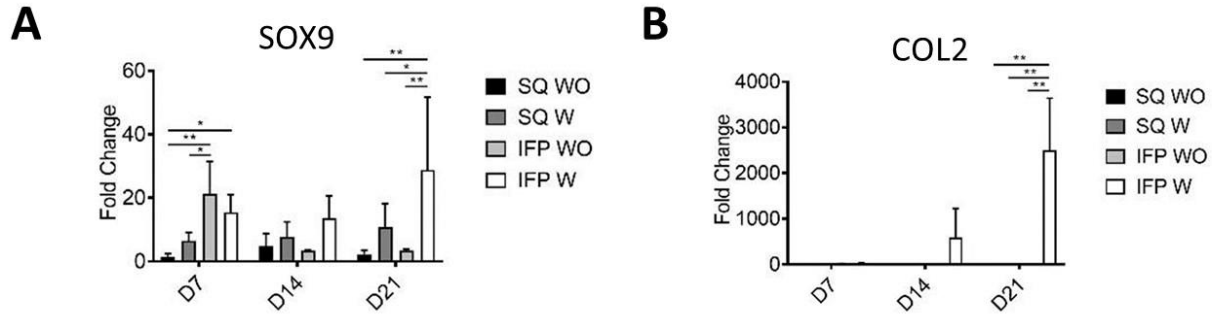


Figure 7. Comparison of IFP-ASCs and SQ-ASCs.

(A) SOX9 gene expression of IFP-ASCs treated with TGF β 3 shows higher expression level when compared to SQ-ASCs with or without TGF β 3 at day 21. At day 7, IFP-ASCs are significantly superior to SQ-ASCs. (B) COL2 gene expression of IFP-ASCs shows higher expression level when compared to SQ-ASCs at day

21. *, $p < 0.05$

2.3.2 Effect of PRP on chondrogenic differentiation in pellet culture

Gross histological observation revealed that the overall influence of PRP exposure was the inhibition of cartilage matrix deposition in IFP-ASC pellet cultures, as shown in Figures S2 and S3. Specifically, increasing PRP concentrations or duration individually, as well as additively, reduced chondrogenesis. To examine the specific effects of PRP, we profiled gene expression, analyzed the biochemical composition, and carried out histological and immunohistochemical examination of pellet cultures during the process of IFP-ASC chondrogenesis, as a function of PRP concentration and treatment duration.

Varying duration of PRP treatment Pellet cultures of BM-MSCs and IFP-ASCs maintained in chondrogenic medium were supplemented with 10% v/v PRP releasate for varying time periods during the 21-day culture. As shown in Figure 2, the magnitude of the PRP effect, i.e., inhibition of chondrogenesis, depending on the duration of treatment. Increasing the duration of PRP

exposure resulted in decreased expression of COL2, ACAN, and COL10, with negligible effects on MMP13 expression, in IFP-ASCs (**Figure 8A**). Varying duration of PRP treatment did not affect cell number, on the basis of dsDNA content, in either IFP-ASC or BM-MSC pellets; however, increasing PRP treatment time resulted in decreasing GAG/DNA content in IFP-ASCs, but not in BM-MSCs (**Figures 8B, 9A**). This effect was supported by histological staining, as increasing duration of PRP supplementation led to decreasing deposition of cartilage-specific extracellular matrix in IFP-ASC pellets, including sulfated GAG and collagen type II (Figure 2C). As a result, the size of the pellet decreased as PRP concentration or treatment duration increased. In BM-MSC pellets, some decrease in cartilage extracellular matrix production was also observed, although the inhibitory effect of PRP was not as strong (**Figure 9B**).

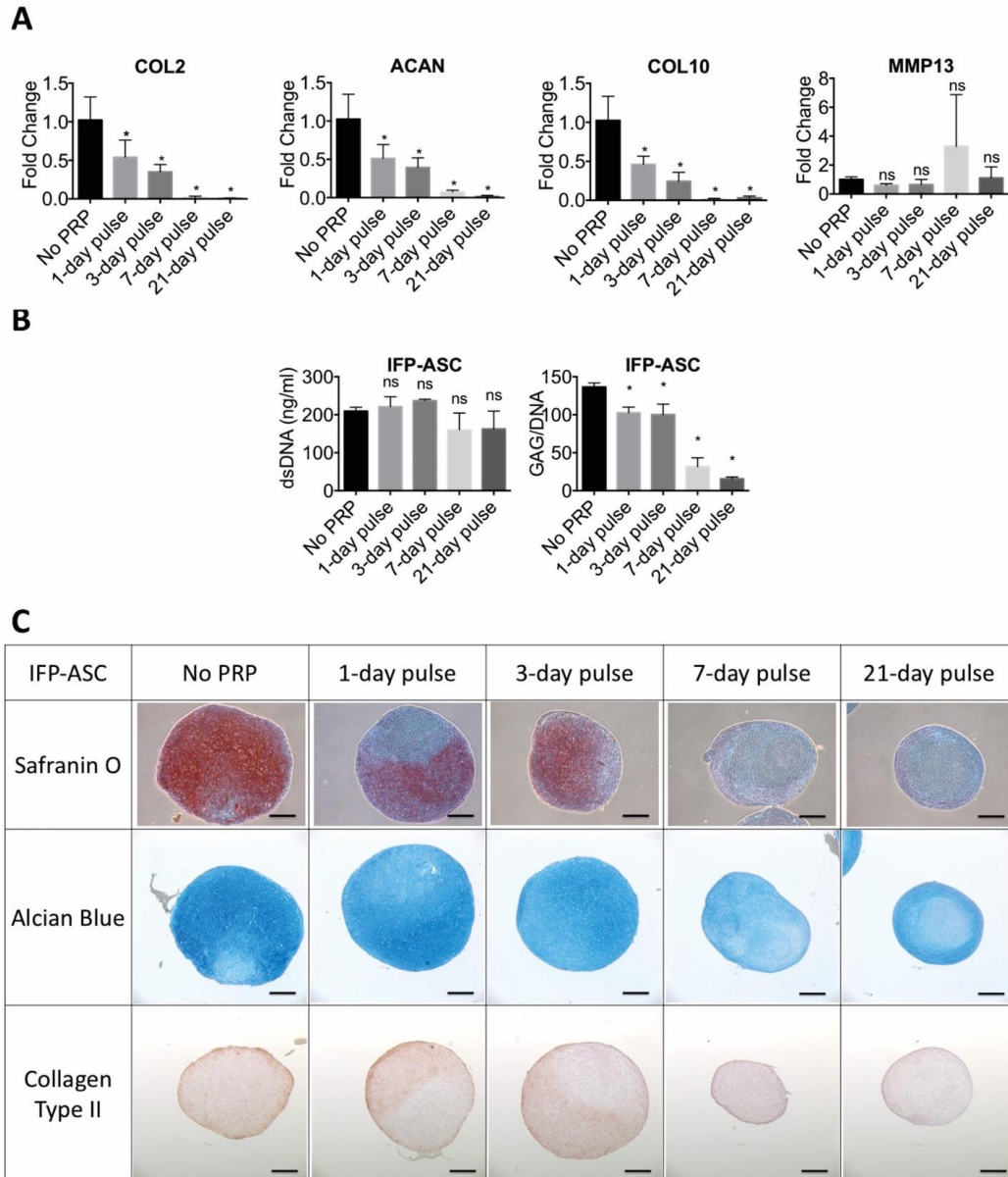


Figure 8. Effect of treatment with 10% PRP for varying durations on IFP-ASC pellet cultures.

(A) Gene expression of IFP-ASCs in 21-day pellet culture. RT-PCR analysis showed longer exposure to PRP resulted in higher reduction of expression of collagen type II, aggrecan, and collagen type X, while expression of MMP13 was unchanged. (B) DNA and GAG content of IFP-ASCs in 21-day pellet culture. No change in DNA content was seen in the various treatment groups, while normalized GAG content decreased with longer exposure to PRP releasate. *, $p < 0.05$; ns, not significant. (C) Histology of IFP-ASCs in 21-day pellet culture. Longer PRP exposure time resulted in higher reduction in matrix proteoglycan histological staining, as well as reduced collagen type II content detected by immunohistochemistry. Bar = 400 μm .

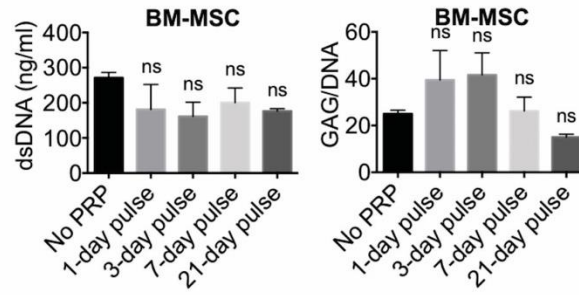
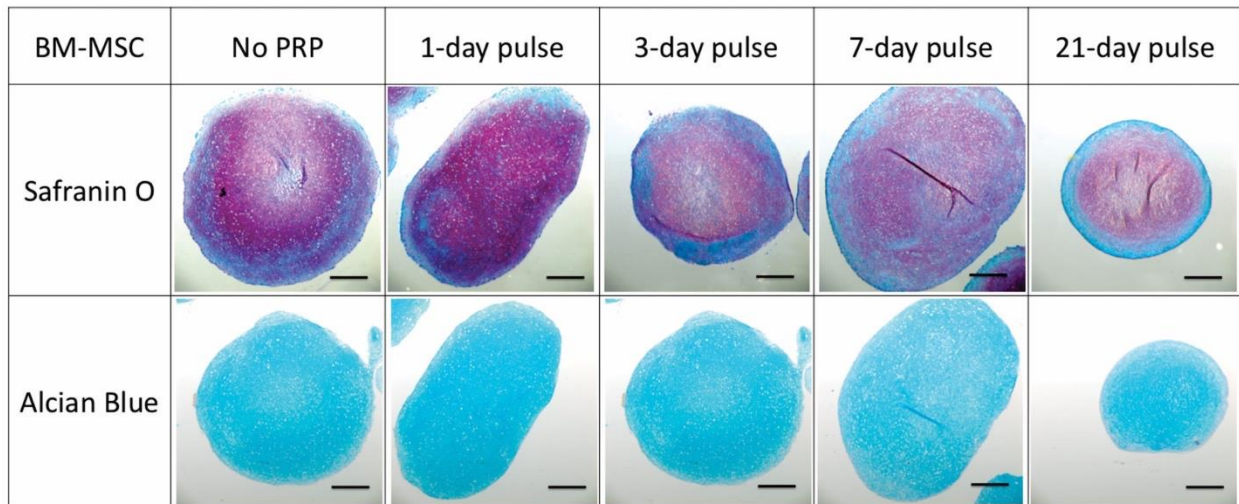
A**B**

Figure 9. Effect of treatment with 10% PRP for varying durations on BM-MSC pellet cultures.

(A) DNA and GAG content of BM-MSC in 21-day pellet culture. No difference in DNA and normalized GAG contents was seen in the various treatment groups. *, $p < 0.05$; ns, not significant. (B) Histology of BM-MSCs in 21-day pellet culture. No difference was seen in histological staining of matrix proteoglycan or immunohistochemically detected collagen type II was observed. Bar = 400 μm .

Varying PRP concentration For this study, transient PRP exposure, as in clinical intra-articular injections (Campbell et al., 2015), was simulated by exposing pellet cultures to PRP releasate supplementation only for the first 24 hours of the 21-day culture period. In IFP-ASC pellets, gene expression profile remained relatively unchanged among the treatment groups exposed to different PRP concentrations (**Figure 10A**), except that at low, 1% PRP, increased

cartilage matrix production and collagen type II deposition was seen, compared to cultures treated with higher PRP concentrations (**Figure 10B**). [Note: The first panel (No PRP) and the fourth panel (10% PRP, 1-day pulse) are repeated from Figure 2C.] In BM-MSC cultures, gene expression of COL2, ACAN, and MMP13 remained unchanged upon treatment with different PRP concentrations for 1 day; however, the hypertrophy associated gene, COL10, was significantly upregulated upon treatment with 20% PRP (**Figure 11A**). Matrix sulfated GAG staining with Safranin O and Alcian Blue appeared similar in the various groups, except for 20% PRP, which showed slightly reduced staining intensity (**Figure 11B**). **Figure 12** and **Figure 13** summarize the Safranin O and Alcian Blue staining of IFP-ASC pellets with different PRP concentrations for varying duration.

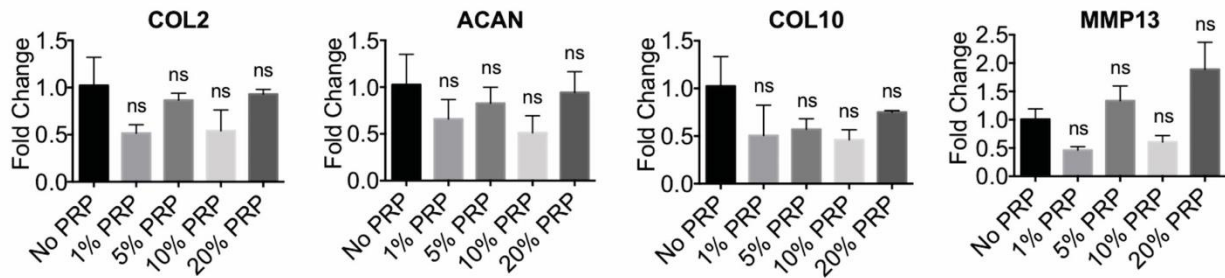
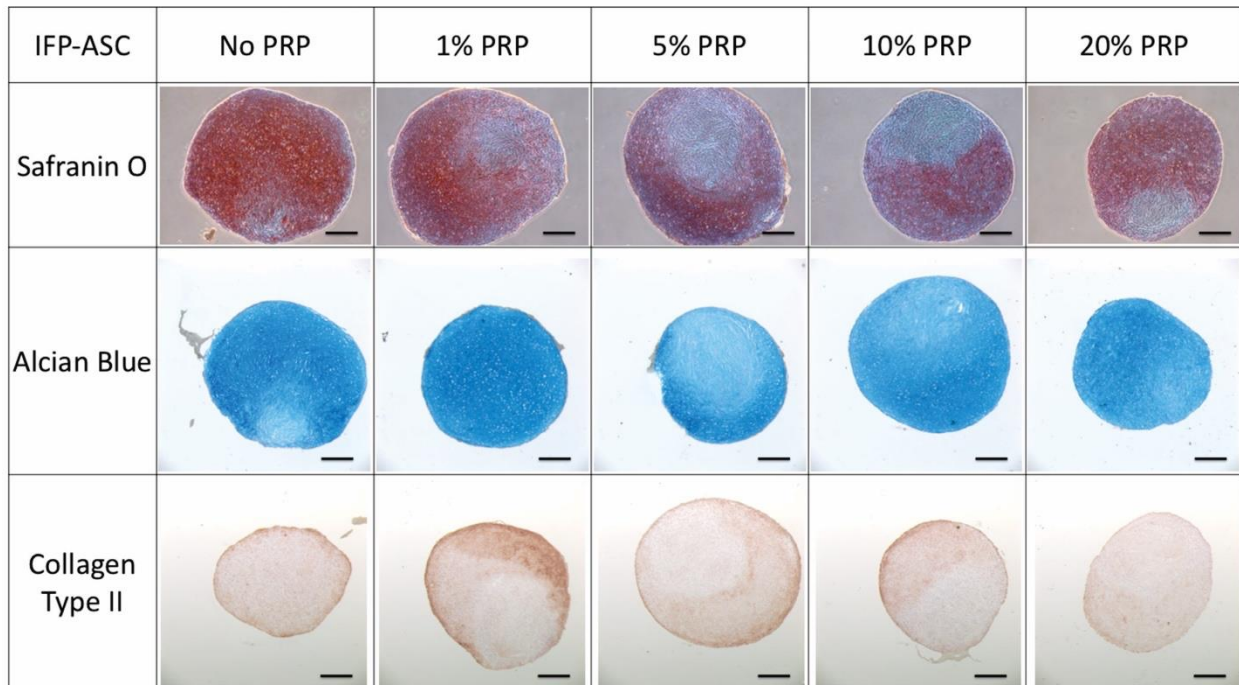
A**B**

Figure 10. Effect of 1-day pulse PRP at varying concentrations on IFP-ASC pellet cultures.

(A) Gene expression profile. No significant difference in gene expression profile was observed in the different PRP treatment groups. *, $p < 0.05$; ns, not significant. (B) Histological analysis. PRP treatment at low concentration (1% PRP) and for short duration (1-day pulse) preserved matrix proteoglycan and collagen type II deposition. Bar = 400 μm .

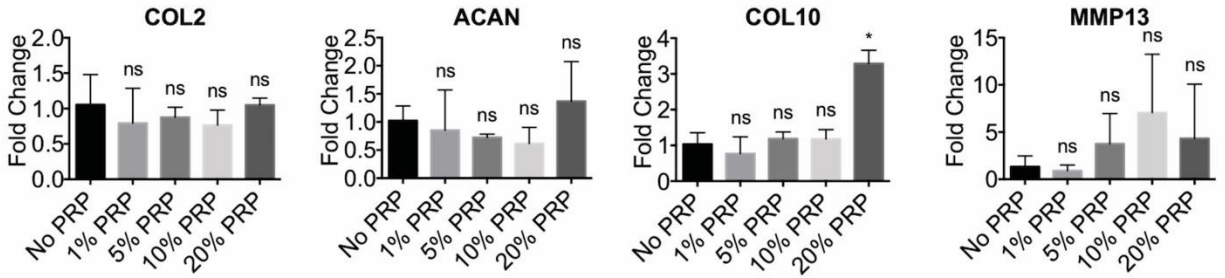
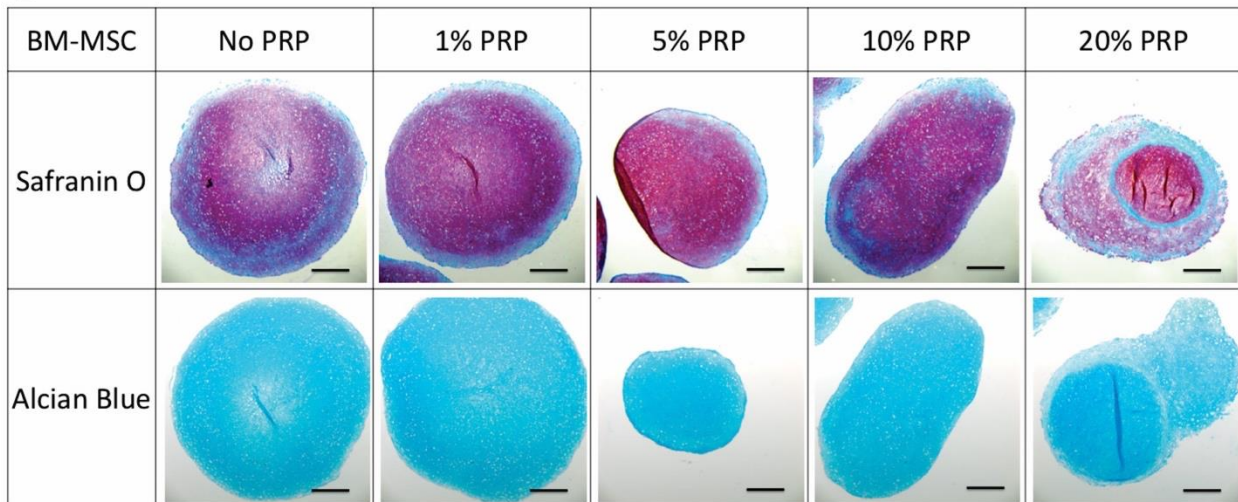
A**B**

Figure 11. Effect of 1-day pulse PRP at varying concentrations on BM-MSC pellet cultures.

(A) Gene expression profile. Gene expression was largely unchanged in the different PRP treatment groups, except for the upregulation of collagen type X in the 20% PRP treatment group. *, $p < 0.05$; ns, not significant. (B) Histological analysis. No difference was observed in proteoglycan deposition and collagen type II production. Bar = 400 μm.

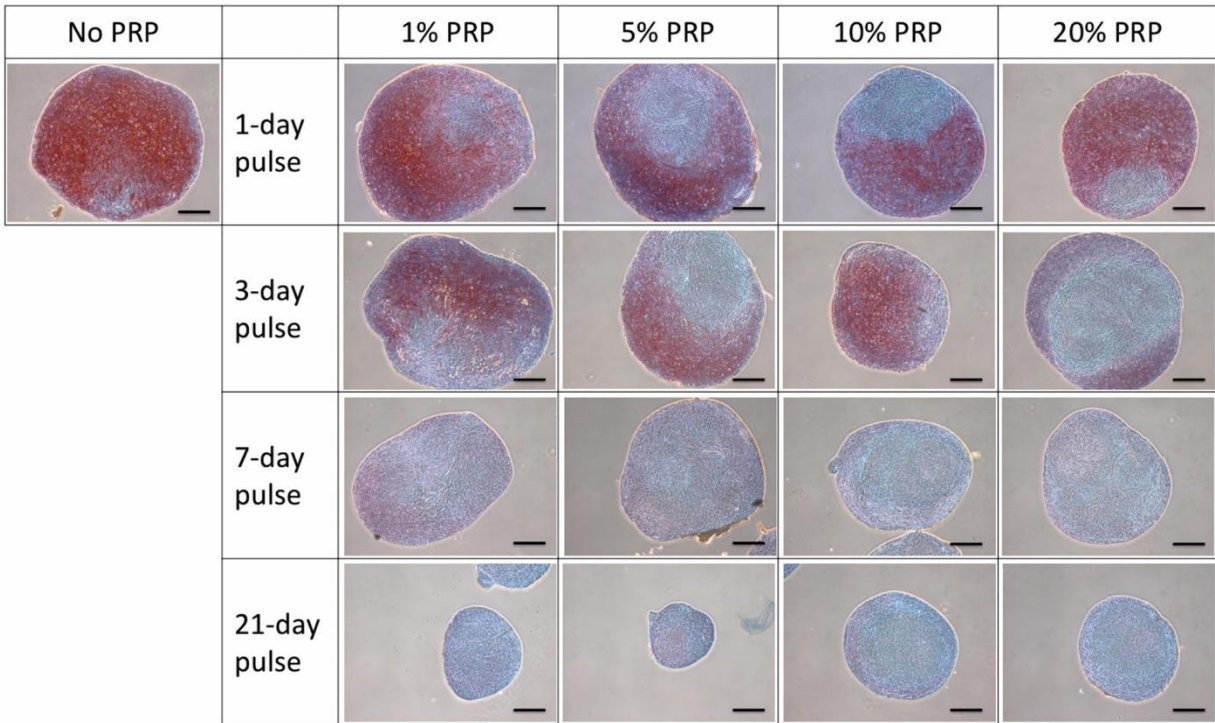


Figure 12. Safranin O staining of IFP-ASC pellet cultures.

As PRP concentration or duration decreases, proteoglycan deposition increases. Bar = 400 μ m.

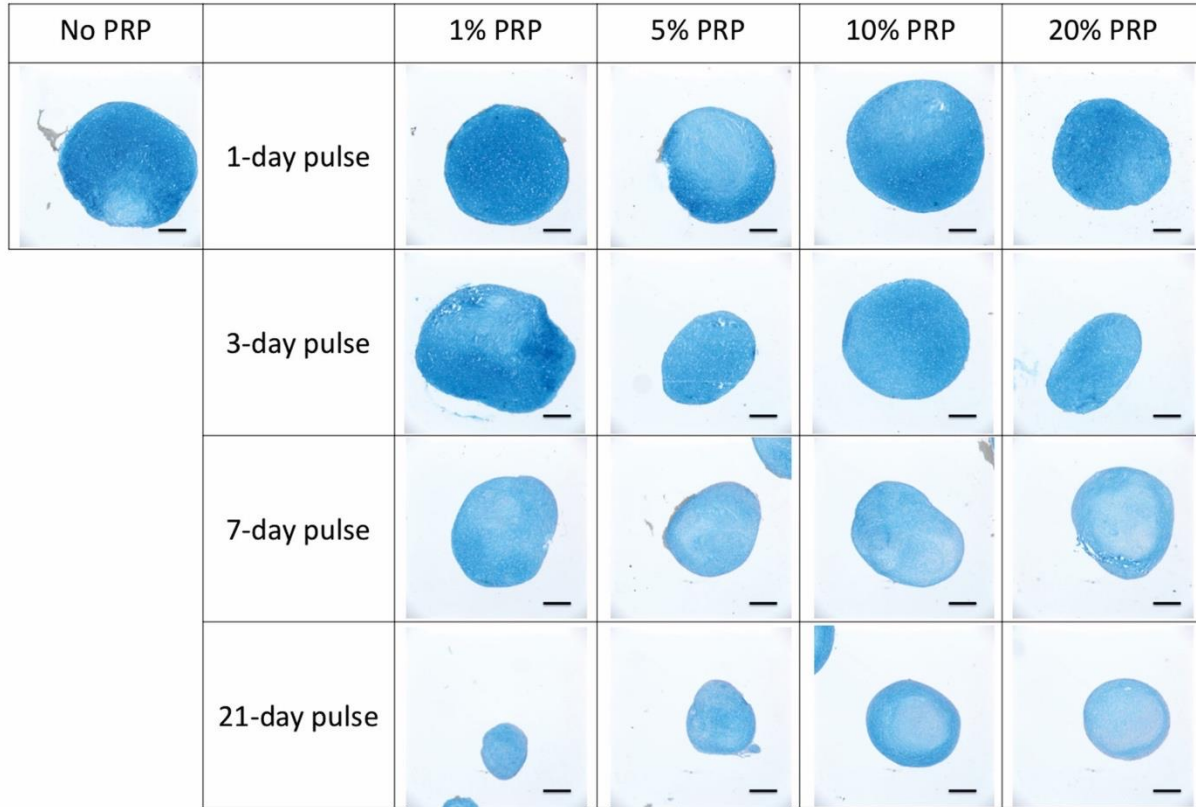


Figure 13. Alcian blue staining of IFP-ASC pellet cultures.

As PRP concentration or duration decreases, proteoglycan deposition increases. Bar = 400 μ m.

2.3.3 Effect of PRP on chondrogenic differentiation in hydrogel culture

Given the preferred practice of encapsulating MSCs in 3D scaffolds for cartilage tissue engineering and repair, we next examined the effect of PRP exposure on chondrogenesis of MSCs in a 3D context, specifically by seeding cells in a photocrosslinkable hydrogel. IFP-ASCs were encapsulated in mGL/mHA hydrogels and cultured for 21 days in chondrogenic medium, with PRP supplementation at different concentrations. Our results showed that, with increasing PRP concentrations, the relative expression of COL2, ACAN, COL10, and MMP13 was reduced (**Figure 14A**). In comparison, BM-MSCs in hydrogel cultures showed significant reduction only

in COL2 and ACAN gene expression (**Figure 15A**). Alcian blue histological staining showed that PRP treatment inhibited pericellular GAG deposition (**Figures 14B, 15B**).

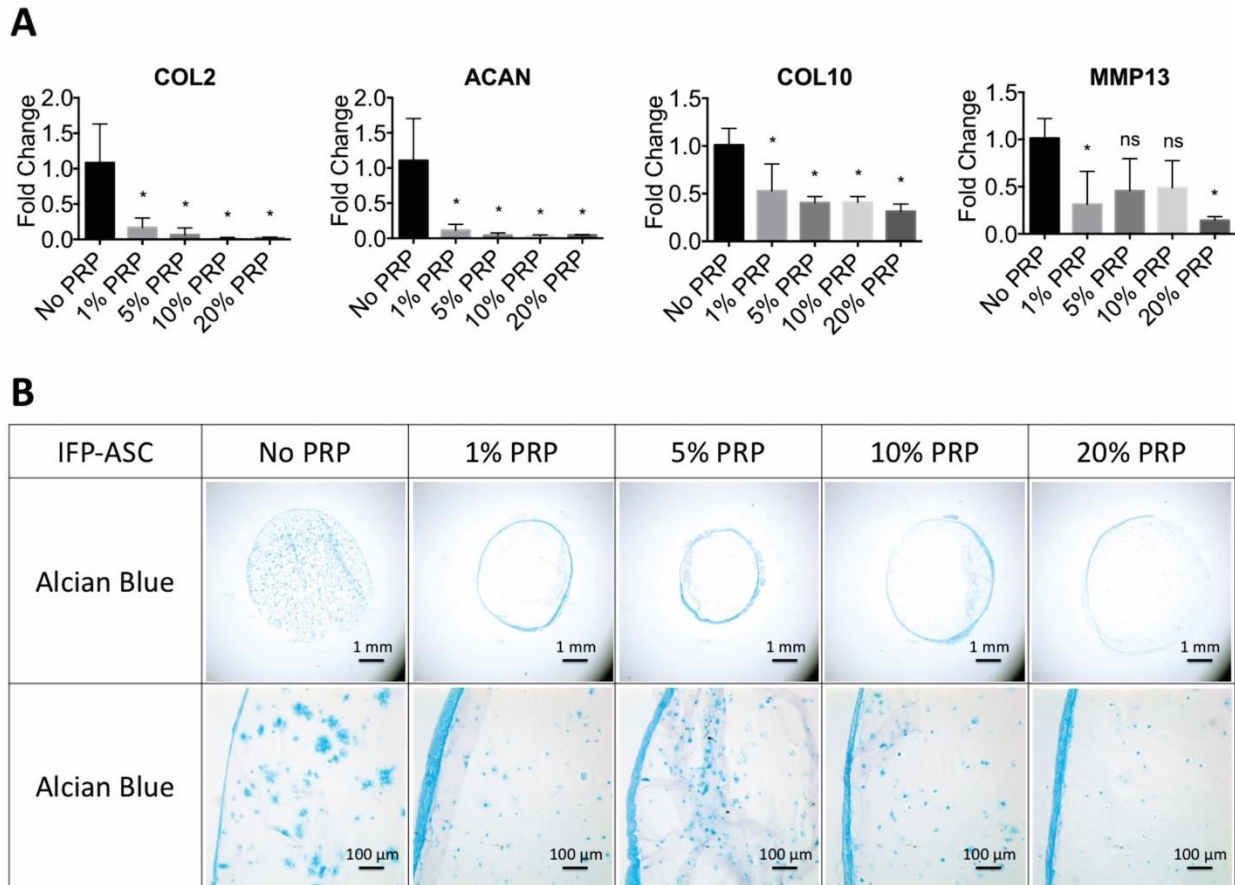


Figure 14. Effect of 21-day PRP at varying concentrations on IFP-ASC hydrogel cultures.

(A) Gene expression profile. Similar to pellet cultures, PRP treatment downregulated the expression of collagen type II, aggrecan, and collagen type X, while expression of MMP13 remained the same. *, $p < 0.05$; ns, not significant. (B) Histological analysis. Cartilage matrix deposition decreased with increasing PRP concentration. Bar = 1 mm & 100 μm .

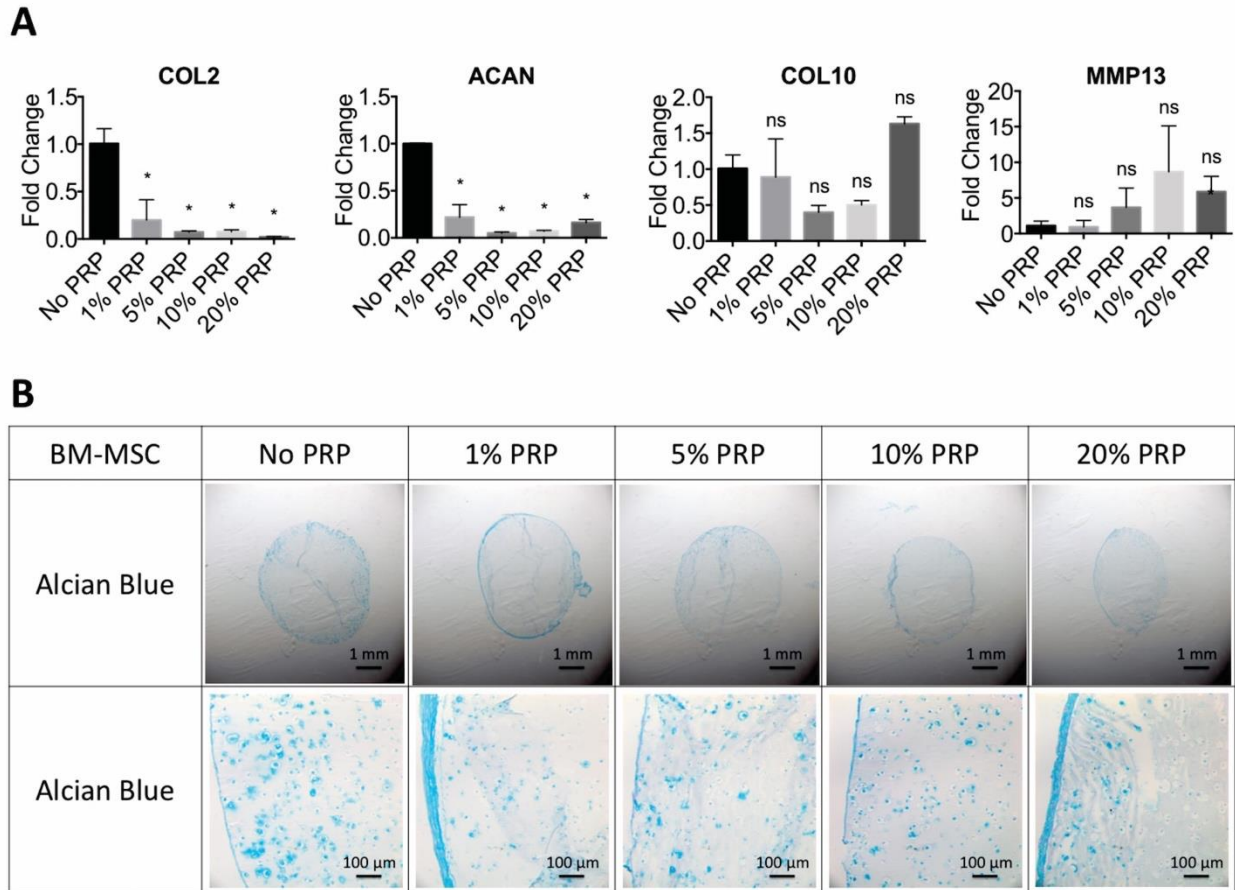


Figure 15. Effect of 21-day PRP at varying concentrations on BM-MSC hydrogel cultures.

(A) Gene expression. Like pellet cultures, PRP treatment downregulated the expression of collagen type II and aggrecan, while expression of collagen type X and MMP13 remained the same. *, $p < 0.05$; ns, not significant.

(B) Histological analysis. No difference in proteoglycan deposition and collagen type II production was observed.

Bar = 1 mm & 100 μm .

2.4 Discussion

PRP has received considerable recent attention as a potential therapeutic agent for tissue repair, including joint tissues; however, whether PRP enhances the formation of hyaline cartilage remains controversial. While some studies have reported pain reduction and improvement of joint

function with PRP treatment (Patel et al., 2013), others have reported no improvement of cartilage repair in *in vivo* models (Brehm et al., 2006; G. Filardo et al., 2015; Giuseppe Filardo et al., 2012; Elizaveta Kon et al., 2010; Xie et al., 2014). In this study, our results clearly showed that PRP did not enhance chondrogenesis of IFP-ASC and BM-MSc *in vitro*.

For adult stem cell therapy, BM-MSc is considered the gold-standard candidate cell type, by virtue of the large body of information currently available on its biological activities and responses (Haleem et al., 2010; Milano et al., 2010; Xie et al., 2012). However, the biological benefits of PRP treatment on BM-MSc, for the purpose of tissue repair and regeneration, are not well understood and remain controversial. For example, Haleem et al. reported a case study that all patients showed improvement 12 months after treatment of autologous BM-MScs along with fibrin-containing PRP (Haleem et al., 2010). However, the advantage of PRP treatment was not observed in a porcine model. Betsch et al. reported that PRP alone or BM-MSc alone significantly improved healing of osteochondral defects 26-week after surgery, but the combination of PRP and BM-MScs did not further enhance wound healing (Betsch et al., 2013). In studying the efficacy of combining PRP and BM-MSc, do Amaral et al. reported that higher concentration of PRP actually impaired chondrogenesis of BM-MSc in pellet cultures (do Amaral et al., 2015).

In this study, we investigated the effect of PRP on BM-MSc in both pellet and 3D hydrogel cultures, the latter to better recapitulate the microenvironment of MSCs encapsulated in 3D biomaterial scaffolds for clinical tissue repair applications. In both types of cultures, treatment dose and durations were varied to assess biologically optimal conditions. At 10% PRP, which approximates PRP concentrations used for intra-articular injections (Pourcho, Smith, Wisniewski, & Sellon, 2014), varying treatment durations (from 1-day pulse to 21-day pulse continuous treatment) did not yield significantly different results in pellet cultures, although PRP treatment

for the first 24 or 72 hours seemed to enhance GAG deposition. In hydrogel cultures, PRP treatment highly downregulated the expression of collagen type II and aggrecan, confirming that PRP does not enhance chondrogenesis in BM-MSC. While some studies have reported that PRP promoted cell proliferation of BM-MSCs (Mishra et al., 2009), we did not observe any PRP-mediated increase in DNA content in any group. In support, Krüger et al. also reported similar findings, namely that PRP co-treatment down-regulated gene expression of aggrecan and collagen type II in TGF β 3-treated pellet cultures of subchondral bone progenitor cells (Krüger et al., 2012).

IFP-ASCs, on the other hand, have not been extensively investigated in terms of their chondrogenic activity. Given the easy access to the IFP, for example via arthroscopic procedures, IFP-ASCs would present a more readily available cell source than BM-MSCs for point-of-care applications. We have therefore performed detailed characterization of the IFP-ASCs, in comparison to BM-MSCs. Our results showed that adipose tissue-derived stem cells expressed high levels of surface epitopes commonly detected in BM-MSCs, including CD44, CD73, CD90, and CD105, with negligible expression of surface markers for epithelial and hematopoietic cells, such as CD31, CD34, and CD45, consistent with reported findings (Amable, Teixeira, Carias, Granjeiro, & Borojevic, 2014; Lopa et al., 2014). Interestingly, we also observed that IFP-ASCs performed better regarding chondrogenesis than SQ-ASCs (Lopa et al., 2014; Pires de Carvalho et al., 2014).

The chondrogenic activity of IFP-ASCs maintained in 3D biomaterial scaffolds has been studied, and cell proliferation and cartilage matrix deposition have been reported for cultures in fibrin, agarose, collagen-hyaluronic acid, and polylactic acid hydrogel *in vitro* (Ahearne, Buckley, & Kelly, 2011; Ahearne, Liu, & Kelly, 2014; Almeida et al., 2014; Y. Liu, Buckley, Almeida, Mulhall, & Kelly, 2014; Luo, Thorpe, Buckley, & Kelly, 2015). At present, only one study has

investigated the combination of IFP-ASCs and PRP. In this Level IV case study, 18 osteoarthritis patients were treated with autologous IFP-ASC and 3 mL of PRP as scaffold via intra-articular injections (Koh et al., 2013). Two-year follow-up showed promising results including pain reduction and joint function restoration. However, in contrast to the potential therapeutic effects reported by these authors, our *in vitro* analysis of the effects of PRP exposure on IFP-ASCs showed that PRP impairs chondrogenesis of IFP-ASC in both pellet and 3D hydrogel cultures. These contrasting findings merit some discussion regarding the potential biological benefits of using PRP to treat joint cartilage related pathologies.

A major complication in assessing the clinical benefit of PRP is the high variability of PRP preparations and the different tissue or disease targets. PRP preparation generally involves a two-step centrifugation: the first step fractionates platelet-poor plasma, buffy coat, and red blood cells; and the second step generates either leukocyte-containing PRP or pure PRP depending on which portion is taken (Dohan Ehrenfest, Rasmusson, & Albrektsson, 2009). In our preparation, we collected both the buffy coat and platelet-poor plasma, resulting in leukocyte-containing PRP, a practice that is used in the majority of clinical practices. In view of these variabilities in PRP preparation, we propose that the following parameters and caveats must be taken into account in considering the efficacy of PRP treatment.

(a) PRP concentration and duration. Our results strongly suggest that PRP, when applied for cartilage-related treatments, must be used at low concentration and for short duration. Results from do Amaral et al. also showed that 2.5% PRP was better than 10% PRP applied in a collagen/hyaluronic acid scaffold *in vitro* (do Amaral et al., 2015). Other studies have also suggested that higher PRP concentration was not better for chondrogenesis (Gaissmaier et al., 2005; Spreafico et al., 2009; S. Y. Yang et al., 2000). Regarding the duration of PRP treatment,

Park et al. reported a continuous increase of bone morphogenetic protein 7 (BMP-7) and vascular endothelial growth factor (VEGF), both involved in bone remodeling, in rabbit chondrocyte cultures exposed to continuous presence of PRP for 10 days (Park, Lee, Kim, Ahn, & Do, 2011). Taken together with our findings reported here, longer duration of PRP treatment very likely will lead to hypertrophy and bone formation.

(b) Platelet number. In our study, we re-suspended platelets at 1.0×10^6 platelets/ μL before calcium activation. Based on the PAW (Platelet, Activation, White Cell) Classification System, our PRP releasate is categorized as P3 ($0.75\sim 1.25 \times 10^6$ platelets/ μL) (DeLong et al., 2012). Of relevance, a recent study showed that higher platelet number (5-fold to whole blood) diminished pro-collagen expression in anterior cruciate ligament fibroblasts (Yoshida, Cheng, & Murray, 2014). Taken together, these findings suggest higher platelet number is not necessarily higher performing for chondrogenesis.

(c) Platelet activation. In our PRP preparation, exogenous calcium chloride was added for platelet activation, since it has been shown to be more effective and inexpensive than bovine thrombin (Textor & Tablin, 2012). Calcium reacts with fibrinogen and forms fibrin clots which are typically removed, resulting in PRP releasate. Dohan Ehrenfest et al. summarized current protocols for pure PRP, leukocyte-rich PRP, pure platelet-rich fibrin, and leukocyte-rich PRF based on the speed and time of centrifugation and portion collected after centrifugation (Dohan Ehrenfest et al., 2009); however, a direct comparison between the four preparations in terms of cartilage repair was not performed. In the operating room, no exogenous platelet activation is required before PRP injections because collagen in the body acts as platelet agonist and activates platelets.

(d) Leukocyte number. As mentioned above, leukocyte-containing PRP was used in this study. Rios et al. showed that after lipopolysaccharide treatment, leukocyte-rich PRP released more growth factors and anti-inflammatory cytokines than pure PRP in healthy cartilage explants (Rios et al., 2015). In a clinical trial, patients treated with leukocyte-containing PRP suffered from more swelling and pain when compared to leukocyte-reduced PRP group (Giuseppe Filardo et al., 2012). However, a prospective study of multiple clinical trials showed no significant difference between leukocyte-poor PRP and leukocyte-rich PRP on cartilage repair (Riboh, Saltzman, Yanke, Fortier, & Cole, 2015). It is possible that inflammatory cytokines released from leukocytes induce inflammation (swelling and pain) in the early stage, but in the long term, leukocytes do not affect cartilage repair.

One of the limitations in this study is lack of information on the nature of the growth factor and cytokine profiles in the PRP preparation, which would vary in different preparations depending on the methods of platelet activation (Textor & Tablin, 2012). Specifically, the levels of chondrogenesis-promoting factors, such as members of the transforming growth factor- β (TGF β) family, may regulate the extent of cartilage formation. Other factors, including vascular endothelial growth factor (VEGF) and epidermal growth factor (EGF), may also impair the chondro-inductive effects of PRP. Matsumoto et al. showed that VEGF-transduced, muscle derived stem cells performed poorly in chondrogenesis in a rat model (Kubo et al., 2009b; Matsumoto et al., 2009). When combined with soluble VEGF receptor 1 (sFlt1), pellet cultures of the sFlt1-PRP treated group showed more collagen type II deposition (Mifune et al., 2013). EGF receptor ligand that was identified in osteoarthritis cartilage promoted chondrocyte catabolic activity, but inhibited anabolic activity in a mouse model (Long, Ulici, Chubinskaya, & Loeser, 2015). These findings suggest that VEGF or EGF, known components of PRP, may negatively

impact the activities of other chondro-inductive components of PRP; thus, specific depletion of such anti-chondrogenesis factors from PRP may enhance the pro-chondrogenesis effect of PRP on MSCs.

Another limitation of our study is that a PRP releasate pooled from several donors was used, in order to examine the overall effects of dosage and treatment duration on MSC chondrogenesis for a given PRP preparation. It is noteworthy that Mazzocca et al. reported that platelet and white blood cell numbers vary between individuals and repetitive withdraws of same individual (Mazzocca, 2012). More extensive future studies using a statistically significant number of PRP preparations from different donors are clearly needed to examine and correlate the biological activities with the variables noted above.

2.5 Conclusion

In 21-day IFP-ASC chondrogenic pellet cultures, high PRP concentrations delivered over days 7-21 increased catabolic gene expression, decreased chondrogenic gene expression, and decreased matrix proteoglycan deposition, compared to TGF β + /PRP- controls. Short duration and low concentration PRP treatment (1-day pulse, 1% PRP) resulted in increased cartilage matrix production and collagen type II deposition, compared to longer durations and higher concentrations. Furthermore, in 21-day 3D hydrogel cultures, PRP treatment highly downregulated chondrogenic gene expression and decreased proteoglycan deposition, compared to TGF β + /PRP- controls. These results showed that high concentration PRP treatment for prolonged period impairs MSC chondrogenesis *in vitro*. Understanding the effects of PRP on MSC chondrogenesis is necessary to further develop strategies for the application of PRP in combination

with cell-based therapy for the repair of focal cartilage defects. For example, autologous MSCs encapsulated in an autologous PRP-containing biocompatible hydrogel may be injected into the defect site, resulting in optimal MSC chondrogenic differentiation and production of cartilage extracellular matrix, and the formation of functional neo-cartilage.

3.0 Vascular Endothelial Growth Factor Impairs Pro-Chondrogenic Activity of Platelet-Rich Plasma on Adipose Stem Cells

3.1 Introduction

Cartilage degeneration affects 27 million people in the United States, and post-traumatic and focal cartilage defects comprise 12% of all cases (approximately 3 million Americans annually) (Brown et al., 2006; R. C. Lawrence et al., 2008). Current surgical techniques for treating focal cartilage defects include osteochondral autograft/allograft transplantation, microfracture, and autologous chondrocyte implantation (ACI). In ACI, autologous chondrocytes are isolated from non-weight bearing cartilage, expanded *ex vivo*, and returned to the chondral defect as a cell suspension covered with a collagen membrane (Huang et al., 2016). More recently, matrix-assisted ACI (MACI) has been developed. In MACI, autologous chondrocytes are seeded within a three-dimensional scaffold before implantation, theoretically provided better integration with the surrounding native cartilage while also providing a biomimetic microenvironment capable of enhancing cartilage neotissue formation (Freyman et al., 2013; E Kon et al., 2013; Makris et al., 2015). Although both ACI and MACI have shown promise, challenges persist. Donor site morbidity is the main challenge. Chondrocyte yield from non-weight bearing cartilage is low, requiring *ex vivo* cell expansion with an accompanying loss of the chondrogenic phenotype (Tuan et al., 2013). As a result, the patient must undergo two surgical procedures and the quality of cartilage repair remains inconsistent. Identification of alternative cell sources and the application of chondroinductive scaffolds are needed to overcome these challenges, permitting a single-step procedure with robust cartilage formation.

Mesenchymal stem cells (MSCs) are capable of undergoing chondrogenic differentiation and have traditionally been isolated from the bone marrow, a painful procedure that yields a relatively low percentage of MSCs. Alternatively, adipose tissue contains a higher percentage of MSCs, is abundantly available, and can be harvested through a minimally invasive lipoaspiration procedure (Hildner et al., 2015). Recently, human MSCs derived from the infrapatellar fat pad (IFP-ASCs) were shown to possess a greater chondrogenic potential than subcutaneous ASCs (SQ-ASCs) (Lopa et al., 2014) and ideally provide a stem cell source in one-step procedures. However, the total cell number of IFP-ASCs is limited compared to SQ-ASCs due to a smaller tissue volume. Therefore, ex vivo culture expansion of IFP-ASCs would likely be required to obtain a sufficient cell number for implantation. Alternatively, it may be possible to promote IFP-ASC proliferation at the site of implantation, thereby allowing the intraoperative isolation of IFP-ASCs and implantation into a chondral defect.

Platelet-rich plasma (PRP) has recently received considerable attention as a potential therapeutic agent for cartilage repair, due to its non-invasive, cost-effective and autologous nature. PRP contains many growth factors and inflammatory mediators that are released from activated platelets, and it has been shown to promote stem cell proliferation and tissue regeneration. We hypothesize that the combination of IFP-ASCs and autologous PRP can overcome the challenge of limited cell number and cell expansion given the proliferative capabilities of IFP-ASCs and the growth factors in PRP. However, the efficacy of PRP is controversial. Some studies have reported pain reduction and improvement of joint function with PRP treatment (Bayar et al., 2008), while others have found no improvement in cartilage formation (Brehm et al., 2006; Elizaveta Kon et al., 2010). Variations in PRP effectiveness include timing of blood draw, individual difference, and preparation protocol which results in varied growth factor and cytokine

profiles. Among all growth factors within PRP, studies have indicated that vascular endothelial growth factor (VEGF) may impair stem cell chondrogenesis and cartilage repair. More specifically, VEGF has been shown to induce endothelial cell migration and proliferation and highly promote angiogenesis in vivo (Carlevaro et al., 2000). VEGF and VEGF receptors are highly expressed in osteoarthritis cartilage indicating that VEGF may be responsible for the degradation of healthy cartilage by the production of matrix metalloproteinases (Enomoto et al., 2003). VEGF-transduced muscle-derived stem cells performed poorly in chondrogenesis and a catabolic role of VEGF on matrix degeneration has been reported in a rat model (Kubo et al., 2009b; Matsumoto et al., 2009). When combined with soluble receptor to block VEGF signaling, soluble receptor-treated group had more collagen type II deposition in pellet culture (Mifune et al., 2013). Subcutaneous, intravenous, or intraarticular administration of anti-VEGF antibody Bevacizumab improved articular cartilage repair in rat and rabbit models (Nagai et al., 2010, 2014; Y. Wang, Da, Li, & Zheng, 2013). All these studies indicate that VEGF may impair the pro-chondrogenic potential of PRP. At the tissue level, VEGF signaling somehow induces degradation by producing MMPs; at the cellular level, VEGF and VEGF receptors lead stem cells or chondrocytes to hypertrophy. After all, cartilage is an avascular tissue. The balance between angiogenic factors and anti-angiogenic factors is crucial in this nature.

VEGF, known as VEGFA, belongs to the superfamily that includes VEGFB, VEGFC, and VEGFD. VEGF, produced by pericytes, binds to two receptor tyrosine kinases VEGFR-1 (Flt-1) and VEGFR-2 (KDR or Flk-1) with different affinities (Ferrara, Gerber, & LeCouter, 2003). Once VEGF binds to the receptor, dimerization and auto-phosphorylation begins and leads to VEGF-induced angiogenesis and vascularization (Murata, Yudoh, & Masuko, 2008; Stutfeld & Ballmer-Hofer, 2009). Known roles of VEGF include mitogenic signal transduction by activation of Ras-

Raf-Mek-Erk pathway and activation of PI3K-Akt pathway for pro-survival signals (Ferrara et al., 2003). Of particular relevance is that, in early embryonic development, VEGF is required for the endochondral ossification (Carlevaro et al., 2000). This process is initiated by mesenchymal condensation, followed by chondrogenic differentiation to form a cartilage template (Carlevaro et al., 2000). Growth and maturation of the cartilage template in a structure known as the growth plate result in chondrocyte hypertrophy, accompanied by the upregulation of VEGF and subsequent vascularization (Carlevaro et al., 2000; Karimian et al., 2011). During this event, the hypertrophic chondrocytes undergo apoptosis, and are replaced by osteoblasts, ultimately resulting in bone formation (Carlevaro et al., 2000; Karimian et al., 2011). The critical key that leads chondrocytes to hypertrophy is still unclear, but VEGF is believed to play an important role.

Therefore, we hypothesize that VEGF impairs IFP-ASC chondrogenesis, and that removal of VEGF from PRP can enhance IFP-ASC chondrogenesis. In this study, we utilized an experimental system of IFP-ASCs as high-density cell pellets in vitro.

3.2 Methods

3.2.1 Materials and Reagents

All chemicals and reagents were purchased from Sigma-Aldrich (St. Louis, MO), unless indicated otherwise.

3.2.2 PRP Releasate Preparation

Platelet-rich plasma (PRP) releasate was prepared according to an adapted protocol (J. Zhang & Wang, 2010). Briefly, anticoagulated human whole blood (Central Blood Bank, Pittsburgh, PA) was distributed into 15 mL conical tubes (Thermo Fisher, Pittsburgh, PA) and centrifuged at 480 x g for 20 minutes at room temperature. Pelleted red blood cells were discarded; the middle layer buffy coat and the supernatant platelet-poor plasma was aspirated and concentrated to obtain a platelet concentration of 1×10^6 platelets/ μL . To activate platelets, 22.8 mM of calcium chloride (Sigma–Aldrich) was added and incubated at 37 °C overnight. After another centrifugation at 2000 x g for 10 minutes at room temperature, the fibrin clot was discarded and the supernatant, referred to as PRP releasate, was aliquoted and stored at -20 °C until future use. PRP releasate from six different donors were pooled in equal volume before each experiment.

3.2.3 Cell Isolation and Preparation

Human infrapatellar fat pad derived adipose stem cells (IFP-ASCs) were isolated from infrapatellar fat pads of three different donors undergoing total knee arthroplasty (48 years old female, 59 years old male, and 65 years old male) under an IRB-approved and exempted protocol (University of Pittsburgh and University of Washington). The tissue was digested with 1 mg/mL type I collagenase (Worthington Biochemical, Lakewood, NJ) and 1 mg/mL trypsin (Invitrogen, Carlsbad, CA) for 3 hours at 37°C in an orbital shaker at 150 rpm. Cells were filtered through a 40-micron cell strainer (Thermo Fisher), centrifuged at 1200 rpm for 5 minutes, and expanded in *growth medium* (DMEM, 10% v/v fetal bovine serum, and 1% v/v antibiotic-antimycotic).

Human bone marrow-derived mesenchymal stem cells (BM-MSCs) were isolated from the bone marrow of three different donors undergoing total knee or hip arthroplasty (65 years old male, 67 years old male, and 68 years old male). The trabecular bone marrow was minced with surgical scissors and rinsed with Minimum Essential Medium Alpha (α MEM; Invitrogen). Cells were filtered through a 40- μ m cell strainer (Thermo Fisher), pelleted by centrifugation at 1300 rpm for 5 minutes, and expanded in growth medium.

Human umbilical vascular endothelial cells (UVECs, #C2517A single donor) and UVEC culture medium (#CC-3162, each 500 mL endothelial growth medium-2 contains 0.5 mL of epidermal growth factor, 0.5 mL of vascular endothelial growth factor, 0.5 mL of R3-insulin-like growth factor, 0.5 mL of ascorbic acid, 0.2 mL of hydrocortisone, 2 mL of fibroblast growth factor 2, 0.5 mL of heparin, 10 mL of fetal bovine serum, and 0.5 mL of gentamicin/amphotericin) were both purchased from Lonza (Basel, Switzerland). Cell culture medium was prepared according to manufacturer's instructions.

3.2.4 PRP Characterization

The profiling of 41 growth factors and cytokines in PRP samples from six different donors (Demography can be found in supplementary table) was quantified by ELISA Microarray (RayBiotech #QAH-BMA-1000, Norcross, GA). Briefly, serial dilutions of cytokine standards and 100 μ L of samples were prepared. Sample diluent was added and incubated for 30 minutes prior to blocking for 1 hour. Biotinylated Antibody and Cy3 Equivalent Dye-Streptavidin were added separately for signal amplification. The sample slide was prepared and shipped to the manufacturer for subsequent analysis.

VEGF concentration was quantified using commercial enzyme-linked immunosorbent assay (ELISA) kits (R&D Systems #DVE00, Minneapolis, MN) according to manufacturer's instructions.

3.2.5 Cell Characterization

The expression of cell surface markers including vascular endothelial growth factor receptors I, II, and III (VEGFR1, VEGFR2, VEGFR3), platelet-derived growth factor receptor beta (PDGFR β) and transforming growth factor beta receptor II (TGF β R2) of IFP-ASCs, BM-MSCs, and UVECs was assessed by flow cytometry.

3.2.6 Monolayer Culture and Proliferation Assay

To determine the metabolic activity, IFP-ASCs were plated on six-well plates as monolayers for up to 7 days in serum-free growth medium (DMEM and 2% ITS) and MTS Cell Proliferation Assay (Promega, Madison, WI) was performed at day 1, day 3, and day 7. At day 7, PicoGreen Assay (Invitrogen, Carlsbad, CA) was also performed to determine relative double-stranded DNA level. Significant difference was determined when $p < 0.05$.

3.2.7 Pellet Culture and Differentiation Assay

To mimic mesenchymal cell condensation in chondrogenesis during embryonic development, 2.5×10^5 IFP-ASCs were pelleted in serum-free chondrogenic medium (DMEM, 1% v/v antibiotic-antimycotic, 10 $\mu\text{g}/\text{mL}$ insulin-transferrin-selenium, 0.1 μM dexamethasone, 40

$\mu\text{g/mL}$ proline, $50 \mu\text{g/mL}$ ascorbic acid, and 10 ng/mL TGF β 3). Culture medium was changed three times a week.

3.2.8 VEGF Knockdown

IFP-ASCs were cultured as monolayers on tissue culture flasks. After 24 hours of plating, cells were washed with PBS and antibiotic-free transfection medium (DMEM with 10% FBS). IFP-ASCs were transfected with either 50 nM Human VEGF ON-TARGET*plus* SMARTpool siRNA (Dharmacon, Lafayette, CO) or 50 nM non-targeting control siRNA ON-TARGET*plus* non-targeting siRNA #2 (Dharmacon, Lafayette, CO) using DharmaFECT1 Transfection Reagent (Dharmacon, Lafayette, CO). DharmaFECT1 and each siRNA were prepared at $10\times$ the final concentration used for transfection in antibiotic-free high glucose DMEM and incubated for 5 min at room temperature. Each siRNA was then mixed 1:1 with the DharmaFECT1 and incubated for 20 min at room temperature. Each siRNA/DharmaFECT mix was then diluted 1:5 in antibiotic-free growth medium and added to washed MSCs at 0.13 ml/cm^2 . The final volume of DharmaFECT used was $0.08 \mu\text{l/cm}^2$. After 24 hours of treatment, the medium was switched to regular growth medium (DMEM, 10% FBS, and 1% antibiotic-antimycotic).

3.2.9 Mechanical Impacts

Bovine articular cartilage explants were isolated from the patellofemoral groove of the hind-leg stifle of 2- to 3-year-old bovine within 24 hours of slaughter (JW Truth and Sons, Baltimore, MD). In brief, 8-mm cartilage discs were removed from the subchondral bone in the articular surface with a steel biopsy punch and immediately place in basal medium (phenol red-

free DMEM with 1% antibiotics). After 24 hours, a central 5-mm core was removed from the 8-mm disc and cultured in serum-free chondrogenic medium (DMEM, 1% v/v antibiotic-antimycotic, 10 µg/mL insulin-transferrin-selenium, 0.1 µM dexamethasone, 40 µg/mL proline, 50 µg/mL ascorbic acid, and 10 ng/mL TGFβ3). After weighing, samples between 38 and 60 mg (approximately 1.8 to 2.2 mm in thickness) were randomly distributed into four different experimental groups for another 24 hours. On the day of the experiment, the cartilage samples were placed in the impact chamber (5 mm in diameter and 2.2 mm in depth), covered with a piece of polyvinyl-enclosed Pressurex Pressure Indicating Sensor Film, and subjected to 36 MPa of impact force. Impacted samples were returned to wells containing fresh chondrogenic medium and cultured for seven days. Medium was changed once at day 3. Four experimental groups: (1) Control, (2) Impacted, (3) PRP-treated, and (4) Impacted & PRP-treated.

3.2.10 Western Blotting

Western blotting was performed to confirm the antibody functions. Cells were seeded in 6-well plates as monolayers and treated with 10 ng/mL of recombinant VEGF (rVEGF) and anti-VEGF (treated with 500 ng/mL of anti-VEGF antibody) or IgG (treated with 500 ng/mL of IgG antibody) with no treatment as the control. Cells were trypsinized at 10, 20, 30 and 60 minutes. Total RNA was isolated for western blotting of VEGF and GAPDH to detect protein expression level of VEGF and GAPDH.

3.2.11 Gene Expression Analysis

Pellet cultures were collected on day 21 and homogenized in Qiazol (Qiagen, Hilden, Germany). Total RNA was isolated with RNeasy Plus Mini Kit (Qiagen). Gene expression levels of chondrogenic markers (transcription factor SOX9, SOX9; collagen type II, COL2; aggrecan, ACAN), hypertrophic markers (collagen type X, COL10; matrix metalloproteinase 13, MMP13), osteogenic markets (collagen type I, COL1; runt-related transcription factor 2, RUNX2), and VEGF signaling pathway markers (vascular endothelial, growth factor, VEGF; VEGF receptor 1, FLT1; VEGF receptor 2 or kinase insert domain receptor 1, KDR1; neuropilin 1, NRP1; neuropilin 2, NRP2) were assessed by real-time RT-PCR. All the gene expression levels were normalized to that of 18S ribosomal RNA (primer sequence shown in Supplementary Table). Relative fold changes were calculated using $\Delta\Delta C_t$ method.

3.2.12 Histological Analysis

For histology, pellets were harvested on day 21, fixed with 4% paraformaldehyde, and embedded in paraffin. Eight-micron sections were stained with Safranin O/Fast Green for proteoglycans and Alcian Blue/Nuclear Fast Red for glycosaminoglycan. Immunohistochemical analysis was performed using anti-human collagen type II antibodies. Briefly, the slides were washed with 0.02% bovine serum albumin and incubated with 0.1 U/mL chondroitinase ABC (Sigma–Aldrich, St. Louis, MO) and 250 U/mL hyaluronidase (Sigma) for antigen retrieval. Three percent hydrogen peroxide (Company, Catalog) and 1% horse serum (Vector) was used for blocking. Samples were then incubated with rabbit anti-human collagen type II (Abcam, Cambridge, United Kingdom) at 4 °C overnight. Biotinylated anti-rabbit secondary antibody was

used to bind the primary antibody. Signals were amplified using ABC reagent (Vector, Burlingame, CA) and visualized with VIP Kit (Vector). Counterstain Hematoxylin QS (Vector) was used before mounting.

3.2.13 Biochemical Analysis

Papain (Sigma-Aldrich) was diluted in digestion buffer (0.1 M sodium acetate, 0.01 M cysteine HCl, 0.05 M EDTA, add ddH₂O to 500 mL, adjust pH to 6.0) at 1:50. Pellets were digested with papain solution at 65°C overnight. Sulfated GAG content was measured with the Blyscan GAG Assay (BioColor, Carrickfergus, United Kingdom) according to the manufacturer's instructions. GAG content was normalized against DNA content determined with PicoGreen Assay (Invitrogen, San Diego, CA).

3.2.14 Statistical Analysis

Gene expression levels, GAG content, and DNA content are shown as mean \pm standard deviation. Three to six independent trials were performed for each experiment. One-way ANOVA and Tukey's multiple comparisons test were performed using GraphPad Prism 7 (GraphPad Software Inc, CA) to determine the significant difference between groups. Significance was determined when $p < 0.05$.

3.3 Results

3.3.1 Growth factor and cytokine profile of PRP

To obtain the growth factor and cytokine profile of PRP, enzyme-linked immunosorbent assay (ELISA) microarray was performed. Forty-one growth factors and cytokines at the protein level were detected, including Activin A, aFGF, Amphiregulin, bFGF, E-Selectin, ICAM-1, IGF1, TNF α , IL1a, IL1b, IL6, IL8, IL11, IL17, MCP1, MCSF, MIP1a, MMP2, MMP3, MMP9, MMP13, Osteoactivin, P-Cadherin, VE-Cadherin, RANK, SDF-1a, Shh-N, TGF β 1, TGF β 2, TGF β 3, BMP2, BMP4, BMP6, BMP7, BMP9, Dkk-1, Osteoprotegrin, Osteopontin, PDGFBB, TRANCE, VCAM-1 (**Figure 16A**). A heat map was generated to facilitate comparison across donors (**Figure 16B**). The demographic information of donors is listed in Appendix.

EGF ELISA was performed and the concentration of EGF was quantified (**Figure 17A**). A variation across six different donors was observed and the concentration ranges between 0 and 1,000 pg/mL. The concentration of VEGF was also quantified (**Figure 17B**). Concentrations averaged 150 pg/mL. This concentration is consistent with the concentration reported by Bertrand-Duchesne et al. (Bertrand-Duchesne, Grenier, & Gagnon, 2010). In their study, the mean of 5 PRP donors was 189 ± 7 pg/mL.

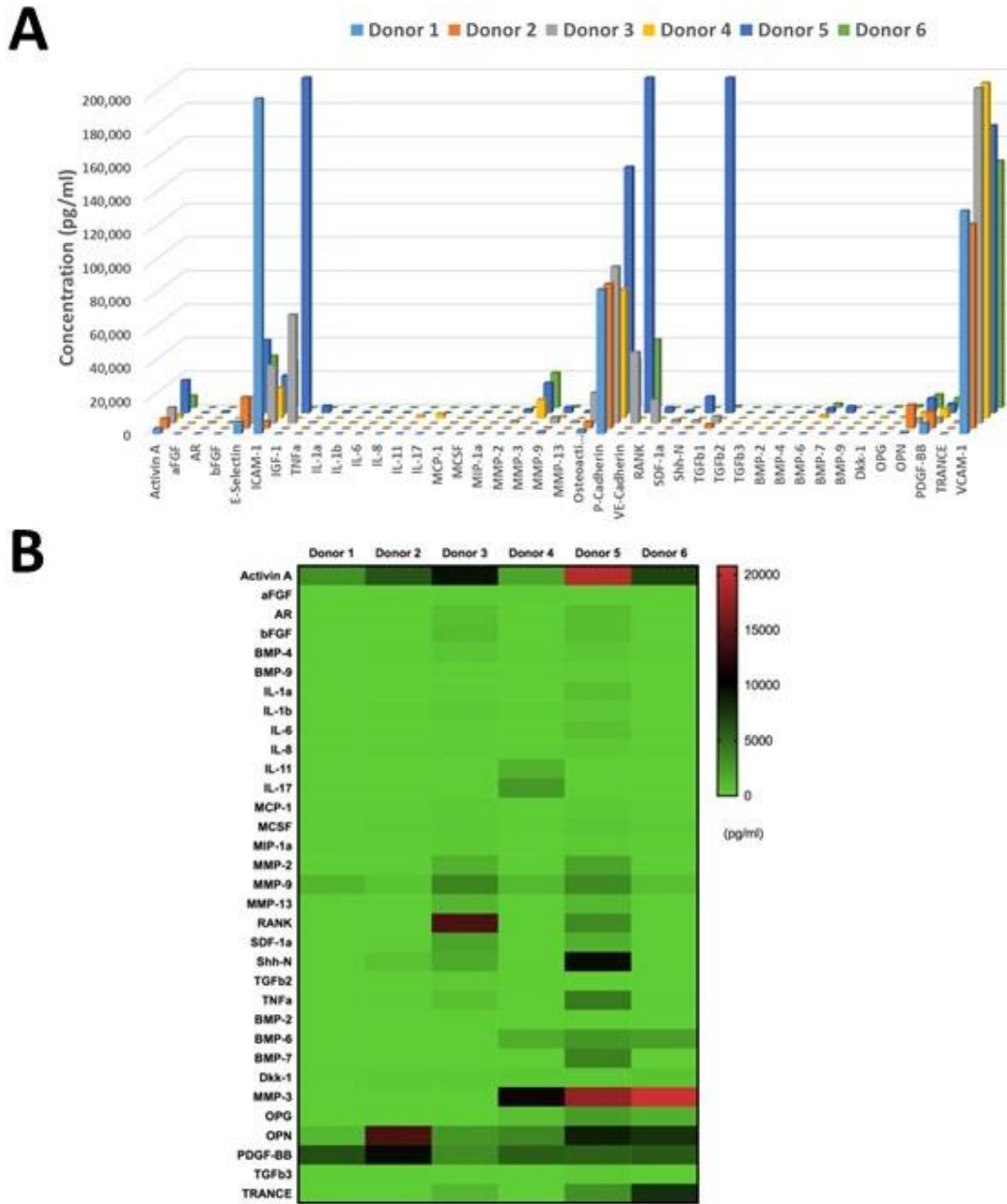


Figure 16. Growth factor and cytokine profile of PRP samples.

(A) ELISA microarray of 41 growth factors and cytokines including proliferative growth factors (aFGF, bFGF), chondrogenic growth factors (TGFβ1, TGFβ2, TGFβ3, BMP2, BMP4, BMP6, BMP7, BMP9), catabolic factors (MMP2, MMP3, MMP9, MMP13), and pro-inflammatory cytokines (TNFa, IL1a, IL1b, IL6, IL8, IL11, IL17), endothelial markers (P-Cadherin, VE-Cadherin) (B) Heat map of 33 growth factors and cytokines that are 20,000 pg/ml or below.

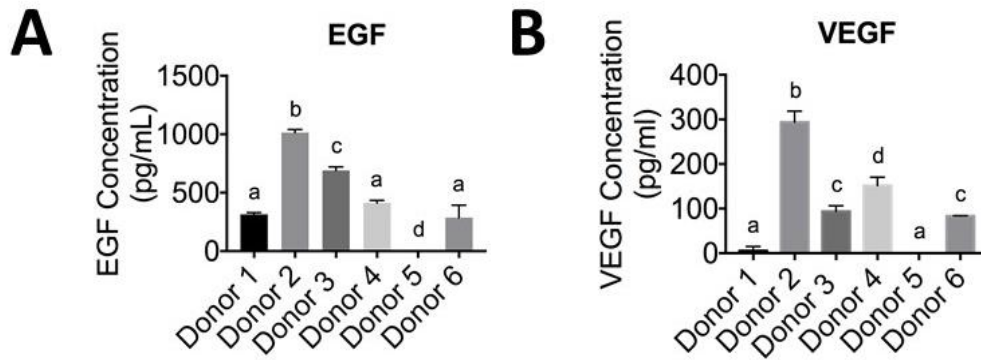


Figure 17. EGF and VEGF protein concentration in PRP samples.

(A) ELISA of EGF shows that EGF concentration is averaged 500 pg/mL (n=3). one-way ANOVA, significant difference between different letters. (B) ELISA of VEGF (n=3). one-way ANOVA, significant difference between different letters.

3.3.2 Effect of PRP on IFP-ASC proliferation

Prior to differentiation assays, the effect of PRP on IFP-ASC proliferation was examined. MTS assays show that 10% (v/v) PRP significantly increased metabolic activity in IFP-ASC monolayer cultures at day 1, day 3, and day 7 (**Figure 18A**). At day 7, PicoGreen assay showed that 10% PRP significantly promoted IFP-ASC proliferation (**Figure 18B**).

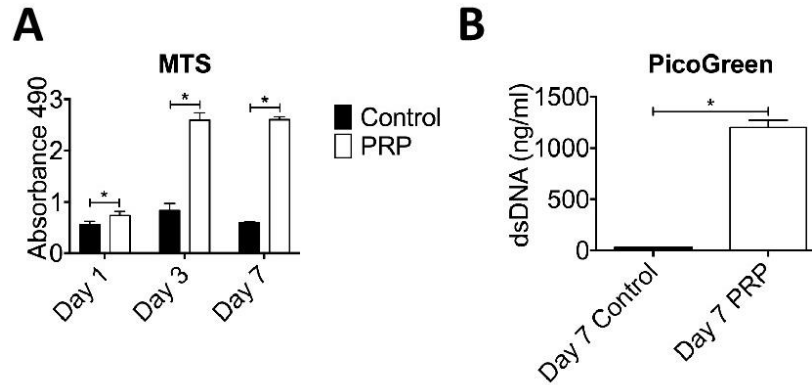


Figure 18. Effect of PRP treatment on IFP-ASC metabolic activity and proliferation.

(A) MTS assay shows 10% (v/v) PRP significantly promotes metabolic activity. (B) PicoGreen assay (cell number) shows 10% PRP significantly promotes cell proliferation.

3.3.3 Effect of exogenous VEGF supplementation

To examine the effect of VEGF on IFP-ASC chondrogenesis, IFP-ASCs were cultured in chondrogenic medium supplemented with PRP and 10 ng/ml recombinant VEGF (rVEGF) and analyzed at day 8. Exogenous rVEGF supplementation downregulated SOX9 and ACAN, while no significant difference was observed in the COL2 expression (**Figure 19**). However, when the rVEGF concentration was increased from 10 to 50 or 100 ng/mL, no significant difference was observed (data not shown).

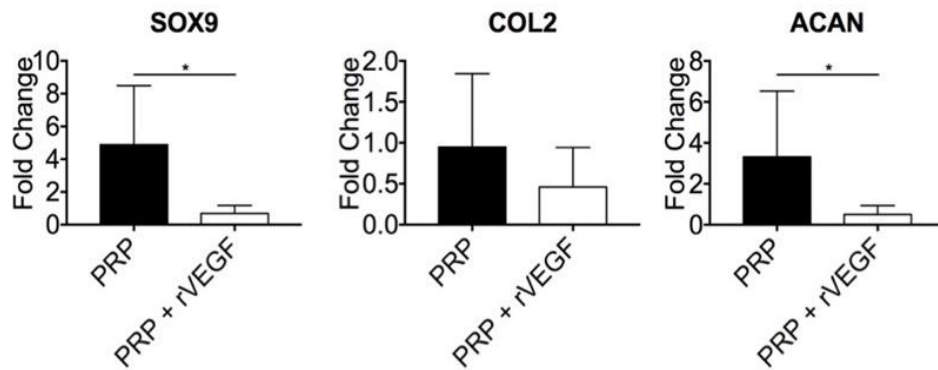


Figure 19. Effect of exogenous VEGF supplementation on IFP-ASC pellet cultures.

PRP pellets (chondrogenic medium supplemented with 10% v/v PRP) and PRP + rVEGF pellets (chondrogenic medium supplemented with 10% v/v PRP and additional 10 ng/mL recombinant VEGF) at day 8 (n=5).

3.3.4 VEGF receptor surface expression

Next, we postulated that the lack of change of chondrogenesis observed as VEGF concentration was increased (i.e., increased ligand concentration) was partially due to the low expression of VEGF receptors on IFP-ASCs. To analyze the cell surface expression of VEGF receptors, IFP-ASCs were cultured as monolayers and then analyzed using flow cytometry. The results showed that IFP-ASCs expressed low level of VEGF receptor 1 (VEGFR1), VEGF receptor 2 (VEGFR2), and VEGF receptor 3 (VEGFR3), but expressed high level of PDGF receptor beta (PDGFRβ). Expression of TGF beta receptor 2 was about 50% of that observed in BM-MSCs and human umbilical vein endothelial cells (HUVECs) (**Figure 20A**). Quantitation of receptor surface expression was shown (**Figure 20B**).

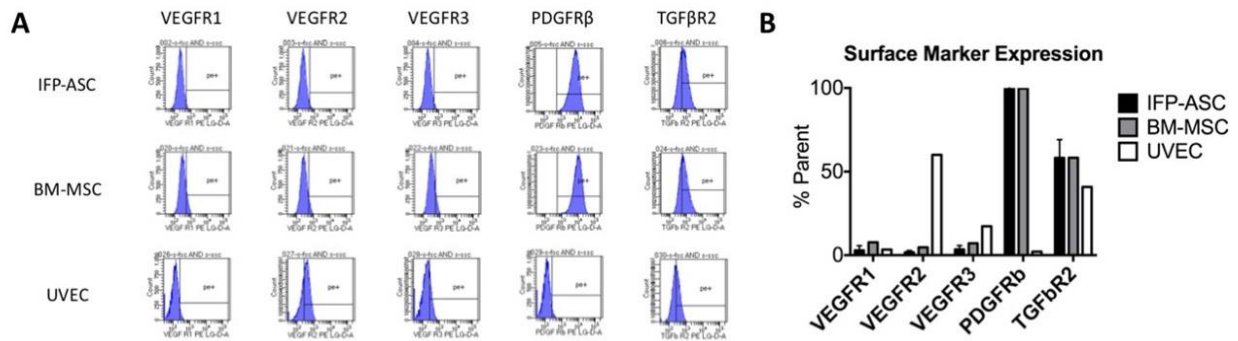


Figure 20. Surface expression of monolayer cultured IFP-ASCs, BM-MSCs, and UVECs.

(A) Characteristics of IFP-ASCs is indicated by high expression of PDGF receptor beta and TGF beta receptor 2 (50% parent) with negligible expression of VEGF receptor 1, VEGF receptor 2, and VEGF receptor 3 (n=3). (B) Quantification of surface expression in IFP-ASC, BM-MSC, and UVEC monolayer cultures.

3.3.5 Effect of anti-VEGF treatment

To manipulate VEGF level, in addition to VEGF supplementation, VEGF was also depleted from PRP by immunoadsorption using anti-VEGF antibody. VEGF antibody was supplemented to chondrogenic medium. [Note: 1 ug/ml was most common concentration of this antibody used in other similar studies (Allerstorfer et al., 2008; Hatfield, Rynning, Corbascio, & Bruserud, 2006).] Our results showed that at day 7, SOX9 expression remained the same; ACAN expression decreased in PRP group but anti-VEGF antibody rescued this reduction (data not shown). At day 21, treatment with anti-VEGF antibodies significantly improved SOX9, COL2, and ACAN expression when compared to the PRP-treated group in high-density pellet cultures (**Figure 21A**). This finding was consistent with changes in the measured value of sulfated GAG content per pellet (**Figure 21B**).

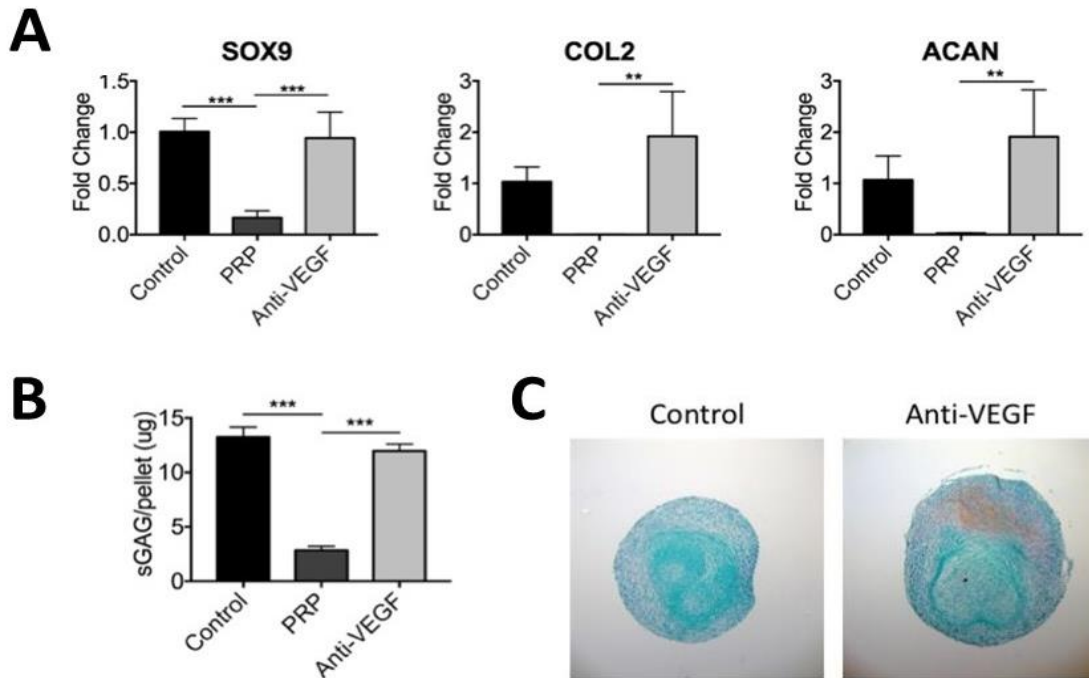


Figure 21. Effect of anti-VEGF treatment on IFP-ASC pellet culture.

(A) Anti-VEGF treatment can recover PRP-induced loss of SOX9, COL2, and ACAN gene expression in IFP-ASC pellet cultures. (B) Anti-VEGF treatment increases sulfated GAG deposition when compared to the PRP group. (C) Safranin O staining of IFP-ASC pellet cultures confirms the beneficial effect of anti-VEGF treatment on IFP-ASC chondrogenic differentiation.

3.3.6 Anti-inflammatory effect of PRP

The anti-inflammatory effect of PRP was also evaluated. The response of IFP-ASC to pro-inflammatory cytokines, IL1 β and IL6, was examined in 21-day pellet cultures. The results showed that IL1 β significantly decreased sulfated glycosaminoglycan deposition in IFP-ASC pellets at 14 days; no significant effect was observed in the IL6-treated group when compared to the control (**Figure 22**). We also tested the effect of IL1 β in hydrogel cultures. Results show that IL1 β

significantly downregulated collagen type II (COL2) and aggrecan (ACAN) expression on day 7 while upregulating matrix metalloproteinase 3 (MMP3) at day 1 (**Figure 23**).

To examine the anti-inflammatory effect of PRP on injured cartilage, bovine cartilage plugs were impact-injured using an impactor custom-designed by our laboratory and then treated with PRP at 10% (v/v) for up to 7 days. No significant difference was detected between *Impacted* and *Impacted & PRP-Treated* groups at the gene expression level of MMP1, MMP3, MMP13, ADAMTS4, ADAMTS5, COX2, iNOS, RUNX2, IHH, SMO, or PTCH (data not shown). Quantitation of the anti-inflammatory cytokines IL4 and IL10 in six PRP samples using ELISA assays showed that the IL4 concentration in all samples was lower than the detection limit at 1 pg/mL (data not shown).

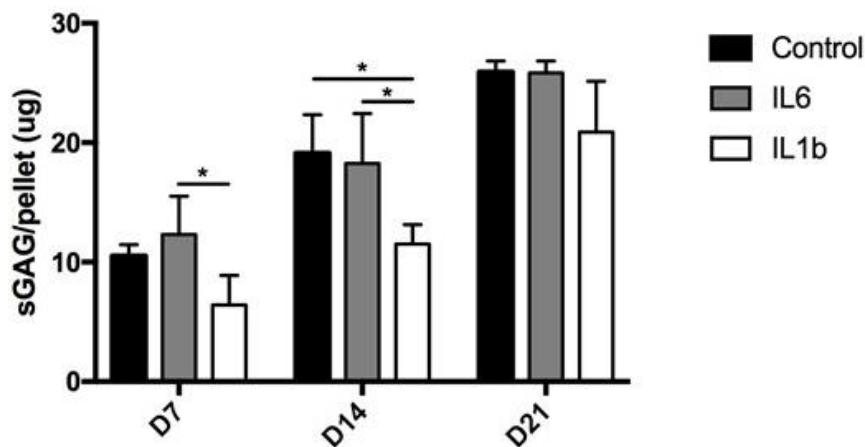


Figure 22. Effect of IL6 and IL1 β on IFP-ASC pellet cultures.

IL1 β significantly decreased GAG/DNA of IFP-ASC pellets at day 7 and day 14. *, $p < 0.05$.

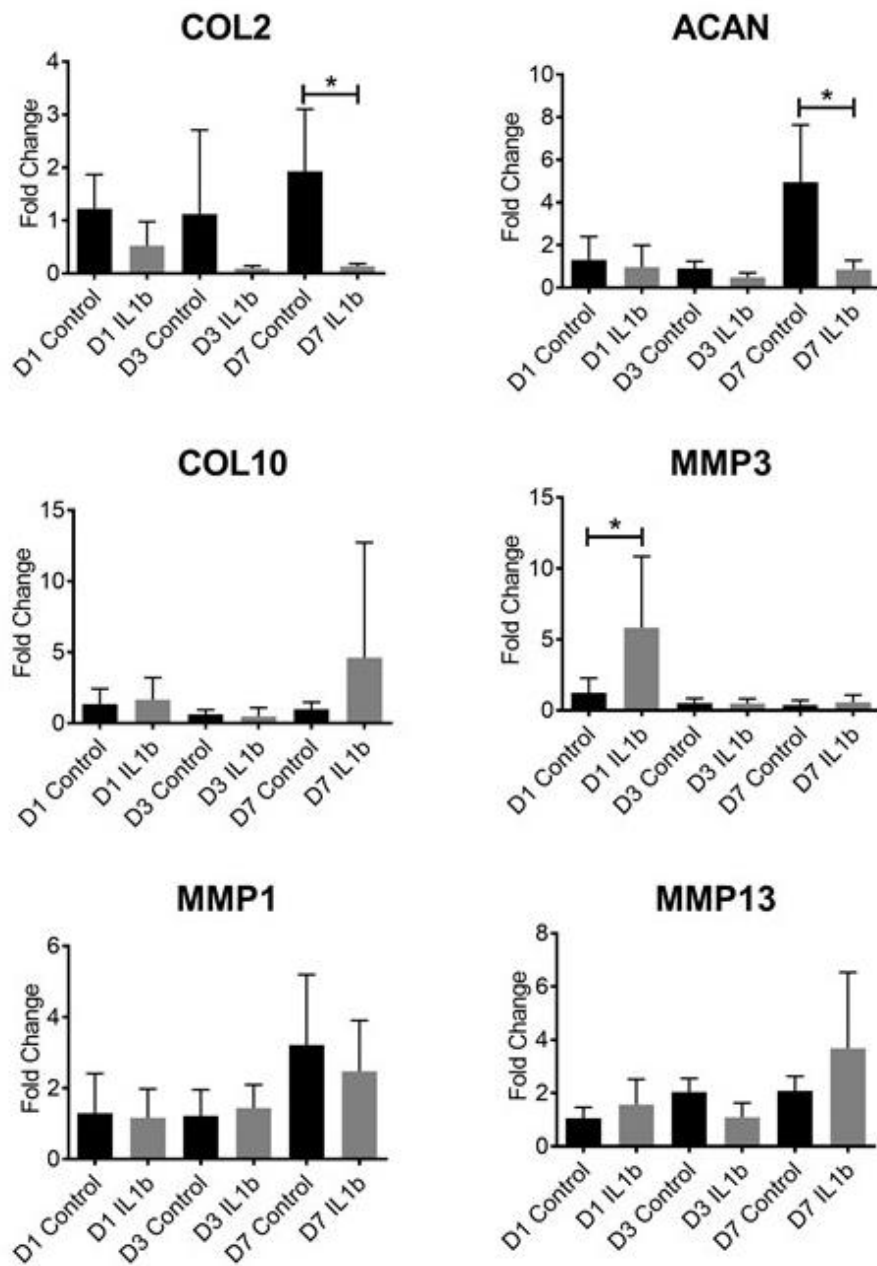


Figure 23. Effect of IL1 β on three-dimensional hydrogel cultures.

IL1 β significantly downregulates COL2 and ACAN at day 7 while at day 1, MMP3 is highly upregulated

in IL1 β treated group. *, $p < 0.05$.

3.4 Discussion

This study provides a perspective of how VEGF, as a component of PRP, can impair IFP-ASC chondrogenic differentiation, and shows that blockage of VEGF can improve chondrogenesis. Exogenous VEGF at 10 ng/mL downregulated chondrogenic gene expression. Lozito et al. also reported no difference between VEGF treatments on BM-MSCs in the absence or presence of 5, 25, or 50 ng/mL of VEGF (Lozito, Kuo, Taboas, & Tuan, 2009). It is possible that this is related to the fact that VEGF receptor expression level in MSCs is low, e.g., less than in endothelial cells (e.g., human umbilical vein endothelial cells). Indeed, our data show that VEGF receptors are barely found on the surface of IFP-ASCs. ASCs derived from subcutaneous tissues had similar surface expression profile – a low expression of VEGF receptors but high expression of PDGF receptor beta (Hutton et al., 2012; Shevchenko et al., 2013).

Among the growth factors that are released from platelets after platelet activation, VEGF is essential for mitogenic and pro-survival signals (Ferrara et al., 2003). In early embryonic development, VEGF is required for the endochondral ossification process of skeletogenesis (Carlevaro et al., 2000). This process is initiated by mesenchymal condensation, followed by mesenchymal chondrogenic differentiation to form a cartilage template (Carlevaro et al., 2000). Growth and maturation of the cartilage template in the growth plate result in chondrocyte hypertrophy, accompanied by the upregulation of VEGF and subsequent vascularization (Carlevaro et al., 2000; Karimian et al., 2011). During this event, the hypertrophic chondrocytes undergo apoptosis and are replaced by osteoblasts, ultimately resulting in bone formation (Carlevaro et al., 2000; Karimian et al., 2011). The critical key that leads to hypertrophy is still unclear, but VEGF is believed to play an important role. Studies have shown hypoxia-inducible factor 1-alpha (HIF1 α) leads to transcriptional activation of the VEGF gene in hypoxic cells. In

the growth plate, reduced oxygen level induces HIF1 α expression which induces VEGF transcriptional activation (Murata et al., 2008), and that HIF1 α and VEGF act coordinately to maintain cartilage metabolism under hypoxic conditions (Nagao et al., 2017). HIF1 α also acts through VEGF-independent mechanisms because overexpression of VEGF in HIF1 α -deficient mice only partially rescues the aberrant hypoxia phenotype (Macs 2012 J Bone Miner Res; Pfander 2003 J Cell Sci; Schipani 2001 Genes Dev). In chondrocytes, HIF1 α increases the expression of VEGF and promotes angiogenesis in the surrounding perichondrium (Wang 2007 J Clin Invest; Riddle 2009 J Mol Med). Overexpression of the HIF1 α target, VEGF, in chondrocytes also results in excessive endochondral bone formation (Macs 2010).

At the cellular level, VEGF controls mitogenic and pro-survival signals through multiple signaling pathways. VEGF, known as VEGFA, belongs to the superfamily that includes VEGFB, VEGFC, and VEGFD. VEGF can bind to two receptor tyrosine kinases VEGFR-1 and VEGFR-2 with different affinities (Ferrara et al., 2003). Once it binds to the receptor, dimerization and auto-phosphorylation begins and turns on downstream signaling cascades (Stuttfield & Ballmer-Hofer, 2009). Most of the proliferation and survival signals come from VEGFR2 (Ferrara et al., 2003), so we hypothesize VEGF actions on chondrogenesis via VEGFR2 signaling.

VEGFR2 signaling can be inhibited via ligand sequestration (e.g., monoclonal antibody or soluble receptor that directly binds to ligand) or receptor blocking (e.g., small molecule inhibitor that binds to ATP pocket and prevents receptor phosphorylation). Among all small inhibitors, VEGF receptor 2 inhibitor SU1498 has been investigated. SU1498 prevents tyrosine kinase phosphorylation, and it inhibits VEGF-induced histone deacetylase stabilization and Akt phosphorylation in embryonic stem cells (Zeng et al., 2006). SU1498 also blocked shear stress-

induced VEGFR2-positive embryonic stem cells differentiating towards endothelial cells, while a VEGF neutralizing antibody did not (Yamamoto et al., 2005).

Gene silencing can also knockdown VEGF signaling. VEGF siRNA has been widely used in cancer research (S. H. Kim, Jeong, Lee, Kim, & Park, 2008), but only in a few studies in the orthopedic field. Among them, most of the gene silencing strategies targeted HIF1 α , an upstream molecule of VEGF signaling (Kakudo, Morimoto, Ogawa, Taketani, & Kusumoto, 2015; L. Lin et al., 2011; C. Zhang, Li, Cornelia, Swisher, & Kim, 2012). However, Prasad et al. treated human umbilical vein endothelial cell (HUVEC)/osteocyte cocultures with VEGF siRNA and found that proliferation, cell migration, tubule formation, or angiogenic gene expression of HUVECs was significantly reduced (Prasad et al., 2014). Conditional deletion of VEGF in chondrocytes caused massive cell death in growth plate chondrocytes and reduced angiogenesis in the primary ossification center (Zelzer et al., 2004).

Gerber et al. inactivated VEGF systemically in mice and found that inhibition of VEGF activity impaired bone formation and expanded hypertrophic chondrocytes with almost complete suppression of blood supply (Gerber et al., 1999). Zelzer et al. generated VEGF knockout mice and found impaired embryonic bone development (Zelzer et al., 2004).

The result from our study is in line with several studies. VEGF-transduced muscle-derived stem cells performed poorly in chondrogenesis in a rat model and reported a catabolic role of VEGF on matrix degeneration (Kubo et al., 2009b; Matsumoto et al., 2009). When combined with the soluble receptor to block VEGF signaling, the soluble receptor-treated group had more collagen type II deposition in pellet culture (Mifune et al., 2013). When treated with anti-VEGF antibody intravenously, antibody treatment improved articular cartilage repair in a rabbit model (Nagai et al., 2010). Nagao et al. demonstrated that conditional knock-down of VEGF attenuates

induced OA and intra-articular anti-VEGF antibodies suppress OA progression in a mouse model (Nagao et al., 2017). A summary of relevant VEGF studies has been summarized in Table 1.

It has been hypothesized that Bevacizumab can function like chondromodulin-1 as an anti-angiogenic factor in maintaining the avascular nature of cartilage tissue (S. Lee, Nemeño, & Lee, 2016). The limitation of this study is that the effect of VEGF was only evaluated in vitro.

Table 1. Effect of VEGF on chondrogenic differentiation for cartilage repair.

Condition	Treatment	Outcome	Reference
Mono-iodoacetate induced arthritis by one IA injection in rats	Gene transduction, IA injection	VEGF-transduced muscle-derived stem cells performed poorly in chondrogenesis in a rat model and reported a catabolic role of VEGF on matrix degeneration.	(Matsumoto et al., 2009)
Osteochondral defect model (1.8 mm diameter 2.0 mm depth) in rats	Gene transduction, IA injection	VEGF-transduced muscle-derived stem cells performed poorly in chondrogenesis in a rat model and reported a catabolic role of VEGF on matrix degeneration.	(Kubo et al., 2009a)
Osteochondral defect (5 mm diameter 3 mm depth) in rabbits	Bevacizumab IV	Intravenous administration of anti-VEGF antibody improved articular cartilage repair compared to defect the only group at one month and three months in a rabbit model.	(Nagai et al., 2010)
No injury in mice	Bevacizumab Hyaluronic acid/fibrin subcutaneous implants	Incorporation of anti-VEGF antibody inhibited host vessel ingrowth but enhanced construct survival rate at three and six weeks. Subcutaneous implantation of nasal chondrocytes-encapsulated fibrin/hyaluronan scaffold and incorporation of Bevacizumab does not affect cartilage matrix deposition in a nude mouse model.	(Centola et al., 2013)
Monosodium iodoacetate induced arthritis by one IA injection in rats	Gene transduction with/without PRP, IA injection	When combined with the soluble receptor to block VEGF signaling, the soluble receptor-treated group had more collagen type II deposition in pellet culture.	(Mifune et al., 2013)
Anterior cruciate ligament transection in rabbits	Bevacizumab IV and IA	IV injections reduced cartilage degeneration and osteophyte formation; IA injections are better than IV injections.	(Nagai et al., 2014)

Table 1 (continued)

No injury in nude mice	Gene transduction, subcutaneous implantation	VEGF blockage by retroviral transduction of sFlk1 does not affect chondrogenic differentiation of nasal chondrocytes in vitro, but the implantation of chondrocyte-encapsulated collagen scaffold increases glycosaminoglycan deposition in a nude mouse model.	(Medeiros Da Cunha et al., 2017)
Surgical induced OA by destabilization of medial meniscus in mice	Conditional knockdown of VEGF, intra-articular injection of anti-VEGF antibodies, and oral administration of VEGFR2 kinase inhibitors (Vandetanib)	Conditional knock-down of VEGF attenuates induced OA. Intra-articular anti-VEGF antibodies suppress OA progression, reduce levels of phosphorylated VEGF receptors. Finally, oral administration of the VEGFR2 kinase inhibitor attenuates OA progression.	(Nagao et al., 2017)

Note: IA: intra-articular; IV: intra-venous; OA: osteoarthritis; VEGF: vascular endothelial growth factor.

3.5 Conclusion

Exogenous VEGF supplementation decreased chondrogenic gene expression in IFP-ASC pellet cultures. PRP treatment decreased chondrogenic gene expression when compared to TGF β 3+/PRP- controls. Anti-VEGF antibodies rescued PRP-induced loss of chondrogenesis. These results showed that VEGF, as one component in PRP, acts to impair MSC chondrogenesis *in vitro*. Understanding the involvement of VEGF in PRP on MSC chondrogenesis is necessary to optimize the application of PRP in combination with cell-based therapy for the repair of focal cartilage defects. For example, autologous MSCs encapsulated mixed with VEGF-depleted PRP in hydrogel may be injected into the defect site, resulting in optimal MSC chondrogenic differentiation and production of cartilage extracellular matrix, and the formation of functional neo-cartilage.

4.0 Discussion

Current clinical treatments for cartilage injuries mostly only target short-term pain and provide temporary restoration of joint function. Surgical procedures, in addition to being destructive in nature, are also associated with risks of infection, inflammation, post-surgery failure, and need for surgical revision. We have reviewed here the principles and progress of current tissue engineering approaches that have the potential to repair or regenerate skeletal soft tissues, specifically cartilage. Critical to the success of a regenerative medicine approach is the development of a biomaterial scaffold that, with the appropriate delivery of requisite growth and inductive factors, can provide cells with the optimal environment and niche to grow and differentiate, and to regenerate a neo-tissue that is able to mature and remodel in concert with and in response to the physiology of the native tissue milieu (**Figure 24**).

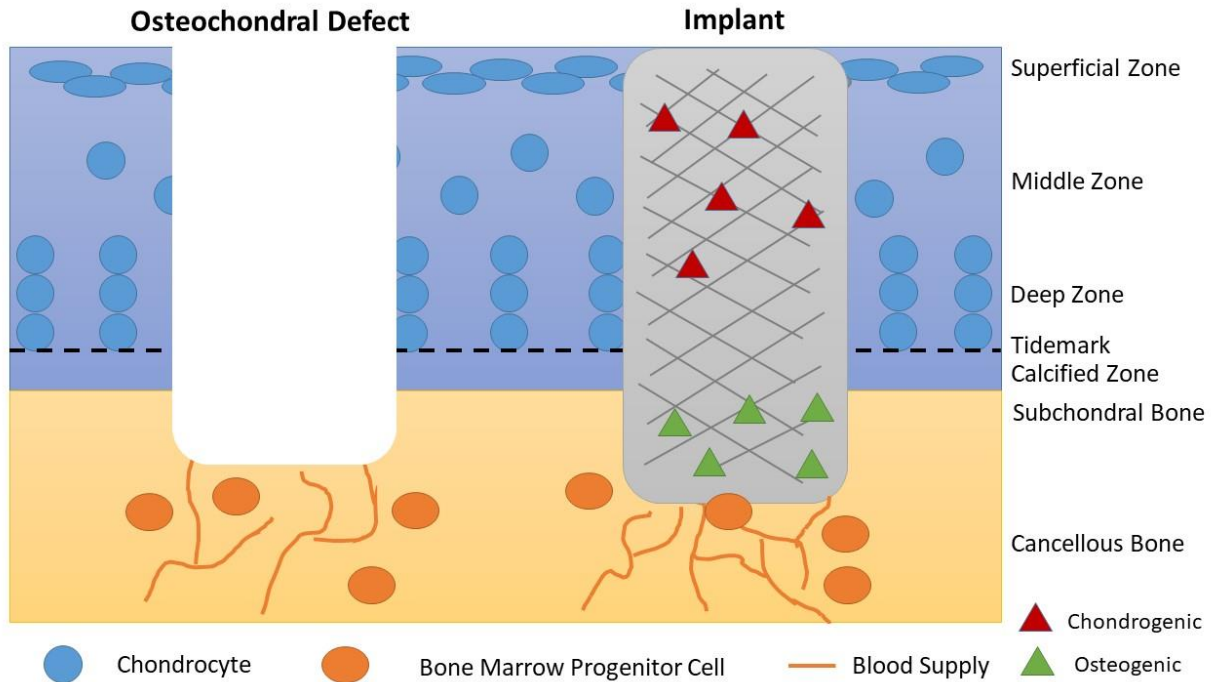


Figure 24. Tissue engineering approach for osteochondral defect repair.

Ultimately, an autologous cell-based therapy is an osteochondral implant that contains cells, bioactive factors, and scaffolds. There are four different zones (superficial zone, middle zone, deep zone, and calcified zone).

Several native and synthetic scaffolds are under investigation for tissue regenerative applications. Native biopolymeric scaffolds have natural extracellular matrix microstructure, which promotes cell adhesion, migration, infiltration, proliferation, and differentiation. However, poor mechanical properties and nonspecific and unregulated inductive activities are the limitations of current biological scaffolds. Synthetic, or polymeric, scaffolds have defined mechanical properties with quality consistency, but are not as biocompatible as native matrix-derived scaffolds. Future development in scaffold technology thus needs to be grounded in the natural history of soft tissue development and biology.

In terms of bioactive factors, the use of PRP remains controversial. Although PRP is a natural product, may be obtained autologously and rapidly implemented, and requires no or little

regulatory clearance, more investigations, particularly controlled clinical trials, are clearly needed to yield conclusive evidence to indicate its value for cartilage regeneration and what the standard procedure should be. In comparison, the bioactive factor, TGF β , while having shown efficacy in improving tissue differentiation and regeneration in cell culture and animal models, does not have FDA approval for clinical use.

The most promising cell type for skeletal soft tissue engineering and regeneration is the MSC, derived from bone marrow or other tissues, such as adipose. MSCs that have undergone minimal or no culture expansion are preferred as they possess more robust proliferative and differentiation potential. MSCs are optimally delivered in 3D scaffolds that are formed in a manner that allows optimal cell encapsulation, and recent developments in 3D bioprinting present interesting options in scaffold design and fabrication. The potential of using allogeneic MSCs should also be explored, particularly given the extensive literature supporting the low, intrinsic immunogenicity of MSCs.

In conclusion, contemporary advances in stem cell biology, developmental biology, and scaffold technologies have provided exciting possibilities in developing regenerative therapeutic approaches for the repair of injuries to cartilage. The potential of functional restoration will significantly alleviate the disease burden of these debilitating injuries and improve the quality of life of a significant segment of society. Sustaining the breakthroughs through the continuous convergence of life science and engineering is critical to reach these goals.

4.1 Summary

The central hypothesis of this dissertation is that PRP modulates IFP-ASC chondrogenesis and that removal of VEGF enhances IFP-ASC chondrogenesis for cartilage tissue engineering. In Aim 1, the effect of PRP on IFP-ASC chondrogenesis was examined in high-density pellet cultures and three-dimensional hydrogel cultures. Results show that treatment with high concentration PRP for extensive time periods impairs IFP-ASC chondrogenesis in both pellet and hydrogel cultures. In Aim 2, the effect of VEGF as a bioactive component of PRP was examined. Results show that exogenous VEGF supplementation downregulates chondrogenic gene expression and treatment of anti-VEGF antibodies was able to rescue PRP-induced loss of chondrogenesis. In Aim 3, PRP in combination with ASCs in hydrogel was examined in a rabbit study for osteochondral defect repair.

As mentioned above, the complexity of PRP research is due to the variability between donors, and how PRP is processed and delivered (**Table 2**). In this dissertation, one growth factor – VEGF – was identified as the chondro-inhibitory factor, providing information on future application for cartilage tissue engineering.

Table 2. Variables of PRP treatments for cartilage repair

Variable	Sub-Variable
Donor	Age (Andia & Maffulli, 2013; Elizaveta Kon et al., 2011), gender, comorbidities, concurrent medications (anti-inflammatory drugs), nutritional status, activity level (J. S. Wang et al., 1994)
Processing	Blood collection and storage conditions, spin protocol (speed, time) (Amable et al., 2013), activation protocol (agent, concentration, timing) (Amable et al., 2013)
Delivery	Form of delivery (gel, solution) (Dohan Ehrenfest et al., 2009), timing of delivery in relation to isolation or activation, injury chronicity, dosing regimen (single, repeat)

Adapted from reference (LaPrade et al., 2016)

4.2 Future Perspectives

4.2.1 Rabbit Model

The following information will be submitted as a manuscript - Liou, J. J., Iseki, T., Rothrauff, B. B., Kihara, S., Alexander, P. G., & Tuan, R. S. (in preparation) Application of platelet-rich plasma in combination with adipose stem cells encapsulated in three-dimensional hydrogel in a rabbit model of cartilage repair.

Rabbit subcutaneous adipose tissue was harvested from the dorsomedial line of six post-breeder New Zealand white rabbits (6-month-old female, average 4.0 kg, average 30 g of tissues

per rabbit) under an IACUC-approved and –exempted protocol (University of Pittsburgh). The adipose tissue was accessed through a longitudinal incision in the dorsomedial line (couple centimeters from the skull in the craniocaudal direction) (**Figure 25**). The adipose tissue was digested with 2 mg/mL Type I collagenase (Worthington Biochemical, Lakewood, NJ), 1 mg/mL trypsin (Invitrogen, Carlsbad, CA), and 2% antibiotic-antimycotic (Invitrogen) in Dulbecco’s Modified Eagle’s Medium (DMEM; Invitrogen) at 2 mL per gram of tissue at 37 °C for 3 hours. After enzyme digestion, rabbit ASCs were filtered, centrifuged at 1,200 rpm for 5 minutes, and expanded in growth medium (DMEM, 10% fetal bovine serum [Gemini Bio Products, West Sacramento, CA], and 1% antibiotic-antimycotic). The demographic profile of rabbit donors is listed in Appendix.

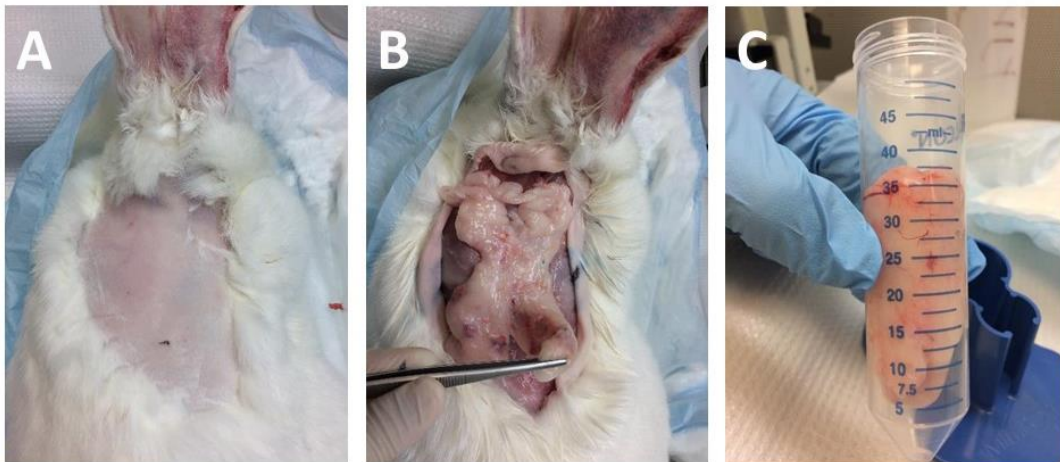


Figure 25. Isolation of rabbit adipose tissue.

(A) Donor rabbits were euthanized, and hair was shaved using a razor. (B) After a 10 cm incision, H-shape fat tissue was exposed. (C) Rabbit adipose tissue was harvested from the dorsomedial line of the donor rabbit and collected in 50 mL conical tubes prior to enzyme digestion (n = 6 rabbits).

Tri-lineage differentiation of rabbit ASCs was analyzed via monolayer culture in: (1) chondrogenic medium (DMEM, 1% v/v antibiotic-antimycotic, 10 µg/mL insulin-transferrin-selenium (ITS; Invitrogen, Carlsbad, CA), 0.1 µM dexamethasone, 40 µg/mL proline, 50 µg/mL ascorbic acid, and 10 ng/mL recombinant human transforming growth factor-β3 [PeproTech #100-36E, Rocky Hill, NJ]); (2) osteogenic medium (DMEM, 10% v/v FBS, 1% v/v antibiotic-antimycotic, 0.1 µM dexamethasone, 10 mM β-glycerophosphate, and 50 µg/mL ascorbic acid); and (3) adipogenic medium (DMEM, 10% v/v FBS, 1% v/v antibiotic-antimycotic, 1 µg/mL ITS, 1 µM dexamethasone, and 0.5 mM 3-isobutyl-1-methylxanthine (IBMX)). On day 21, the cultures were stained with Alcian Blue, Alizarin Red, and Oil Red O, using standard histological staining protocols, to assess chondrogenesis, osteogenesis, and adipogenesis, respectively.

Briefly, 15 grams of gelatin (Sigma-Aldrich) was dissolved in 500 mL H₂O at 37°C, and 15 mL of methacrylic anhydride (Sigma-Aldrich) was added dropwise (H. Lin, Cheng, et al., 2014). The mixture was incubated with shaking at 150 rpm for 24 hours, then dialyzed against water for four days, and methacrylated gelatin lyophilized for storage. The photoinitiator, lithium phenyl-2,4,6-trimethylbenzoylphosphinate (LAP), was prepared as described by Fairbanks et al. For methacrylated hyaluronic acid, 5 gram of sodium hyaluronate (66kDa, Lifecore Biomedical, Chaska, MN) was dissolved in 500 mL H₂O at 37°C, and 15 mL of methacrylic anhydride (Sigma-Aldrich) was added dropwise. At the end of every hour in the first 5 hours, pH was adjusted to 7. The mixture was then incubated with shaking at 150 rpm for 24 hours, dialyzed against water for four days, and lyophilized for storage. To fabricate hydrogels, methacrylated gelatin and methacrylated hyaluronic acid were dissolved in Hank's Balanced Salt Solution (HBSS) with final concentration at 9% and 1% (w/v), respectively. pH was adjusted to 7.4 with 10 N NaOH and 1% antibiotic-antimycotic and 0.15% w/v LAP were added.

Nine ml of blood from each New Zealand White Rabbit was drawn and collected into 1 ml of filter sterilized 3.8% Na-citrate (3.8 g in 100 ml ddH₂O) pre-loaded into the collection syringe. A 50 μ l aliquot was removed from the syringe to obtain the platelet concentration, total white blood cell count, and neutrophil cell count. The rest of the syringe was immediately transferred to a 15 ml conical tube and centrifuged for 10 min at 200 x g. The clear layer (approximately 3 ml) was removed from the red blood cell pellet being careful not to remove any of the leukocyte-rich white interface. The clear layer was spun again for 10 min at 1000 x g. The supernatant was carefully removed leaving lower 500 μ l and the pellet undisturbed. The supernatant was placed in a separate 15 ml conical as platelet-poor plasma (PPP), from which a platelet count was obtained. The pellet in the remaining 500 μ l was resuspended and considered the platelet-rich plasma (PRP). Platelets were counted in both fractions and the whole blood after red blood cell lysis using a standard hemocytometer and an inverted microscope with 40X objective. At this point, the autologous PRP was ready for use. Detailed information of each rabbit PRP was listed in Appendix. One mL of whole blood or PRP was collected and sent to Marshfield Labs (Marshfield Labs, Marshfield, WI) for complete blood count (CBC) with automated differential within 24 hours at ambient temperature. CBC data included platelet number, white blood cell number, and the percentage of neutrophils, lymphocytes, monocytes, eosinophils, and basophils.

Another one mL of PRP was aliquoted and frozen for ELISA microarray. A 41-growth factor and cytokine profile were quantified using ELISA Microarray (RayBiotech #QAH-BMA-1000, Norcross, GA). Briefly, serial dilutions of cytokine standards and 100 μ L of samples were prepared. Sample diluent was added and incubated for 30 minutes prior to blocking for 1 hour. Biotinylated Antibody and Cy3 Equivalent Dye-Streptavidin were added separately for signal

amplification. The sample slide was prepared and shipped to the manufacturer for subsequent analysis. Each sample for each protein was four replicates.

Thirty mature New Zealand white rabbits (9-month-old, averaged 4 kg, 15 male and 15 female) were divided into six experimental groups: (1) sham (sham control), joint capsule was cut open and closed; (2) defect (defect only control), defect was left without treatment and closed; (3) hydrogel (scaffold only control), defect was filled with 10% methacrylated gelatin/1% methacrylated hyaluronic acid/0.15% photoinitiator (hereinafter GelMA); (4) hydrogel + ASC, defect was filled with cell suspension at 20×10^6 cells/ml in 10% GelMA; (5) hydrogel + PRP, defect was filled with PRP in 10% GelMA; and (6) hydrogel + ASC + PRP, defect was filled with cell suspension at 20×10^6 cells/ml and PRP in GelMA.

Each group had five rabbits, and each rabbit was operated bilaterally (n=10 knees per group). Briefly, the knee joints were opened via a medial parapatellar incision, and the patella was reflected laterally to expose the femoral articular surface of the joint. A critical-sized defect of 5 mm in diameter and 5 mm in depth was created on the trochlear groove. To differentiate the donor cells from host cells, ASCs were pre-treated with CellTracker CM-DiI Dye (Thermo Fisher, Pittsburgh, PA) at 37 °C for 5 minutes and cooled on ice for 15 minutes before cell implantation. For ASC-containing groups, ASC pellets were then resuspended in GelMA solution at a final concentration of 20×10^6 cells/mL, and the suspension transferred to a 1.5 mL tube, and 100 μ L was injected to the defect. The cell/monomer mixture was subjected to photoillumination (395 nm) for 5 minutes, forming a cell-laden GelMA hydrogel. For PRP-containing groups, autologous PRP was mixed with allogenic ASC suspension prior to injection to the defect sites. The demographic information of 30 rabbits can be found in Appendix.

In this study, ASCs obtained from rabbit subcutaneous tissues were used in allogeneic cell transplantation. Rabbit ASCs from all six donor rabbits were able to differentiate into adipogenic, osteogenic, and chondrogenic lineages (**Figure 26**). Pellet cultures consisting of 2.5×10^5 ASCs were maintained in chondrogenic medium for 3 weeks.

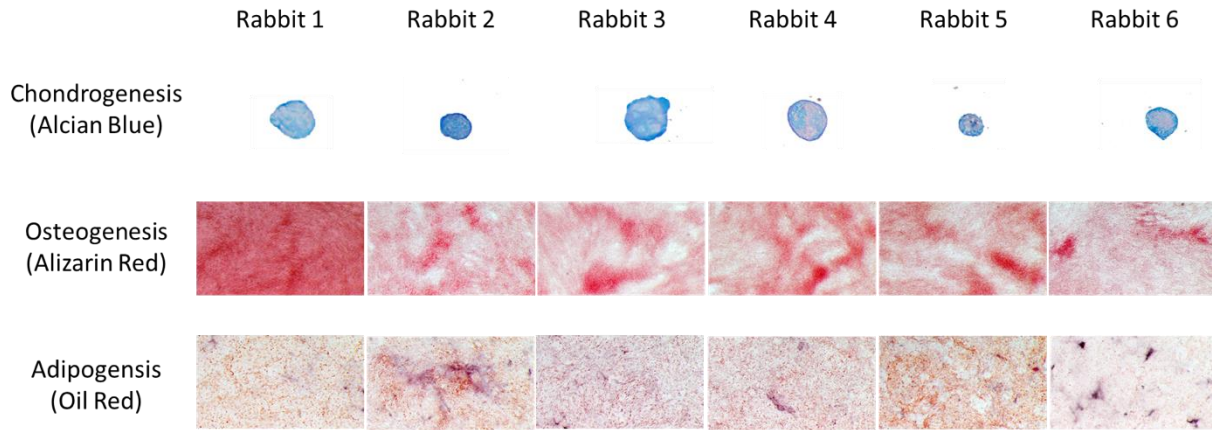


Figure 26. Tri-lineage differentiation of rabbit ASCs.

Rabbit ASCs were cultured in chondrogenic, osteogenic, or adipogenic medium for 21 days and stained with Alcian Blue, Alizarin Red, and Oil Red O, respectively.

Thirty New Zealand white rabbits were divided into 6 treatment groups: defect only (negative control), hydrogel only, hydrogel+cells, hydrogel+PRP, hydrogel+cells+PRP, and sham (positive control). An incision was made from the lateral side of the articular joint. The joint capsule was open and trochlear groove was exposed (**Figure 27A**). For all groups except Sham, an osteochondral defect with 5 mm in diameter and 5 mm in depth was created on the trochlear groove using sterilized drill bits (**Figure 27B**). For hydrogel groups, 0.1 mL of photocrosslinkable hydrogel solution (or cell-containing hydrogel solution) was injected to the defect and photopolymerized for 5 minutes (**Figure 27C**). The joint capsule and the skin layers were closed.

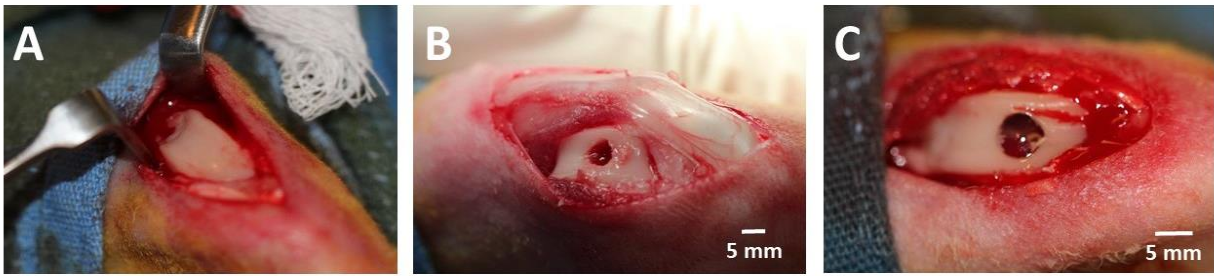


Figure 27. Cell implantation in rabbit osteochondral defects.

(A) An incision was made from lateral side and joint capsule was open to expose the trochlear groove. (B) An osteochondral defect (5 mm diameter, 5 mm depth) was created on the trochlear groove. (C) Photocrosslinkable hydrogel solution (0.1 mL) was injected to the defect and photo-polymerized for five minutes before wound closure.

An application of VEGF-depleted PRP is presented and compared to the outcomes of whole PRP, cell only control, hydrogel only control, defect (negative control), and sham (positive control). The novelty of this study is: (1) to the best of our knowledge, the application of VEGF-depleted PRP has not been examined in a translational context; (2) most of the osteochondral defect repair studies do not report the outcomes of sham or positive control, which would be more informative of how PRP treatment benefits osteochondral defect repair; and (3) lastly, almost all published studies do not report the mechanical properties of neo-tissue. As mentioned earlier, the mechanical strength is the critical factor to the restoration of cartilage function.

Previously, a study of BMSCs and ADSCs seeded within PRP scaffold in a rabbit model with an osteochondral defect of 4 mm diameter and 3 mm depth was analyzed at nine weeks (Xie et al., 2012). This study compared the four different groups of unfilled (untreated group), PRP, PRP-ADSC, and PRP-BMSC, with 9 rabbits (18 defects) each and found that PRP-BMSC group significantly improved cartilage repair (Xie et al., 2012). However, cell only group was not

included; therefore, it was difficult to conclude whether the PRP or cells contributed to the improvement of cartilage repair.

Lee et al. tested the effects of rabbit synovial membrane-derived mesenchymal stem cells and rabbit PRP on osteochondral defect (4 mm diameter 3 mm depth) repair in 81 rabbits (J.-C. C. Lee et al., 2013). In the first four weeks, PRP-SDSC group showed significant improvement on defect repair; however, the repair level was very similar between the groups with and without stem cells at 12 weeks and 24 weeks (J.-C. C. Lee et al., 2013).

A comparison of rabbit PRP and saline (placebo) was performed in an osteochondral defect model (3 mm diameter 5 mm depth) in 12 rabbits at 3, 6, and 12 weeks. ICRS histological score was significantly better in PRP group (Smyth et al., 2016). However, no biochemical or mechanical analysis was performed, and the sample size might be too small to reach significant difference (Smyth et al., 2016).

Liu et al. reported that the use of a photo-crosslinkable PRP hydrogel, compared to non-crosslinkable PRP hydrogel and defect only groups, significantly improved cartilage repair at 12 weeks in a rabbit model (Xiaolin Liu et al., 2017). Unfortunately, manipulation of autologous PRP is not yet allowed in the operating room and to commercialize this photo-crosslinkable PRP hydrogel is challenging.

Several studies compared PRP treatment (usually in cell-containing scaffolds) to defect only group. These comparisons make the data interpretation complicated due to the following reasons: (i) PRP acts as an adjunct that provides growth factors and anti-inflammatory mediators. Rather than making extracellular matrix itself, the cells derived either from cell implantation or subchondral bleeding could contribute to the production of cartilage extracellular matrix, including collagen and aggrecan. (ii) The defect size is smaller than the critical size in most of the studies.

The critical size of a cartilage defect in rabbits is 5 mm in diameter (Ahern, Parvizi, Boston, & Schaer, 2009; Chu, Szczodry, & Bruno, 2010; Xiaohua Liu, Jin, & Ma, 2011). Smaller diameters may lead to endogenous healing and misinterpretation of treatment outcomes. It is difficult to differentiate between the contribution of endogenous healing versus cell-based therapy (Ahern et al., 2009; Chu et al., 2010; Xiaohua Liu et al., 2011). In fact, studies have shown that for chondral or osteochondral defect smaller than the critical size, the defect heals naturally. (iii) PRP preparation protocol and composition are not reported in detail. Dohan Ehrenfest et al. summarized current protocols for pure PRP, leukocyte-rich PRP, pure platelet-rich fibrin (PRF), and leukocyte-rich PRF based on the speed and time of centrifugation and portion collected after centrifugation (Dohan Ehrenfest et al., 2009). Lack of information on whether it is PRP or PRF would make it challenging to compare between studies; we, therefore, summarize several relevant rabbit PRP studies for comparison (**Table 3**).

One of the limitations of our study is that the TGF β 3 release profile of hydrogel in all groups was not evaluated in vitro. Prior to cell implantation, 2 μ g/mL of TGF β 3 was added to the hydrogel solution. This concentration is two hundred times higher than the standard concentration of 10 ng/mL for in vitro experiments.

Recently, leukocytes were reported to be an inhibitory factor in PRP, acting to suppress chondrogenesis and cartilage repair (Xu et al., 2017). A research study compared PRP with leukocyte-reduced PRP and concluded that leukocytes in PRP downregulated the synthesis of collagen types I and III (González, López, Álvarez, Pérez, & Carmona, 2016). PRP also inhibited the mechanically induced catabolic and inflammatory responses in chondrocytes in vitro, with early addition of PRP showing the most significant benefits. The effect of leukocyte on cartilage repair was not compared in our study. Another limitation is that the PRP used in our study is the

liquid form of platelet-rich plasma. Several studies have suggested that platelet-rich fibrin, known as PRF, has better healing potential when compared to liquid-like platelet-rich plasma (Maruyama et al., 2017).

In conclusion, the application of VEGF-depleted PRP is presented and compared to the outcomes of whole PRP, cell only control, hydrogel only control, defect (negative control), and sham (positive control) in our study. We provided the information on the potential application of VEGF-depleted PRP for cartilage repair.

Table 3. Relevant PRP rabbit studies

Condition	Intervention	PRP Specifics	Outcome	Reference
4 mm diameter 3 mm depth on trochlear groove	3 groups: defect, PRP, and PRP+SDSC (n=9 each) 4, 12, 24 weeks	Pure PRP or leukocyte-rich PRP (2000 rpm for 5 min, 3000 rpm for 10 min)	Both PRP and PRP+SDSC have neo-cartilage formation based on Safranin O staining and collagen type II staining; PRP+SDSC had regular cartilage surface integration compared to PRP group.	(J.-C. C. Lee et al., 2013)
5 mm diameter 4 mm depth defect on trochlear groove	3 groups: defect, PLGA, and PLGA+PRP (n=8 each)	Pure PRP or leukocyte-rich PRP (800 rpm for 15 min, 2000 rpm for 15 min)	PLGA+PRP group has the best tissue morphology, matrix staining and total score.	(Y. Sun, Feng, Zhang, Chen, & Cheng, 2010)
3 mm diameter 5 mm depth defect on femoral condyles	2 groups: intra-articular injection of PRP or saline (n=4 each) 3, 6, 12 weeks	Leukocyte-rich PRP (1200 x g for 17 min)	No significant improvement was detected because of PRP administration.	(Smyth et al., 2016)
5 mm diameter 5 mm depth trochlear groove	3 groups: defect, PRP, or injectable PRF (n=4 each) 4 and 12 weeks	Pure PRP (900 x g for 5 min, 2000 x g for 15 min); leukocyte-rich PRF (60 x g for 5 min)	At week 12, no significant difference was observed between macroscopically but injectable PRF had the highest ICRS score microscopically.	(Abd El Raouf et al., 2017)
4 mm diameter 3 mm depth trochlear groove	6 groups: defect, PRP, PRF, gelatin+SDF1, PRP+SDF1, or PRF+SDF1 (n=6 each) 4 weeks	Pure PRP or leukocyte-rich PRP (2000 rpm for 5 min, 3000 rpm for 10 min) ; CaCl ₂ added before use; leukocyte-rich PRF (3000 rpm for 10 min)	PRF+SDF1 is the best based on collagen type II staining and toluidine blue staining among all six groups at 4 weeks.	(Bahmanpour, Ghasemi, Sadeghi-Naini, & Kashani, 2016)

Table 3 (continued)

Trochlear groove	4 groups: control, hydrogel, hydrogel+cells, +cells+PRP 4 weeks	Pure PRP or leukocyte-rich PRP (1500 rpm for 10 min, 3000 rpm for 10 min)	Hydrogel+cells+PRP is the best at 4 weeks.	(H. R. Lee, Park, Joung, Park, & Do, 2012)
Trochlear groove	3 groups: defect, PRP gel, photo-crosslinkable PRP gel (n=8 each) 12 weeks	Pure PRP or leukocyte-rich PRP (800 rpm for 15 min, 2000 rpm for 15 min)	Photo-crosslinkable PRP gel has controlled release of TGF β and the best staining of collagen type II at 12 weeks.	(Xiaolin Liu et al., 2017)

Note: PLGA: poly(lactic-co-glycolic acid); SDSC: synovial membrane-derived mesenchymal stem cells; SDF1: stromal cell-derived factor-1.

4.2.2 Goat Model

Under IACUC-approved and -exempted protocol #17081143, we also examined the application of PRP, more specifically, anti-VEGF neutralized PRP, in a caprine model. The demographic information can be found in the Appendix. The two treatment groups were hydrogel and cells with or without anti-VEGF neutralized leukocyte-poor PRP. Cells were derived from the stromal vascular fraction of infrapatellar fat pad. More specifically, infrapatellar fat pad was surgically removed and collected in the operating room. Fat was minced and digested in 0.6 % collagenase type I at 37 degrees C for 60 minutes. Stromal vascular fraction was prepared for each goat and resuspended in 10% methacrylated gelatin and 1% methacrylated hyaluronan containing 2 ug/ml TGF β 3. The cell-hydrogel mixture was prepared for cartilage defect implantation.

The significance of this model is that goat knee is large, active, and anatomically similar to human knee. The proportions of cartilage and subchondral bone in goats are closer to humans than other animal models. We utilized caprine model to assess the clinical application for articular

cartilage implants. Previously, studies have reported the mechanical and/or histological performance of implants for cartilage repair and usually included 3-6 animals per group (Jurgens et al., 2013; Levingstone et al., 2016; Lind, Larsen, Clausen, Osther, & Everland, 2008; Miot et al., 2012; Pei, Fan, Zhang, Zhang, & Yu, 2014; van Bergen et al., 2013; Zhu, Zhang, Man, Ma, & Hu, 2011). We also reviewed literature for appropriate experimental design and sample size (Fortier, Hackett, & Cole, 2011; Johnson & Frisbie, 2016). A comparison of saline and leukocyte-rich PRP (Biomet: 3200 rpm 15 min) for osteochondral defect repair was reported; however no significant difference was detected between the saline and the PRP group at 24 weeks (n=8 each) (van Bergen et al., 2013).

The novelty of this study is we utilized autologous cells from infrapatellar fat pads that is translational to clinics. To the best of our knowledge, no studies have yet reported the application of anti-VEGF neutralized leukocyte-poor PRP. In Chapter 3, we identified the potential inhibitory effect of VEGF; literatures have indicated the implications of leukocyte in cartilage repair; therefore, we expect the anti-VEGF neutralization can improve the potential application of PRP.

4.2.3 Future Directions

One of the limitations in this dissertation is that PRP pooled from several donors was used, to examine the overall effect of dosage and treatment duration on IFP-ASC chondrogenesis for a given PRP preparation. It is noteworthy that Mazzocca et al. reported that platelet and white blood cell numbers vary between individuals and repetitive withdraws of the same individual (Mazzocca, 2012). We may increase the sample size and examine the effect of different donors individually. We may also perform ELISA microarray to quantify the growth factor and cytokine concentration in each PRP preparation, and correlate the observed chondrogenic potential to the individual

growth factor and cytokine profile, in order to identify more chondro-inhibitory and/or -stimulatory factors and optimize the PRP treatments.

Another limitation is that the effect of leukocyte- and platelet-rich plasma (L-PRP) and pure platelet-rich plasma (P-PRP) was not compared in this dissertation. Several studies have reported that L-PRP and P-PRP prepared from the same batch of whole blood have significantly different growth factor and cytokine profile and different osteochondral defect repair outcome in animal models (Osterman et al., 2015; Sundman, Cole, & Fortier, 2011; Xu et al., 2017).

As mentioned earlier, PRP can be in liquid form or gel form (known as platelet-rich fibrin or PRF), dependent on the preparation protocol and the presence of platelet activator. It has been shown that PRP and PRF also have different repair outcomes in animal models (Maruyama et al., 2017).

These directions can provide information on the potential application of PRP in combination with cell-based therapy for cartilage repair. Our goal is to develop an optimal cell and biologic formulation for a potential point-of-care treatment of post-traumatic and focal cartilage defects, for the restoration of joint function and improvement of the quality of life.

Appendix A

Table 4. Demography of human whole blood donors

Whole Blood Donors	Gender	Age
Donor 1	F	48
Donor 2	M	17
Donor 3	F	55
Donor 4	F	24
Donor 5	M	39
Donor 6	M	26

Table 5. Sequences of human RT-PCR primers

Gene	Forward Sequence (5' to 3')	Reverse Sequence (5' to 3')
18S rRNA	GTA ACC CGT TGA ACC CCA TT	CCA TCC AAT CGG TAG TAG CG
SOX9	CTG AGC AGC GAC GTC ATC TC	GTT GGG CGG CAG GTA CTG
COL2	GGA TGG CTG CAC GAA ACA TAC CGG	CAA GAA GCA GAC CGG CCC TAT G
ACAN	GCT ACA CTG GCG AGC ACT GTA ACA T	GCG CCA GTT CTC AAA TTG CAT GGG
COL10	GTG TTT TAC GCT GAA CGA TAC CAA	ACC TGG TTT CCC TAC AGC TGA TG
MMP13	ACT GAG AGG CTC CGA GAA ATG	GAA CCC CGC ATC TTG GCT T
COL1	GGG CTC TAA TGA TGT TGA ACT TGT	ATG ATT GTC TTT CCC CAT TCA TTT
RUNX2	CAA CCA CAG AAC CAC AAG TGC G	TGT TTG ATG CCA TAG TCC CTC C
VEGF	GCC TTG CCT TGC TGC TCT AC	GCA TGG TGA TGT TGG ACT CCT C
KDR1	AGA CGG ACA GTG GTA TGG TTC	CCG AGT CAG GCT GGA GAA TC
FLT1	TTG ATG ACT ACC AGG GCG ACA G	GGA GTA CAG GAC CAC CGA GTT G
NRP1	GGC TCT CAC AAG ACC TTC TG	ACT CCT CTG GCT TCT GGT AG
NRP2	AAA CGG CAA GGA CTG GGA ATA C	TGG TTG TCT CTT CGC TCT TCA C

Table 6. Antibodies for flow cytometry and antibody neutralization

Antibody	Company	Catalog Number	Isotype	Application
CD31	BD Biosciences	558068	Mouse IgG	Flow Cytometry
CD34	BD Biosciences	550761	Mouse IgG	Flow Cytometry
CD44	BD Biosciences	550989	Mouse IgG	Flow Cytometry
CD45	BD Biosciences	560975	Mouse IgG	Flow Cytometry
CD73	BD Biosciences	550257	Mouse IgG	Flow Cytometry
CD90	BD Biosciences	555595	Mouse IgG	Flow Cytometry
CD105	BD Biosciences	560839	Mouse IgG	Flow Cytometry
VEGFR1	R&D Systems	FAB321P	Mouse IgG	Flow Cytometry
VEGFR2	R&D Systems	FAB357P	Mouse IgG	Flow Cytometry
VEGFR3	R&D Systems	FAB3492P	Mouse IgG	Flow Cytometry
TGF β R2	R&D Systems	FAB2411P	Goat IgG	Flow Cytometry
PDGFR β	BD Biosciences	558821	Mouse IgG	Flow Cytometry
VEGF	R&D Systems	MAB293	Mouse IgG	Antibody Neutralization
IgG	R&D Systems	MAB004	Mouse IgG	Antibody Neutralization
VEGFR1	Abcam	ab32152	Rabbit IgG	Antibody Neutralization
VEGFR2	Abcam	ab2349	Rabbit IgG	Antibody Neutralization

Table 7. Demographic profile of donor rabbits for rabbit cell isolation

Rabbit Donors	Gender	Weight (kg)	Adipose Tissue (g)	Stromal Vascular Fraction
Rabbit 1	F	4.4	61.0	1.0 x 10 ⁷ cells
Rabbit 2	F	3.7	33.9	1.6 x 10 ⁷ cells
Rabbit 3	F	3.6	19.7	1.5 x 10 ⁷ cells
Rabbit 4	F	3.6	23.7	1.6 x 10 ⁷ cells
Rabbit 5	F	4.0	36.8	1.8 x 10 ⁷ cells
Rabbit 6	F	3.1	14.9	0.2 x 10 ⁷ cells

Under IACUC-approved and -exempted protocol #15063708 and #16025372

Table 8. Information of rabbit implantation

Rabbit #	DLAR #	Gender	Treatment	Operation Date	Sacrifice Date
1	R691-17	F	Hydrogel	2/26/2018	5/21/2018
2	R692-17	F	Hydrogel + Cells	2/26/2018	5/21/2018
3	R695-17	F	Defect	3/1/2018	5/24/2018
4	R696-17	F	Hydrogel	3/1/2018	5/24/2018
5	R698-17	F	Sham	3/5/2018	5/28/2018
6	R699-17	F	Sham	3/5/2018	5/28/2018
7	R704-17	M	Sham	3/5/2018	5/28/2018
8	R702-17	F	Defect	3/8/2018	5/31/2018
9	R707-17	M	Defect	3/8/2018	5/31/2018
10	R708-17	M	Defect	3/8/2018	5/31/2018
11	R689-17	F	Hydrogel + Cells	3/21/2018	6/13/2018
12	R690-17	F	Hydrogel + Cells	3/21/2018	6/13/2018
13	R709-17	M	Hydrogel + Cells	3/21/2018	6/13/2018
14	R710-17	M	Hydrogel + Cells	3/21/2018	6/13/2018
15	R700-17	F	Hydrogel	3/28/2018	6/20/2018
16	R701-17	F	Hydrogel	3/28/2018	6/20/2018
17	R711-17	M	Sham	3/28/2018	6/20/2018
18	R712-17	M	Hydrogel + Cells + PRP	3/28/2018	6/20/2018
19	R703-17	F	Hydrogel + PRP	4/2/2018	6/25/2018
20	R713-17	M	Hydrogel + PRP	4/2/2018	6/25/2018
21	R714-17	M	Hydrogel + PRP	4/2/2018	6/25/2018
22	R693-17	F	Hydrogel + Cells + PRP	4/9/2018	7/2/2018
23	R716-17	M	Hydrogel + Cells + PRP	4/9/2018	7/2/2018
24	R717-17	M	Hydrogel + Cells + PRP	4/9/2018	7/2/2018
25	R718-17	M	Hydrogel + Cells + PRP	4/9/2018	7/2/2018
26	R314-18	M	Hydrogel + PRP	5/10/2018	8/2/2018
27	R315-18	M	Sham	5/10/2018	8/2/2018
28	R316-18	M	Defect	5/10/2018	8/2/2018
29	R317-18	F	Hydrogel + PRP	5/14/2018	8/6/2018
30	R318-18	F	Hydrogel + Cells + PRP	5/14/2018	8/6/2018
31	R319-18	F	Hydrogel + Cells + PRP	5/14/2018	8/6/2018

Under IACUC-approved and -exempted protocol #17106357; data updated on May 14, 2018.

Table 9. Complete blood count of whole blood and PRP for rabbit surgery

DLAR #		Platelet x 10³/μL	WBC x 10³/μL	Neutrophil	Lymphocyte	Monocyte	Eosinophil	Basophil
R693-17	WB	152	5.5	25%	65%	7%	1%	2%
	PRP	331	1.5	26%	48%	22%	4%	*
R703-17	WB	252	6.6	30%	54%	4%	2%	10%
	PRP	389	0.3	*	*	*	*	*
R712-17	WB	*	*	*	*	*	*	*
	PRP	63	0.1	*	*	*	*	*
R713-17	WB	300	5.4	34%	60%	1%	2%	3%
	PRP	392	0.1	*	*	*	*	*
R714-17	WB	217	7.4	41%	48%	6%	3%	2%
	PRP	147	0.3	*	*	*	*	*
R717-17	WB	308	7.2	30%	62%	5%	1%	2%
	PRP	420	1.0	*	*	*	*	*
R718-17	WB	449	4.8	45%	49%	6%	*	*
	PRP	942	0.1	*	*	*	*	*
R314-18	WB	324	6.4	27%	64%	4%	3%	2%
	PRP	563	1.3	*	*	*	*	*
R317-18	WB	249	5.9	31%	62%	4%	1%	2%
	PRP	238	1.6	*	*	*	*	*

Under IACUC-approved and -exempted protocol #17106357; WB: whole blood; PRP: platelet-rich plasma; WBC: white blood cell; *: no results; data updated on May 14, 2018.

Table 10. Information of goat implantation

Goat #	DLAR #	Gender	Treatment	Surgery Date	Sacrifice Date
1	G2-18	F	Hydrogel + Cells	2/22/2018	8/22/2018
2	G3-18	F	Hydrogel + Cells	2/22/2018	8/22/2018
3	G9-18	F	Hydrogel + Cells	3/15/2018	9/15/2018
4	G10-18	F	Hydrogel + Cells	3/15/2018	9/15/2018
5	G1-18	F	Hydrogel + Cells	3/22/2018	9/22/2018
6	G4-18	F	Hydrogel + Cells	3/22/2018	9/22/2018
7	G5-18	F	Hydrogel + Cells + Anti VEGF Neutralized PRP	3/26/2018	9/26/2018
8	G6-18	F	Hydrogel + Cells + Anti VEGF Neutralized PRP	3/26/2018	9/26/2018
9	G7-18	F	Hydrogel + Cells + Anti VEGF Neutralized PRP	3/29/2018	9/29/2018
10	G8-18	F	Hydrogel + Cells + Anti VEGF Neutralized PRP	3/29/2018	9/29/2018

Under IACUC-approved and -exempted protocol #17081143; data updated on May 14, 2018.

Bibliography

- Abd El Raouf, M., Wang, X., Miusi, S., Chai, J., Mohamed AbdEl-Aal, A. B., Nefissa Helmy, M. M., ... Miron, R. J. (2017). Injectable-platelet rich fibrin using the low speed centrifugation concept improves cartilage regeneration when compared to platelet-rich plasma. *Platelets*, pp. 1–9. <http://doi.org/10.1080/09537104.2017.1401058>
- Ahearne, M., Buckley, C. T., & Kelly, D. J. (2011). A growth factor delivery system for chondrogenic induction of infrapatellar fat pad-derived stem cells in fibrin hydrogels. *Biotechnology and Applied Biochemistry*, *58*(5), 345–52. <http://doi.org/10.1002/bab.45>
- Ahearne, M., Liu, Y., & Kelly, D. J. (2014). Combining freshly isolated chondroprogenitor cells from the infrapatellar fat pad with a growth factor delivery hydrogel as a putative single stage therapy for articular cartilage repair. *Tissue Engineering. Part A*, *20*(5–6), 930–9. <http://doi.org/10.1089/ten.TEA.2013.0267>
- Ahern, B. J., Parvizi, J., Boston, R., & Schaefer, T. P. (2009). Preclinical animal models in single site cartilage defect testing: a systematic review. *Osteoarthritis and Cartilage*, *17*(6), 705–713. <http://doi.org/10.1016/j.joca.2008.11.008>
- Akens, M. K., & Hurtig, M. B. (2005). Influence of species and anatomical location on chondrocyte expansion. *BMC Musculoskeletal Disorders*, *6*, 23. <http://doi.org/10.1186/1471-2474-6-23>
- Alegre-Aguarón, E., Desportes, P., García-Álvarez, F., Castiella, T., Larrad, L., & Martínez-Lorenzo, M. J. (2012). Differences in Surface Marker Expression and Chondrogenic Potential among Various Tissue-Derived Mesenchymal Cells from Elderly Patients with Osteoarthritis. *Cells Tissues Organs*, *196*(1), 231–240. <http://doi.org/10.1159/000334400>
- Allan, K. S., Pilliar, R. M., Wang, J., Grynblas, M. D., & Kandel, R. a. (2007). Formation of biphasic constructs containing cartilage with a calcified zone interface. *Tissue Engineering*, *13*(1), 167–177. <http://doi.org/10.1089/ten.2007.13.ft-302>
- Allerstorfer, S., Sonvilla, G., Fischer, H., Spiegl-Kreinecker, S., Gaughhofer, C., Setinek, U., ... Berger, W. (2008). FGF5 as an oncogenic factor in human glioblastoma multiforme: autocrine and paracrine activities. *Oncogene*, *27*(30), 4180–4190. <http://doi.org/10.1038/onc.2008.61>
- Almeida, H. V, Liu, Y., Cunniffe, G. M., Mulhall, K. J., Matsiko, A., Buckley, C. T., ... Kelly, D. J. (2014). Controlled release of transforming growth factor- β 3 from cartilage-extra-cellular-matrix-derived scaffolds to promote chondrogenesis of human-joint-tissue-derived stem cells. *Acta Biomaterialia*, *10*(10), 4400–9. <http://doi.org/10.1016/j.actbio.2014.05.030>

- Amable, P. R., Carias, R. B. V., Teixeira, M. V. T., da Cruz Pacheco, I., Corrêa do Amaral, R. J. F., Granjeiro, J. M., & Borojevic, R. (2013). Platelet-rich plasma preparation for regenerative medicine: optimization and quantification of cytokines and growth factors. *Stem Cell Research & Therapy*, *4*(3), 67. <http://doi.org/10.1186/scrt218>
- Amable, P. R., Teixeira, M. V. T., Carias, R. B. V., Granjeiro, J. M., & Borojevic, R. (2014). Mesenchymal stromal cell proliferation, gene expression and protein production in human platelet-rich plasma-supplemented media. *PLoS ONE*, *9*(8), e104662. <http://doi.org/10.1371/journal.pone.0104662>
- Andia, I., & Maffulli, N. (2013). Platelet-rich plasma for managing pain and inflammation in osteoarthritis. *Nature Reviews. Rheumatology*, *9*(12), 721–30. <http://doi.org/10.1038/nrrheum.2013.141>
- Bahmanpour, S., Ghasemi, M., Sadeghi-Naini, M., & Kashani, I. R. (2016). Effects of platelet-rich plasma & platelet-rich fibrin with and without Stromal cell-derived factor-1 on repairing full-thickness cartilage defects in knees of rabbits. *Iranian Journal of Medical Sciences*, *41*(6), 507–517.
- Bayar, A., Turhan, E., Ozer, T., Keser, S., Ege, A., & Erdem, Z. (2008). The fate of patellar tendon and infrapatellar fat pad after arthroscopy via central portal. *Knee Surgery, Sports Traumatology, Arthroscopy: Official Journal of the ESSKA*, *16*(12), 1114–20. <http://doi.org/10.1007/s00167-008-0612-0>
- Beitzel, K., Allen, D., Apostolakos, J., Russell, R. P., McCarthy, M. B. et., Gallo, G. J., ... Mazzocca, A. D. (2015). US definitions, current use, and FDA stance on use of platelet-rich plasma in sports medicine. *The Journal of Knee Surgery*, *28*(1), 29–34. <http://doi.org/10.1055/s-0034-1390030>
- Bertrand-Duchesne, M.-P., Grenier, D., & Gagnon, G. (2010). Epidermal growth factor released from platelet-rich plasma promotes endothelial cell proliferation in vitro. *Journal of Periodontal Research*, *45*(1), 87–93. <http://doi.org/10.1111/j.1600-0765.2009.01205.x>
- Betsch, M., Schnependahl, J., Thuns, S., Herten, M., Sager, M., Jungbluth, P., ... Abdel Aziz, M. T. (2013). Bone marrow aspiration concentrate and platelet rich plasma for osteochondral repair in a porcine osteochondral defect model. *PloS One*, *8*(8), e71602. <http://doi.org/10.1371/journal.pone.0071602>
- Bhumiratana, S., Eton, R. E., Oungoulian, S. R., Wan, L. Q., Ateshian, G. a, & Vunjak-Novakovic, G. (2014). Large, stratified, and mechanically functional human cartilage grown in vitro by mesenchymal condensation. *Proceedings of the National Academy of Sciences of the United States of America*, *111*(19), 6940–5. <http://doi.org/10.1073/pnas.1324050111>
- Brehm, W., Aklin, B., Yamashita, T., Rieser, F., Trüb, T., Jakob, R. P., ... Mainil-Varlet, P. (2006). Repair of superficial osteochondral defects with an autologous scaffold-free cartilage construct in a caprine model: implantation method and short-term results. *Osteoarthritis and Cartilage*, *14*(12), 1214–1226. <http://doi.org/10.1016/j.joca.2006.05.002>

- Brittberg, M., Lindahl, A., Nilsson, A., Ohlsson, C., Isaksson, O., & Peterson, L. (1994). Treatment of deep cartilage defects in the knee with autologous chondrocyte transplantation. *The New England Journal of Medicine*, 331(14), 889–95. <http://doi.org/10.1056/NEJM199410063311401>
- Brittberg, M., Nilsson, A., Lindahl, A., Ohlsson, C., & Peterson, L. (1996). Rabbit articular cartilage defects treated with autologous cultured chondrocytes. *Clinical Orthopaedics and Related Research*, (326), 270–83.
- Brown, T. D., Johnston, R. C., Saltzman, C. L., Marsh, J. L., & Buckwalter, J. A. (2006). Posttraumatic osteoarthritis: a first estimate of incidence, prevalence, and burden of disease. *Journal of Orthopaedic Trauma*, 20(10), 739–44. <http://doi.org/10.1097/01.bot.0000246468.80635.ef>
- Bruder, S. P., Jaiswal, N., & Haynesworth, S. E. (1997). Growth kinetics, self-renewal, and the osteogenic potential of purified human mesenchymal stem cells during extensive subcultivation and following cryopreservation. *Journal of Cellular Biochemistry*, 64(2), 278–294. [http://doi.org/10.1002/\(SICI\)1097-4644\(199702\)64:2<278::AID-JCB11>3.0.CO;2-F](http://doi.org/10.1002/(SICI)1097-4644(199702)64:2<278::AID-JCB11>3.0.CO;2-F)
- Campbell, K. A., Saltzman, B. M., Mascarenhas, R., Khair, M. M., Verma, N. N., Bach, B. R., & Cole, B. J. (2015). Does Intra-articular Platelet-Rich Plasma Injection Provide Clinically Superior Outcomes Compared with Other Therapies in the Treatment of Knee Osteoarthritis? A Systematic Review of Overlapping Meta-analyses. *Arthroscopy - Journal of Arthroscopic and Related Surgery*. <http://doi.org/10.1016/j.arthro.2015.03.041>
- Carlevaro, M. F., Cermelli, S., Cancedda, R., & Descalzi Cancedda, F. (2000). Vascular endothelial growth factor (VEGF) in cartilage neovascularization and chondrocyte differentiation: auto-paracrine role during endochondral bone formation. *Journal of Cell Science*, 113, 59–69.
- Centola, M., Abbruzzese, F., Scotti, C., Barbero, A., Vadalà, G., Denaro, V., ... Marsano, A. (2013). Scaffold-Based Delivery of a Clinically Relevant Anti-Angiogenic Drug Promotes the Formation of In Vivo Stable Cartilage. *Tissue Engineering Part A*, 19(17–18), 1960–1971. <http://doi.org/10.1089/ten.tea.2012.0455>
- Cerza, F., Carnì, S., Carcangiu, A., Di Vavo, I., Schiavilla, V., Pecora, A., ... Ciuffreda, M. (2012). Comparison between hyaluronic acid and platelet-rich plasma, intra-articular infiltration in the treatment of gonarthrosis. *American Journal of Sports Medicine*, 40(12), 2822–2827. <http://doi.org/10.1177/0363546512461902>
- Chu, C. R., Szczodry, M., & Bruno, S. (2010). Animal Models for Cartilage Regeneration and Repair. *Tissue Engineering Part B: Reviews*, 16(1), 105–115. <http://doi.org/10.1089/ten.teb.2009.0452>
- Delong, J. M., Russell, R. P., & Mazzocca, A. D. (2012). Platelet-rich plasma: The PAW classification system. *Arthroscopy - Journal of Arthroscopic and Related Surgery*, 28(7), 998–1009. <http://doi.org/10.1016/j.arthro.2012.04.148>

- Djouad, F., Rackwitz, L., Song, Y., Janjanin, S., & Tuan, R. S. (2009). ERK1/2 activation induced by inflammatory cytokines compromises effective host tissue integration of engineered cartilage. *Tissue Engineering. Part A*, *15*(10), 2825–2835. <http://doi.org/10.1089/ten.tea.2008.0663>
- do Amaral, R. J., Matsiko, A., Tomazette, M. R., Rocha, W. K., Cordeiro-Spinetti, E., Levingstone, T. J., ... Balduino, A. (2015). Platelet-rich plasma releasate differently stimulates cellular commitment toward the chondrogenic lineage according to concentration. *Journal of Tissue Engineering*, *6*, 1–14. <http://doi.org/10.1177/2041731415594127>
- Dohan Ehrenfest, D. M., Rasmusson, L., & Albrektsson, T. (2009). Classification of platelet concentrates: from pure platelet-rich plasma (P-PRP) to leucocyte- and platelet-rich fibrin (L-PRF). *Trends in Biotechnology*, *27*(3), 158–167. <http://doi.org/10.1016/j.tibtech.2008.11.009>
- Dragoo, J. L., Johnson, C., & McConnell, J. (2012). Evaluation and treatment of disorders of the infrapatellar fat pad. *Sports Medicine*. <http://doi.org/10.2165/11595680-000000000-00000>
- Dragoo, J. L., Samimi, B., Zhu, M., Hame, S. L., Thomas, B. J., Lieberman, J. R., ... Benhaim, P. (2003). Tissue-engineered cartilage and bone using stem cells from human infrapatellar fat pads. *The Journal of Bone and Joint Surgery. British Volume*, *85*(5), 740–747. <http://doi.org/10.1302/0301-620X.85B5.13587>
- Enomoto, H., Inoki, I., Komiya, K., Shiomi, T., Ikeda, E., Obata, K., ... Okada, Y. (2003). Vascular Endothelial Growth Factor Isoforms and Their Receptors Are Expressed in Human Osteoarthritic Cartilage. *The American Journal of Pathology*, *162*(1), 171–181. [http://doi.org/10.1016/S0002-9440\(10\)63808-4](http://doi.org/10.1016/S0002-9440(10)63808-4)
- Fairbanks, B. D., Schwartz, M. P., Bowman, C. N., & Anseth, K. S. (2009). Photoinitiated polymerization of PEG-diacrylate with lithium phenyl-2,4,6-trimethylbenzoylphosphinate: polymerization rate and cytocompatibility. *Biomaterials*, *30*(35), 6702–6707. <http://doi.org/10.1016/j.biomaterials.2009.08.055>
- Fedorovich, N. E., Schuurman, W., Wijnberg, H. M., Prins, H.-J., van Weeren, P. R., Malda, J., ... Dhert, W. J. A. (2012). Biofabrication of osteochondral tissue equivalents by printing topologically defined, cell-laden hydrogel scaffolds. *Tissue Engineering. Part C, Methods*, *18*(1), 33–44. <http://doi.org/10.1089/ten.TEC.2011.0060>
- Ferrara, N., Gerber, H.-P. P., & LeCouter, J. (2003). The biology of VEGF and its receptors. *Nature Medicine*, *9*(6), 669–676. <http://doi.org/10.1038/nm0603-669>
- Filardo, G., Kon, E., Pereira Ruiz, M. T., Vaccaro, F., Guitaldi, R., Di Martino, A., ... Marcacci, M. (2012). Platelet-rich plasma intra-articular injections for cartilage degeneration and osteoarthritis: Single- versus double-spinning approach. *Knee Surgery, Sports Traumatology, Arthroscopy*, *20*(10), 2082–2091. <http://doi.org/10.1007/s00167-011-1837-x>

- Filardo, G., Kon, E., Roffi, A., Di Matteo, B., Merli, M. L., & Marcacci, M. (2015). Platelet-rich plasma: why intra-articular? A systematic review of preclinical studies and clinical evidence on PRP for joint degeneration. *Knee Surgery, Sports Traumatology, Arthroscopy*, 23(9), 2459–2474. <http://doi.org/10.1007/s00167-013-2743-1>
- Fortier, L. A., Hackett, C. H., & Cole, B. J. (2011). The Effects of Platelet-Rich Plasma on Cartilage: Basic Science and Clinical Application. *Operative Techniques in Sports Medicine*, 19(3), 154–159. <http://doi.org/10.1053/j.otsm.2011.03.004>
- Freymann, U., Petersen, W., & Kaps, C. (2013). Cartilage regeneration revisited: entering of new one-step procedures for chondral cartilage repair. *Oapublishinglondon.Com*, 1(1964), 1–6.
- Gaissmaier, C., Fritz, J., Krackhardt, T., Flesch, I., Aicher, W. K., & Ashammakhi, N. (2005). Effect of human platelet supernatant on proliferation and matrix synthesis of human articular chondrocytes in monolayer and three-dimensional alginate cultures. *Biomaterials*, 26(14), 1953–1960. <http://doi.org/10.1016/j.biomaterials.2004.06.031>
- Gerber, H. P., Vu, T. H., Ryan, A. M., Kowalski, J., Werb, Z., & Ferrara, N. (1999). VEGF couples hypertrophic cartilage remodeling, ossification and angiogenesis during endochondral bone formation. *Nature Medicine*, 5(6), 623–628. <http://doi.org/10.1038/9467>
- González, J. C., López, C., Álvarez, M. E., Pérez, J. E., & Carmona, J. U. (2016). Autologous leukocyte-reduced platelet-rich plasma therapy for Achilles tendinopathy induced by collagenase in a rabbit model. *Scientific Reports*, 6. <http://doi.org/10.1038/srep19623>
- Haleem, A. M., Singergy, A. A. El, Sabry, D., Atta, H. M., Rashed, L. A., Chu, C. R., ... Abdel Aziz, M. T. (2010). The Clinical Use of Human Culture-Expanded Autologous Bone Marrow Mesenchymal Stem Cells Transplanted on Platelet-Rich Fibrin Glue in the Treatment of Articular Cartilage Defects: A Pilot Study and Preliminary Results. *Cartilage*, 1(4), 253–261. <http://doi.org/10.1177/1947603510366027>
- Han, E., Chen, S. S., Klisch, S. M., & Sah, R. L. (2011). Contribution of proteoglycan osmotic swelling pressure to the compressive properties of articular cartilage. *Biophysical Journal*, 101(4), 916–924. <http://doi.org/10.1016/j.bpj.2011.07.006>
- Hatfield, K., Ryningen, A., Corbascio, M., & Bruserud, O. (2006). Microvascular endothelial cells increase proliferation and inhibit apoptosis of native human acute myelogenous leukemia blasts. *International Journal of Cancer*, 119(10), 2313–2321. <http://doi.org/10.1002/ijc.22180>
- Hildner, F., Eder, M. J., Hofer, K., Aberl, J., Redl, H., van Griensven, M., ... Peterbauer-Scherb, A. (2015). Human platelet lysate successfully promotes proliferation and subsequent chondrogenic differentiation of adipose-derived stem cells: a comparison with articular chondrocytes. *Journal of Tissue Engineering and Regenerative Medicine*, 9(7), 808–18. <http://doi.org/10.1002/term.1649>
- Huang, B., Hu, J., & Athanasiou, K. (2016). Cell-based tissue engineering strategies used in the clinical repair of articular cartilage. *Biomaterials*, 98, 1–22.

- Hutton, D. L., Logsdon, E. A., Moore, E. M., Gabhann, F. Mac, Gimble, J. M., & Grayson, W. L. (2012). Vascular Morphogenesis of Adipose-Derived Stem Cells is Mediated by Heterotypic Cell-Cell Interactions. *Tissue Engineering. Part A*, 18(15–16), 1729–1740. <http://doi.org/10.1089/ten.tea.2011.0599>
- Johnson, S. A., & Frisbie, D. D. (2016). Cartilage Therapy and Repair in Equine Athletes. *Operative Techniques in Orthopaedics*, 26(3), 155–165. <http://doi.org/10.1053/j.oto.2016.06.005>
- Jurgens, W. J. F. M., Kroeze, R. J., Zandieh-Doulabi, B., van Dijk, A., Renders, G. A. P., Smit, T. H., ... Helder, M. N. (2013). One-Step Surgical Procedure for the Treatment of Osteochondral Defects with Adipose-Derived Stem Cells in a Caprine Knee Defect: A Pilot Study. *BioResearch Open Access*, 2(4), 315–325. <http://doi.org/10.1089/biores.2013.0024>
- Kakudo, N., Morimoto, N., Ogawa, T., Taketani, S., & Kusumoto, K. (2015). Hypoxia enhances proliferation of human adipose-derived stem cells via HIF-1 α activation. *PLoS ONE*, 10(10). <http://doi.org/10.1371/journal.pone.0139890>
- Karimian, E., Chagin, A. S., & Sävendahl, L. (2011). Genetic regulation of the growth plate. *Frontiers in Endocrinology*, 2, 113. <http://doi.org/10.3389/fendo.2011.00113>
- Kickler, T. S. (2006). Platelet biology - an overview. *Transfusion Alternatives in Transfusion Medicine*, 8(2), 79–85. <http://doi.org/10.1111/j.1778-428X.2006.00013.x>
- Kim, H.-J., Yeom, J. S., Koh, Y.-G., Yeo, J.-E., Kang, K.-T., Kang, Y.-M., ... Lee, C.-K. (2014). Anti-inflammatory effect of platelet-rich plasma on nucleus pulposus cells with response of TNF- α and IL-1. *Journal of Orthopaedic Research : Official Publication of the Orthopaedic Research Society*, 32(4), 551–6. <http://doi.org/10.1002/jor.22532>
- Kim, S. H., Jeong, J. H., Lee, S. H., Kim, S. W., & Park, T. G. (2008). Local and systemic delivery of VEGF siRNA using polyelectrolyte complex micelles for effective treatment of cancer. *Journal of Controlled Release*, 129(2), 107–116. <http://doi.org/10.1016/j.jconrel.2008.03.008>
- Koh, Y.-G., & Choi, Y.-J. (2012). Infrapatellar fat pad-derived mesenchymal stem cell therapy for knee osteoarthritis. *The Knee*, 19(6), 902–7. <http://doi.org/10.1016/j.knee.2012.04.001>
- Koh, Y.-G., Jo, S.-B., Kwon, O.-R., Suh, D.-S., Lee, S.-W., Park, S.-H., & Choi, Y.-J. (2013). Mesenchymal stem cell injections improve symptoms of knee osteoarthritis. *Arthroscopy : The Journal of Arthroscopic & Related Surgery : Official Publication of the Arthroscopy Association of North America and the International Arthroscopy Association*, 29(4), 748–55. <http://doi.org/10.1016/j.arthro.2012.11.017>
- Kohli, N., Wright, K. T., Sammons, R. L., Jeys, L., Snow, M., & Johnson, W. E. B. (2015). An In Vitro Comparison of the Incorporation, Growth, and Chondrogenic Potential of Human Bone Marrow versus Adipose Tissue Mesenchymal Stem Cells in Clinically Relevant Cell Scaffolds Used for Cartilage Repair. *Cartilage*, 6(4), 252–63. <http://doi.org/10.1177/1947603515589650>

- Kon, E., Filardo, G., Delcogliano, M., Fini, M., Salamanna, F., Giavaresi, G., ... Marcacci, M. (2010). Platelet autologous growth factors decrease the osteochondral regeneration capability of a collagen-hydroxyapatite scaffold in a sheep model. *BMC Musculoskeletal Disorders*, *11*, 220. <http://doi.org/10.1186/1471-2474-11-220>
- Kon, E., Filardo, G., Di Matteo, B., Perdisa, F., & Marcacci, M. (2013). Matrix assisted autologous chondrocyte transplantation for cartilage treatment: A systematic review. *Bone & Joint Research*, *2*(2), 18–25. <http://doi.org/10.1302/2046-3758.22.2000092>
- Kon, E., Mandelbaum, B., Buda, R., Filardo, G., Delcogliano, M., Timoncini, A., ... Marcacci, M. (2011). Platelet-rich plasma intra-articular injection versus hyaluronic acid viscosupplementation as treatments for cartilage pathology: from early degeneration to osteoarthritis. *Arthroscopy*, *27*(11), 1490–1501. <http://doi.org/10.1016/j.arthro.2011.05.011>
- Kondo, M., Yamaoka, K., Sakata, K., Sonomoto, K., Lin, L., Nakano, K., & Tanaka, Y. (2015). Contribution of the Interleukin-6/STAT-3 Signaling Pathway to Chondrogenic Differentiation of Human Mesenchymal Stem Cells. *Arthritis Rheumatol*, *67*(5), 1250–1260. <http://doi.org/10.1002/art.39036>
- Kronenberg, H. M. (2003). Developmental regulation of the growth plate. *Nature*. <http://doi.org/10.1038/nature01657>
- Krüger, J. P., Hondke, S., Endres, M., Pruss, A., Siclari, A., & Kaps, C. (2012). Human platelet-rich plasma stimulates migration and chondrogenic differentiation of human subchondral progenitor cells. *Journal of Orthopaedic Research : Official Publication of the Orthopaedic Research Society*, *30*(6), 845–52. <http://doi.org/10.1002/jor.22005>
- Kubo, S., Cooper, G. M., Matsumoto, T., Phillippi, J. A., Corsi, K. A., Usas, A., ... Huard, J. (2009a). Blocking vascular endothelial growth factor with soluble Flt-1 improves the chondrogenic potential of mouse skeletal muscle-derived stem cells. *Arthritis and Rheumatism*, *60*(1), 155–165. <http://doi.org/10.1002/art.24153>
- Kubo, S., Cooper, G. M., Matsumoto, T., Phillippi, J. a, Corsi, A., Usas, A., ... Huard, J. (2009b). Blocking VEGF with sFlt1 improves the chondrogenic potential of mouse skeletal muscle-derived stem cells, *60*(1), 155–165. <http://doi.org/10.1002/art.24153>.Blocking
- Kuo, C. K., Marturano, J. E., & Tuan, R. S. (2010). Novel strategies in tendon and ligament tissue engineering: Advanced biomaterials and regeneration motifs. *Sports Medicine, Arthroscopy, Rehabilitation, Therapy & Technology : SMARTT*, *2*(1), 20. <http://doi.org/10.1186/1758-2555-2-20>
- Langhans, M. T., Yu, S., & Tuan, R. S. (2015). Stem Cells in Skeletal Tissue Engineering: Technologies and Models. *Current Stem Cell Research & Therapy*.
- LaPrade, R. F., Dragoo, J. L., Koh, J. L., Murray, I. R., Geeslin, A. G., & Chu, C. R. (2016). AAOS research symposium updates and consensus: Biologic treatment of orthopaedic injuries. In *Journal of the American Academy of Orthopaedic Surgeons* (Vol. 24, pp. e62–e78). <http://doi.org/10.5435/JAAOS-D-16-00086>

- Lawrence, R. C., Felson, D. T., Helmick, C. G., Arnold, L. M., Choi, H., Deyo, R. A., ... Wolfe, F. (2008). Estimates of the prevalence of arthritis and other rheumatic conditions in the United States. Part I. *Arthritis and Rheumatism*, 58(1), 26–35. <http://doi.org/10.1002/art.23176>
- Lawrence, T. (2009). The Nuclear Factor NF- κ B Pathway in Inflammation. *Cold Spring Harbor Perspectives in Biology*, 1(6), 1–10. <http://doi.org/10.1101/cshperspect.a001651>
- Lee, C. H., Cook, J. L., Mendelson, A., Muioli, E. K., Yao, H., & Mao, J. J. (2010). Regeneration of the articular surface of the rabbit synovial joint by cell homing: A proof of concept study. *The Lancet*, 376(9739), 440–448. [http://doi.org/10.1016/S0140-6736\(10\)60668-X](http://doi.org/10.1016/S0140-6736(10)60668-X)
- Lee, H. R., Park, K. D. K. M., Joung, Y. K., Park, K. D. K. M., & Do, S. H. (2012). Platelet-rich plasma loaded hydrogel scaffold enhances chondrogenic differentiation and maturation with up-regulation of CB1 and CB2. *Journal of Controlled Release*, 159(3), 332–337. <http://doi.org/10.1016/j.jconrel.2012.02.008>
- Lee, J.-C. C., Min, H. J., Park, H. J., Lee, S., Seong, S. C., & Lee, M. C. (2013). Synovial membrane-derived mesenchymal stem cells supported by platelet-rich plasma can repair osteochondral defects in a rabbit model. *Arthroscopy - Journal of Arthroscopic and Related Surgery*, 29(6), 1034–1046. <http://doi.org/10.1016/j.arthro.2013.02.026>
- Lee, J. K., Lee, S., Han, S. A., Seong, S. C., & Lee, M. C. (2014). The effect of platelet-rich plasma on the differentiation of synovium-derived mesenchymal stem cells. *Journal of Orthopaedic Research*, 32(10), 1317–1325. <http://doi.org/10.1002/jor.22668>
- Lee, S., Nemeño, J. G. E., & Lee, J. I. (2016). Repositioning Bevacizumab: A Promising Therapeutic Strategy for Cartilage Regeneration. *Tissue Engineering Part B: Reviews*, 22(5), 341–357. <http://doi.org/10.1089/ten.teb.2015.0300>
- Levingstone, T. J., Ramesh, A., Brady, R. T., Brama, P. A. J., Kearney, C., Gleeson, J. P., & O'Brien, F. J. (2016). Cell-free multi-layered collagen-based scaffolds demonstrate layer specific regeneration of functional osteochondral tissue in caprine joints. *Biomaterials*, 87, 69–81. <http://doi.org/10.1016/j.biomaterials.2016.02.006>
- Lin, H., Cheng, A. W.-M., Alexander, P. G., Beck, A. M., & Tuan, R. S. (2014). Cartilage Tissue Engineering Application of Injectable Gelatin Hydrogel with In Situ Visible-Light-Activated Gelation Capability in both Air and Aqueous Solution. *Tissue Engineering. Part A*, 20(17), 2402–2411. <http://doi.org/10.1089/ten.TEA.2013.0642>
- Lin, H., Lozito, T. P., Alexander, P. G., Gottardi, R., & Tuan, R. S. (2014). Stem cell-based microphysiological osteochondral system to model tissue response to interleukin-1 β . *Molecular Pharmaceutics*, 11(7), 2203–2212. <http://doi.org/10.1021/mp500136b>
- Lin, L., Shen, Q., Leng, H., Duan, X., Fu, X., & Yu, C. (2011). Synergistic inhibition of endochondral bone formation by silencing Hif1 α and Runx2 in trauma-induced heterotopic ossification. *Molecular Therapy: The Journal of the American Society of Gene Therapy*, 19(8), 1426–1432. <http://doi.org/10.1038/mt.2011.101>

- Lind, M., Larsen, A., Clausen, C., Osther, K., & Everland, H. (2008). Cartilage repair with chondrocytes in fibrin hydrogel and MPEG polylactide scaffold: An in vivo study in goats. *Knee Surgery, Sports Traumatology, Arthroscopy*, *16*(7), 690–698. <http://doi.org/10.1007/s00167-008-0522-1>
- Liu, X., Jin, X., & Ma, P. X. (2011). Nanofibrous hollow microspheres self-assembled from star-shaped polymers as injectable cell carriers for knee repair. *Nature Materials*, *10*(5), 398–406. <http://doi.org/10.1038/nmat2999>
- Liu, X., Yang, Y., Niu, X., Lin, Q., Zhao, B., Wang, Y., & Zhu, L. (2017). An in situ photocrosslinkable platelet rich plasma – Complexed hydrogel glue with growth factor controlled release ability to promote cartilage defect repair. *Acta Biomaterialia*, *62*, 179–187. <http://doi.org/10.1016/j.actbio.2017.05.023>
- Liu, Y., Buckley, C. T., Almeida, H. V, Mulhall, K. J., & Kelly, D. J. (2014). Infrapatellar fat pad-derived stem cells maintain their chondrogenic capacity in disease and can be used to engineer cartilaginous grafts of clinically relevant dimensions. *Tissue Engineering. Part A*, *20*(21–22), 3050–62. <http://doi.org/10.1089/ten.TEA.2014.0035>
- Long, D. L., Ulici, V., Chubinskaya, S., & Loeser, R. F. (2015). Heparin-binding epidermal growth factor-like growth factor (HB-EGF) is increased in osteoarthritis and regulates chondrocyte catabolic and anabolic activities. *Osteoarthritis and Cartilage*, *23*(9), 1523–1531. <http://doi.org/10.1016/j.joca.2015.04.019>
- Lopa, S., Colombini, A., Stanco, D., de Girolamo, L., Sansone, V., & Moretti, M. (2014). Donor-matched mesenchymal stem cells from knee infrapatellar and subcutaneous adipose tissue of osteoarthritic donors display differential chondrogenic and osteogenic commitment. *European Cells and Materials*, *27*, 298–311.
- Lozito, T. P., Kuo, C. K., Taboas, J. M., & Tuan, R. S. (2009). Human mesenchymal stem cells express vascular cell phenotypes upon interaction with endothelial cell matrix. *Journal of Cellular Biochemistry*, *107*(4), 714–722. <http://doi.org/10.1002/jcb.22167>
- Luo, L., Thorpe, S. D., Buckley, C. T., & Kelly, D. J. (2015). The effects of dynamic compression on the development of cartilage grafts engineered using bone marrow and infrapatellar fat pad derived stem cells. *Biomedical Materials (Bristol, England)*, *10*(5), 55011. <http://doi.org/10.1088/1748-6041/10/5/055011>
- Ma, B., Xie, J., Jiang, J., Shuler, F. D., & Bartlett, D. E. (2013). Rational design of nanofiber scaffolds for orthopedic tissue repair and regeneration. *Nanomedicine (London, England)*, *8*(9), 1459–81. <http://doi.org/10.2217/nnm.13.132>
- Makris, E. A., Gomoll, A. H., Malizos, K. N., Hu, J. C., & Athanasiou, K. A. (2015). Repair and tissue engineering techniques for articular cartilage. *Nature Reviews. Rheumatology*, *11*(1), 21–34. <http://doi.org/10.1038/nrrheum.2014.157>

- Marión, R. M., & Blasco, M. a. (2010). Telomeres and telomerase in adult stem cells and pluripotent embryonic stem cells. *Advances in Experimental Medicine and Biology*, 695, 118–31. http://doi.org/10.1007/978-1-4419-7037-4_9
- Maruyama, M., Satake, H., Suzuki, T., Honma, R., Naganuma, Y., Takakubo, Y., & Takagi, M. (2017). Comparison of the Effects of Osteochondral Autograft Transplantation With Platelet-Rich Plasma or Platelet-Rich Fibrin on Osteochondral Defects in a Rabbit Model. *American Journal of Sports Medicine*, 45(14), 3280–3288. <http://doi.org/10.1177/0363546517721188>
- Masouros, S. D., Bull, A. M. J., & Amis, A. A. (2010). (i) Biomechanics of the knee joint. *Orthopaedics and Trauma*, 24(2), 84–91. <http://doi.org/10.1016/j.mporth.2010.03.005>
- Matsumoto, T., Cooper, G. M., Gharaibeh, B., Meszaros, L. B., Li, G., Usas, A., ... Huard, J. (2009). Cartilage repair in a rat model of osteoarthritis through intraarticular transplantation of muscle-derived stem cells expressing bone morphogenetic protein 4 and soluble Flt-1. *Arthritis and Rheumatism*, 60(5), 1390–1405. <http://doi.org/10.1002/art.24443>
- Matsumura, E., Tsuji, K., Komori, K., Koga, H., Sekiya, I., & Muneta, T. (2017). Pretreatment with IL-1 β enhances proliferation and chondrogenic potential of synovium-derived mesenchymal stem cells. *Cytotherapy*, 19(2), 181–193. <http://doi.org/10.1016/j.jcyt.2016.11.004>
- Mazzocca, A. D. (2012). Platelet-Rich Plasma Differs According to Preparation Method and Human Variability. *The Journal of Bone and Joint Surgery (American)*, 94(4), 308. <http://doi.org/10.2106/JBJS.K.00430>
- Medeiros Da Cunha, C. M., Perugini, V., Bernegger, P., Centola, M., Barbero, A., Guildford, A. L., ... Marsano, A. (2017). Vascular endothelial growth factor sequestration enhances in vivo cartilage formation. *International Journal of Molecular Sciences*, 18(11). <http://doi.org/10.3390/ijms18112478>
- Mifune, Y., Matsumoto, T., Takayama, K., Ota, S., Li, H., Meszaros, L. B., ... Huard, J. (2013). The effect of platelet-rich plasma on the regenerative therapy of muscle derived stem cells for articular cartilage repair. *Osteoarthritis and Cartilage / OARS, Osteoarthritis Research Society*, 21(1), 175–85. <http://doi.org/10.1016/j.joca.2012.09.018>
- Milano, G., Sanna Passino, E., Deriu, L., Careddu, G., Manunta, L., Manunta, A., ... Fabbriani, C. (2010). The effect of platelet rich plasma combined with microfractures on the treatment of chondral defects: An experimental study in a sheep model. *Osteoarthritis and Cartilage*, 18(7), 971–980. <http://doi.org/10.1016/j.joca.2010.03.013>
- Miot, S., Brehm, W., Dickinson, S., Sims, T., Wixmerten, A., Longinotti, C., ... Martin, I. (2012). Influence of in vitro maturation of engineered cartilage on the outcome of osteochondral repair in a goat model. *European Cells and Materials*, 23, 222–236. <http://doi.org/vol023a17> [pii]

- Mishra, A., Tummala, P., King, A., Lee, B., Kraus, M., Tse, V., & Jacobs, C. R. (2009). Buffered platelet-rich plasma enhances mesenchymal stem cell proliferation and chondrogenic differentiation. *Tissue Engineering. Part C, Methods*, 15(3), 431–5. <http://doi.org/10.1089/ten.tec.2008.0534>
- Mouser, V. H. M., Levato, R., Bonassar, L. J., D’Lima, D. D., Grande, D. A., Klein, T. J., ... Malda, J. (2017). Three-Dimensional Bioprinting and Its Potential in the Field of Articular Cartilage Regeneration. *Cartilage*. <http://doi.org/10.1177/1947603516665445>
- Moutos, F. T., Glass, K. A., Compton, S. A., Ross, A. K., Gersbach, C. A., Guilak, F., & Estes, B. T. (2016). Anatomically shaped tissue-engineered cartilage with tunable and inducible anticytokine delivery for biological joint resurfacing. *Proceedings of the National Academy of Sciences*, 201601639. <http://doi.org/10.1073/pnas.1601639113>
- Murata, M., Yudoh, K., & Masuko, K. (2008). The potential role of vascular endothelial growth factor (VEGF) in cartilage: how the angiogenic factor could be involved in the pathogenesis of osteoarthritis? *Osteoarthritis Cartilage*, 16(3), 279–286. <http://doi.org/10.1016/j.joca.2007.09.003>
- Nagai, T., Sato, M., Kobayashi, M., Yokoyama, M., Tani, Y., & Mochida, J. (2014). Bevacizumab, an anti-vascular endothelial growth factor antibody, inhibits osteoarthritis. *Arthritis Research & Therapy*, 16(5), 427. <http://doi.org/10.1186/s13075-014-0427-y>
- Nagai, T., Sato, M., Kutsuna, T., Kokubo, M., Ebihara, G., Ohta, N., & Mochida, J. (2010). Intravenous administration of anti-vascular endothelial growth factor humanized monoclonal antibody bevacizumab improves articular cartilage repair. *Arthritis Research & Therapy*, 12(5), R178. <http://doi.org/10.1186/ar3142>
- Nagao, M., Hamilton, J. L., Kc, R., Berendsen, A. D., Duan, X., Cheong, C. W., ... Olsen, B. R. (2017). Vascular Endothelial Growth Factor in Cartilage Development and Osteoarthritis. *Scientific Reports*, 7(1), 1–16. <http://doi.org/10.1038/s41598-017-13417-w>
- National Research Council and the Institute of Medicine. (2001). *Musculoskeletal Disorders and the Workplace: Low Back and Upper Extremities*. Panel on Musculoskeletal Disorders and the Workplace. Commission on Behavioral and Social Sciences and Education. Washington, DC: National Academy Press.
- Ohba, S., Yano, F., & Chung, U. (2009). Tissue engineering of bone and cartilage. *IBMS BoneKEy*, 6(11), 405–419. <http://doi.org/10.1138/20090406>
- Osterman, C., McCarthy, M. B. R., Cote, M. P., Beitzel, K., Bradley, J., Polkowski, G., & Mazzocca, a. D. (2015). Platelet-Rich Plasma Increases Anti-inflammatory Markers in a Human Coculture Model for Osteoarthritis. *The American Journal of Sports Medicine*. <http://doi.org/10.1177/03635465155570463>
- Park, S. Il, Lee, H. R., Kim, S., Ahn, M. W., & Do, S. H. (2011). Time-sequential modulation in expression of growth factors from platelet-rich plasma (PRP) on the chondrocyte cultures. *Molecular and Cellular Biochemistry*, pp. 1–9. <http://doi.org/10.1007/s11010-011-1081-1>

- Patel, S., Dhillon, M. S., Aggarwal, S., Marwaha, N., & Jain, A. (2013). Treatment with platelet-rich plasma is more effective than placebo for knee osteoarthritis: a prospective, double-blind, randomized trial. *The American Journal of Sports Medicine*, *41*(2), 356–64. <http://doi.org/10.1177/0363546512471299>
- Pei, Y., Fan, J. J., Zhang, X. Q., Zhang, Z. Y., & Yu, M. (2014). Repairing the osteochondral defect in goat with the tissue-engineered osteochondral graft preconstructed in a double-chamber stirring bioreactor. *BioMed Research International*, *2014*. <http://doi.org/10.1155/2014/219203>
- Pires de Carvalho, P., Hamel, K. M., Duarte, R., King, A. G. S., Haque, M., Dietrich, M. A., ... Dasa, V. (2014, October). Comparison of infrapatellar and subcutaneous adipose tissue stromal vascular fraction and stromal/stem cells in osteoarthritic subjects. *Journal of Tissue Engineering and Regenerative Medicine*, pp. 757–62. <http://doi.org/10.1002/term.1565>
- Pourcho, A. M., Smith, J., Wisniewski, S. J., & Sellon, J. L. (2014). Intraarticular platelet-rich plasma injection in the treatment of knee osteoarthritis: review and recommendations. *American Journal of Physical Medicine & Rehabilitation / Association of Academic Physiatrists*, *93*(11 Suppl 3), S108-21. <http://doi.org/10.1097/PHM.0000000000000115>
- Prasadam, I., Zhou, Y., Du, Z., Chen, J., Crawford, R., & Xiao, Y. (2014). Osteocyte-induced angiogenesis via VEGF-MAPK-dependent pathways in endothelial cells. *Molecular and Cellular Biochemistry*, *386*(1–2), 15–25. <http://doi.org/10.1007/s11010-013-1840-2>
- Pricola, K. L., Kuhn, N. Z., Haleem-Smith, H., Song, Y., & Tuan, R. S. (2009). Interleukin-6 maintains bone marrow-derived mesenchymal stem cell stemness by an ERK1/2-dependent mechanism. *Journal of Cellular Biochemistry*, *108*(3), 577–588. <http://doi.org/10.1002/jcb.22289>
- Riboh, J. C., Saltzman, B. M., Yanke, A. B., Fortier, L., & Cole, B. J. (2015). Effect of Leukocyte Concentration on the Efficacy of Platelet-Rich Plasma in the Treatment of Knee Osteoarthritis. *The American Journal of Sports Medicine*. <http://doi.org/10.1177/0363546515580787>
- Rios, D. L., Lopez, C., Carmona, J. U. U., Ríos, D. L., López, C., Carmona, J. U. U., ... Carmona, J. U. U. (2015). Evaluation of the anti-inflammatory effects of two platelet-rich gel supernatants in an in vitro system of cartilage inflammation. *Cytokine*, *76*(2), 1–9. <http://doi.org/10.1016/j.cyto.2015.07.008>
- Rose-John, S. (2012). Il-6 trans-signaling via the soluble IL-6 receptor: Importance for the proinflammatory activities of IL-6. *International Journal of Biological Sciences*. <http://doi.org/10.7150/ijbs.4989>
- Rothrauff, B. B., Coluccino, L., Gottardi, R., Ceseracciu, L., Scaglione, S., Goldoni, L., & Tuan, R. S. (2018). Efficacy of thermoresponsive, photocrosslinkable hydrogels derived from decellularized tendon and cartilage extracellular matrix for cartilage tissue engineering. *Journal of Tissue Engineering and Regenerative Medicine*, *12*(1), e159–e170. <http://doi.org/10.1002/term.2465>

- Ruijtenberg, S., & van den Heuvel, S. (2016). Coordinating cell proliferation and differentiation: Antagonism between cell cycle regulators and cell type-specific gene expression. *Cell Cycle*. <http://doi.org/10.1080/15384101.2015.1120925>
- Sánchez, M., Fiz, N., Azofra, J., Usabiaga, J., Aduriz Recalde, E., Garcia Gutierrez, A., ... Anitua, E. (2012). A randomized clinical trial evaluating plasma rich in growth factors (PRGF-Endoret) versus hyaluronic acid in the short-term treatment of symptomatic knee osteoarthritis. *Arthroscopy - Journal of Arthroscopic and Related Surgery*, 28(8), 1070–1078. <http://doi.org/10.1016/j.arthro.2012.05.011>
- Schuurman, W., Khristov, V., Pot, M. W., Van Weeren, P. R., Dhert, W. J. A., & Malda, J. (2011). Bioprinting of hybrid tissue constructs with tailorable mechanical properties. *Biofabrication*, 3(2). <http://doi.org/10.1088/1758-5082/3/2/021001>
- Shevchenko, E. K., Makarevich, P. I., Tsokolaeva, Z. I., Boldyreva, M. A., Sysoeva, V. Y., Tkachuk, V. A., & Parfyonova, Y. V. (2013). Transplantation of modified human adipose derived stromal cells expressing VEGF165 results in more efficient angiogenic response in ischemic skeletal muscle. *Journal of Translational Medicine*, 11, 138. <http://doi.org/10.1186/1479-5876-11-138>
- Smyth, N. A., Haleem, A. M., Ross, K. A., Hannon, C. P., Murawski, C. D., Do, H. T., & Kennedy, J. G. (2016). Platelet-Rich Plasma May Improve Osteochondral Donor Site Healing in a Rabbit Model. *Cartilage*, 7(1), 104–111. <http://doi.org/10.1177/1947603515599190>
- Spreafico, A., Chellini, F., Frediani, B., Bernardini, G., Niccolini, S., Serchi, T., ... Santucci, A. (2009). Biochemical investigation of the effects of human platelet releasates on human articular chondrocytes. *Journal of Cellular Biochemistry*, 108(5), 1153–1165. <http://doi.org/10.1002/jcb.22344>
- Stuttfield, E., & Ballmer-Hofer, K. (2009). Structure and function of VEGF receptors. *IUBMB Life*, 61(9), 915–22. <http://doi.org/10.1002/iub.234>
- Sun, L., Wang, X., & Kaplan, D. L. (2011). A 3D cartilage - Inflammatory cell culture system for the modeling of human osteoarthritis. *Biomaterials*, 32(24), 5581–5589. <http://doi.org/10.1016/j.biomaterials.2011.04.028>
- Sun, Y., Feng, Y., Zhang, C. Q., Chen, S. B., & Cheng, X. G. (2010). The regenerative effect of platelet-rich plasma on healing in large osteochondral defects. *International Orthopaedics*, 34(4), 589–597. <http://doi.org/10.1007/s00264-009-0793-2>
- Sundman, E. a., Cole, B. J., & Fortier, L. a. (2011). Growth Factor and Catabolic Cytokine Concentrations Are Influenced by the Cellular Composition of Platelet-Rich Plasma. *The American Journal of Sports Medicine*, 39(10), 2135–2140. <http://doi.org/10.1177/0363546511417792>
- Takahashi, K., Tanabe, K., Ohnuki, M., Narita, M., Ichisaka, T., Tomoda, K., & Yamanaka, S. (2007). Induction of Pluripotent Stem Cells from Adult Human Fibroblasts by Defined Factors. *Cell*, 107(5), 861–872. <http://doi.org/10.1016/j.cell.2007.11.019>

- Takahashi, K., & Yamanaka, S. (2006). Induction of Pluripotent Stem Cells from Mouse Embryonic and Adult Fibroblast Cultures by Defined Factors. *Cell*, *126*(4), 663–676. <http://doi.org/10.1016/j.cell.2006.07.024>
- Textor, J. A., & Tablin, F. (2012). Activation of equine platelet-rich plasma: Comparison of methods and characterization of equine autologous thrombin. *Veterinary Surgery*, *41*(7), 784–794. <http://doi.org/10.1111/j.1532-950X.2012.01016.x>
- Tuan, R. S., Chen, A. F., & Klatt, B. A. (2013). Cartilage regeneration. *The Journal of the American Academy of Orthopaedic Surgeons*, *21*(5), 303–11. <http://doi.org/10.5435/JAAOS-21-05-303>
- van Bergen, C. J. a, Kerkhoffs, G. M. M. J., Marsidi, N., Korstjens, C. M., Everts, V., van Ruijven, L. J., ... Blankevoort, L. (2013). Osteochondral Defects of the Talus: A Novel Animal Model in the Goat. *Tissue Engineering. Part C, Methods*, *19*(6). <http://doi.org/10.1089/ten.TEC.2012.0401>
- van Buul, G. M., Koevoet, W. L. M., Kops, N., Bos, P. K., Verhaar, J. a. N., Weinans, H., ... van Osch, G. J. V. M. (2011). Platelet-Rich Plasma Releasate Inhibits Inflammatory Processes in Osteoarthritic Chondrocytes. *The American Journal of Sports Medicine*, *39*(11), 2362–2370. <http://doi.org/10.1177/0363546511419278>
- Wang, J. S., Jen, C. J., Kung, H. C., Lin, L. J., Hsiue, T. R., & Chen, H. I. (1994). Different effects of strenuous exercise and moderate exercise on platelet function in men. *Circulation*, *90*(6), 2877–2885. <http://doi.org/10.1161/01.CIR.90.6.2877>
- Wang, Y., Da, G., Li, H., & Zheng, Y. (2013). Avastin exhibits therapeutic effects on collagen-induced arthritis in rat model. *Inflammation*, *36*(6), 1460–1467. <http://doi.org/10.1007/s10753-013-9687-y>
- Wernig, M., Meissner, A., Foreman, R., Brambrink, T., Ku, M., Hochedlinger, K., ... Jaenisch, R. (2007). In vitro reprogramming of fibroblasts into a pluripotent ES-cell-like state. *Nature*, *448*(7151), 318–324. <http://doi.org/10.1038/nature05944>
- Woodfield, T. B. F., Malda, J., De Wijn, J., Péters, F., Riesle, J., & Van Blitterswijk, C. A. (2004). Design of porous scaffolds for cartilage tissue engineering using a three-dimensional fiber-deposition technique. *Biomaterials*, *25*(18), 4149–4161. <http://doi.org/10.1016/j.biomaterials.2003.10.056>
- Woodfield, T. B. F., Van Blitterswijk, C. a, De Wijn, J., Sims, T. J., Hollander, a P., & Riesle, J. (2005). Polymer scaffolds fabricated with pore-size gradients as a model for studying the zonal organization within tissue-engineered cartilage constructs. *Tissue Engineering*, *11*(9–10), 1297–1311. <http://doi.org/10.1089/ten.2005.11.1297>
- Xie, X., Wang, Y., Zhao, C., Guo, S., Liu, S., Jia, W., ... Zhang, C. (2012). Comparative evaluation of MSCs from bone marrow and adipose tissue seeded in PRP-derived scaffold for cartilage regeneration. *Biomaterials*, *33*(29), 7008–7018. <http://doi.org/10.1016/j.biomaterials.2012.06.058>

- Xie, X., Zhang, C., & Tuan, R. S. (2014). Biology of platelet-rich plasma and its clinical application in cartilage repair. *Arthritis Research & Therapy*, *16*(1), 204. <http://doi.org/10.1186/ar4493>
- Xu, Z., Yin, W., Zhang, Y., Qi, X., Chen, Y., Xie, X., & Zhang, C. (2017). Comparative evaluation of leukocyte- and platelet-rich plasma and pure platelet-rich plasma for cartilage regeneration. *Scientific Reports*, *7*, 43301. <http://doi.org/10.1038/srep43301>
- Yamamoto, K., Sokabe, T., Watabe, T., Miyazono, K., Yamashita, J. K., Obi, S., ... Ando, J. (2005). Fluid shear stress induces differentiation of Flk-1-positive embryonic stem cells into vascular endothelial cells in vitro. *American Journal of Physiology. Heart and Circulatory Physiology*, *288*(4), H1915–H1924. <http://doi.org/10.1152/ajpheart.00956.2004>
- Yamanaka, S. (2007). Strategies and New Developments in the Generation of Patient-Specific Pluripotent Stem Cells. *Cell Stem Cell*. <http://doi.org/10.1016/j.stem.2007.05.012>
- Yang, J., Zhang, Y. S., Yue, K., & Khademhosseini, A. (2017). Cell-laden hydrogels for osteochondral and cartilage tissue engineering. *Acta Biomaterialia*. <http://doi.org/10.1016/j.actbio.2017.01.036>
- Yang, P. J., & Temenoff, J. S. (2009). Engineering orthopedic tissue interfaces. *Tissue Engineering. Part B, Reviews*, *15*(2), 127–141. <http://doi.org/10.1089/ten.teb.2008.0371>
- Yang, S. Y., Ahn, S. T., Rhie, J. W., Lee, K. Y., Choi, J. H., Lee, B. J., & Oh, G. T. (2000). Platelet supernatant promotes proliferation of auricular chondrocytes and formation of chondrocyte mass. *Ann Plast Surg*, *44*(4), 405–411.
- Yoshida, R., Cheng, M., & Murray, M. M. (2014). Increasing platelet concentration in platelet-rich plasma inhibits anterior cruciate ligament cell function in three-dimensional culture. *Journal of Orthopaedic Research*, *32*(2), 291–295. <http://doi.org/10.1002/jor.22493>
- Yu, G., Wu, X., Dietrich, M. A., Polk, P., Scott, L. K., Ptitsyn, A. A., & Gimble, J. M. (2010). Yield and characterization of subcutaneous human adipose-derived stem cells by flow cytometric and adipogenic mRNA analyzes. *Cytotherapy*, *12*(4), 538–546. <http://doi.org/10.3109/14653241003649528>
- Yu, J., Vodyanik, M. A., Smuga-Otto, K., Antosiewicz-Bourget, J., Frane, J. L., Tian, S., ... Thomson, J. A. (2007). Induced pluripotent stem cell lines derived from human somatic cells. *Science (New York, N.Y.)*, *318*(5858), 1917–20. <http://doi.org/10.1126/science.1151526>
- Zelzer, E., Mamluk, R., Ferrara, N., Johnson, R. S., Schipani, E., & Olsen, B. R. (2004). VEGFA is necessary for chondrocyte survival during bone development. *Development (Cambridge, England)*, *131*(9), 2161–2171. <http://doi.org/10.1242/dev.01053>
- Zeng, L., Xiao, Q., Margariti, A., Zhang, Z., Zampetaki, A., Patel, S., ... Xu, Q. (2006). HDAC3 is crucial in shear- and VEGF-induced stem cell differentiation toward endothelial cells. *Journal of Cell Biology*, *174*(7), 1059–1069. <http://doi.org/10.1083/jcb.200605113>

- Zhang, C., Li, Y., Cornelia, R., Swisher, S., & Kim, H. (2012). Regulation of VEGF expression by HIF-1 α in the femoral head cartilage following ischemia osteonecrosis. *Scientific Reports*, 2, 2–7. <http://doi.org/10.1038/srep00650>
- Zhang, J., & Wang, J. H.-C. H.-C. (2010). Platelet-rich plasma releasate promotes differentiation of tendon stem cells into active tenocytes. *The American Journal of Sports Medicine*, 38(12), 2477–2486. <http://doi.org/10.1177/0363546510376750>
- Zhu, S., Zhang, B., Man, C., Ma, Y., & Hu, J. (2011). NEL-like molecule-1-modified bone marrow mesenchymal stem cells/poly lactic-co-glycolic acid composite improves repair of large osteochondral defects in mandibular condyle. *Osteoarthritis and Cartilage*, 19(6), 743–750. <http://doi.org/10.1016/j.joca.2011.02.015>
- Zuscik, M. J., Hilton, M. J., Zhang, X., Chen, D., & O’Keefe, R. J. (2008). Regulation of chondrogenesis and chondrocyte differentiation by stress. *Journal of Clinical Investigation*, 118(2), 429–438. <http://doi.org/10.1172/JCI34174>